

Weak sensitivity of the terrestrial water budget to global soil texture maps in the ORCHIDEE land surface model

Salma TAFASCA¹, Agnès DUCHARNE¹, Christian VALENTIN²

Reply to Anonymous Referee #1

We sincerely thank the reviewer for taking the time to review our manuscript and for the very constructive comments he/she provided. We provide below a point-by-point response to these comments, numbered from C1 to C26 for convenience.

C1: The paper by Tafasca et al. uses the ORCHIDEE land surface model to test the effect of using different soil texture maps on the water budget at the global scale and concludes that, given the similarities between the tested maps, the choice of input soil texture map is not crucial for large scale modeling (compared to the bias due to the choice of, for example, meteorological forcings). I think that the study of the impact of biases in the estimates in soil properties on water and energy budgets is of great importance for assessing the accuracy of LSM simulations as well as to guide their parameterization.

However, the manuscript by Tafasca and co-authors, in its current form, lacks a clear definition of its objectives and novelty. Most of the paper is devoted to showing the correct performance of a widely used model in modeling rainfall partitioning in different soil texture – this seems more a reality check for the model, than a novel analysis. The model is then used to conclude that, given the similarity of the tested maps, at the scales under consideration the resulting bias in the hydrologic response is negligible (a result that could have been guessed without performing heavy numerical simulations).

I believe the manuscript would better benefit from a more detailed (and quantitative) analysis of the relationship between the soil input bias and resulting hydrologic bias across scales, as detailed below.

The above points are further expanded below and we tried to carefully address them in the following. Overall, we mostly agree with the analysis, and we propose to augment the paper with additional analyses, as suggested by the reviewer. The revised version of the paper will have the following structure, with proposed changes highlighted in italic:

1. Introduction

New paragraph at the end clarifying the scientific objectives of the paper and outlining the structure of the paper.

2. Materials and methods

2.1. Soil texture in the ORCHIDEE LSM

2.2. Simulation protocol

2.3. Calculation of median diameter dm for each of the 12 USDA soil texture classes

2.4. Evaluation datasets

3. Results

3.1. Comparison of the tested soil texture maps

This new subsection will detail the similarities and differences between the three tested soil maps. A detailed description of this section is found in C22.

3.2. Point scale sensitivity to the 12 USDA texture classes

This section corresponds to the original section 3.1 of the submitted version of the paper, *the description of Figure 4 will be more detailed here..*

3.3. Spatial patterns of simulated fluxes and evapotranspiration bias

This subsection will analyze Figures 6 and 7 of the submitted paper, which correspond to paragraphs 2 and 3 of section 3.2 of the submitted version. *We will also add and discuss the new Figure A5, which is described in C17.*

3.4. Regional zooms on greatly impacted areas

This subsection will highlight areas with important differences induced by the soil map changes (Figure A1). It will also include the discussion on clays found the closing section of the submitted manuscript

3.5. Sensitivity of the simulated water budget to global soil texture maps at different scales

In addition to analyzing the global water budgets resulting from the different soil texture maps, *we propose to add an analysis of the impact of the upscaling resolution on the simulated water fluxes (see C5).*

4. Discussion and conclusions

Most of the discussion about clays will be removed (transferred to subsection 3.4), and *the main conclusions will be rephrased to fit the updated results. In particular, the weak sensitivity of the simulated water fluxes to the prescribed soil texture maps is mostly found at coarse scales (global water cycle), but the texture maps can have a large impact at small scales.*

The propositions detailed in the following would lead to add 5 new figures, and change one figure (Fig. 8) into 2 tables, thus leading to a total of 12 figures and 4 tables.

MAJOR COMMENTS:

C2: 1. It is not clear what the novelty and the overall goal of the paper is. As it stands, it seems more of a modeling exercise using different soil maps, but without a clear scientific objective being proposed.

The main objective of the study was and remains to examine the impact of various soil texture maps on the simulated hydrologic fluxes, from grid-point to continental scales. As discussed below, there is no consensus on what is the “best” soil texture map for global LSM applications, and the identification of the “best” soil map is thus an important scientific question for land surface modelers.

Given our results and the bibliography, we can postulate at least two reasons for this lack of consensus on the “best” global soil texture map: (1) There is no paper trying to identify it; (2) The overall impact of changing the soil texture map on the simulated fluxes is quite small apart from specific areas. This weak sensitivity is probably a reason why there has been no publication on this topic until now, apart from De Lannoy et al., (2014), who document the improvement of one specific global soil texture map.

In this framework, the result we chose to focus on in the submitted manuscript was the weak sensitivity of the simulated water budget to the tested maps, because we felt it had useful practical consequences. Indeed, it means that the choice of the soil texture map, among the ones that are routinely available, is not a major issue for global scale modeling. The choice of the meteorological forcing dataset, for instance, has a much stronger impact. Yet, we perfectly understand the reviewer’s point of view regarding the interest of identifying where the soil texture maps do matter, and we will add a specific sub-section of the Results (3.4) on this point.

As for the scientific goals of the paper, they will be clarified in an expanded paragraph at the end of the Introduction, given in response to comment C8.

C3: 2. The authors use soil texture maps that are similar and conclude that they give similar results. If the soil maps are indeed not too different, how could the authors expect to observe any difference in the results (especially in terms of global fluxes where the main local differences are averaged out)?

The reviewer is right, but the similarity of the soil texture maps is not *a priori* knowledge, as might be suggested by the abstract: it is actually an outcome of our study. At first sight, it is not straightforward that the three tested soil maps are similar (Fig. 1 of the paper), nurturing the question of the “best” soil texture map. It is after getting our results that we analyzed the similarities between the different soil maps to understand why the large-scale simulated fluxes are largely similar. Based on reviewer’s suggestion C22, we propose to add a new sub-section in the Results (3.1) where we analyze the similarities and differences between the soil texture maps. We will also rephrase the abstract.

C4: Along these lines, while the global/average water budget is similar, how different are the extremes (i.e., where the maps actually differ, what is the bias in the results)? In these terms, I think that a more detailed analysis of the biases induced in those areas where the maps differ would be more useful.

We agree, and in the revised version, we will add a dedicated subsection (3.4). We propose to add Figures A1 and A2 below, where we zoomed on four 40°x60° areas where the ET bias is greatly impacted by soil texture map. Based on Figs. 3 and 4 of the submitted manuscript, the largest changes in ET and total runoff are expected where soil texture changes between medium and extreme (Clay or Sand) textures. Hence, the absence of Clay in the Zobler map results in important increase of ET bias (Fig. A1 and Fig. A2). In contrast, the Oxisols mapped as Clay in the Reynolds map correspond to a large negative ET bias (e.g. South America in Fig. A1 and Fig. A2). Another example is found in Central America, where the SoilGrids texture map provided by the SP-MIP team shows a large amount of Clay, which turns the ET bias from positive (with the Reynolds and Zobler maps) to negative. It must be underlined that the original 1km SoilGrids does not show this dominance of Clay in Mexico, and we think that this feature is an error of the SP-MIP map. Since we noticed some non-negligible differences between the original SoilGrids map and the one provided by SP-MIP which is used in this study, we decided to refer to the latter by the SP-MIP map rather than the SoilGrids map. This will be changed and clarified in the revised version of the paper.

The text describing Figures A1 and A2 in the new subsection will be based on the one already present in the Discussion of the submitted version, but without any supporting figure, which shows the importance of better describing the Clay texture, and calls for a soil texture map that distinguishes the two clay types which have different hydrologic behaviors: the Oxisols and the Vertisols. The other extreme soil texture (Sand) is mostly found in arid areas where water is a limiting factor, so the soil map change does not greatly impact the ET bias. It is the case in the Arabian Peninsula and the Sahara, where the sandy soils mapped in SoilGrids are absent in Zobler and only weakly present in Reynolds, but the ET bias hardly changes and remains negative.

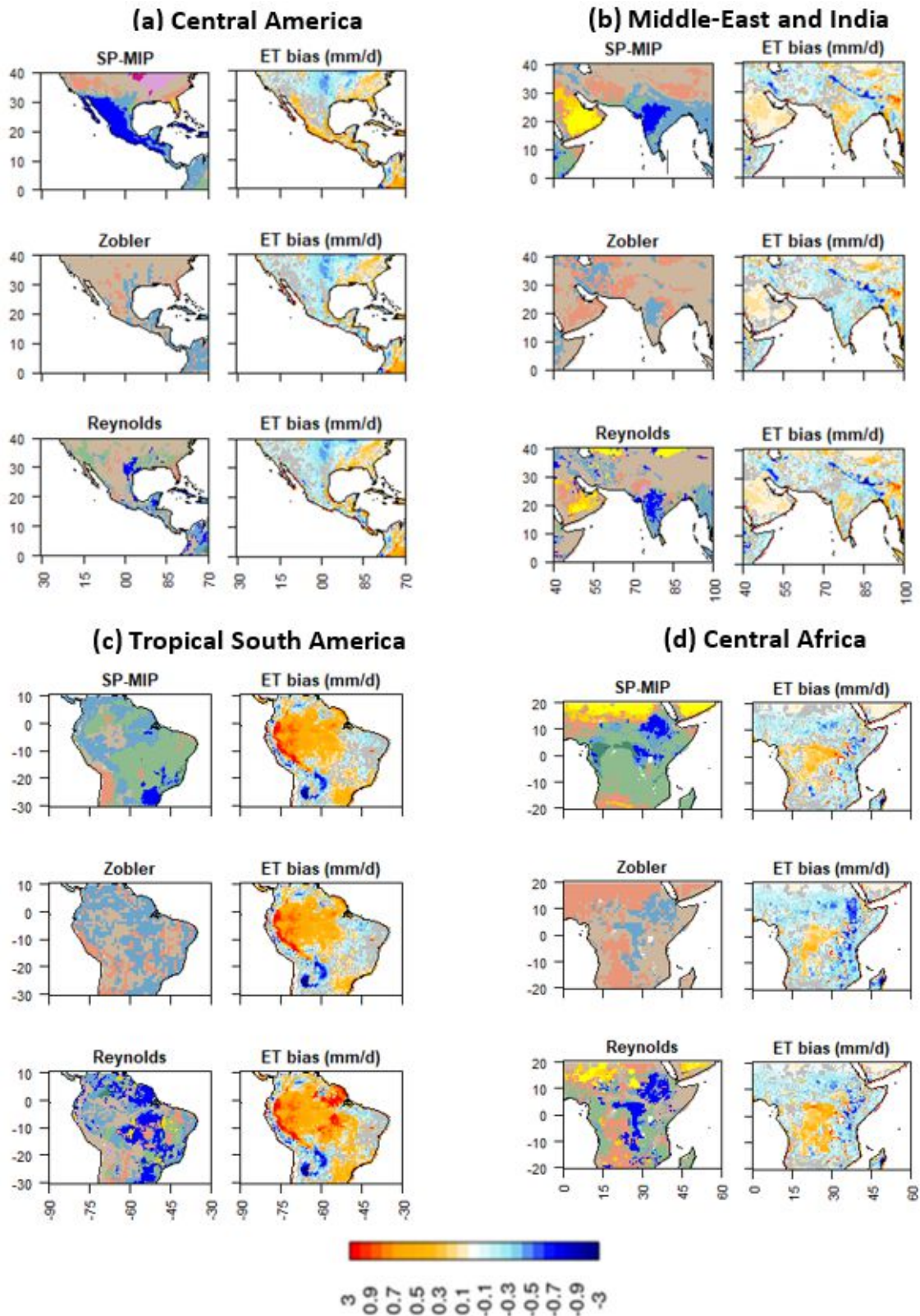


Figure A1 Regional zooms on soil texture maps and the corresponding evapotranspiration bias maps (with respect to the GLEAM product) in four different areas. The colors scale on the right corresponds to the evapotranspiration bias maps, in which the grey color indicates that the bias is not statistically significant using Student's t -test with a p -value < 0.05 . The colors of the soil texture maps are defined in Figure 1d.

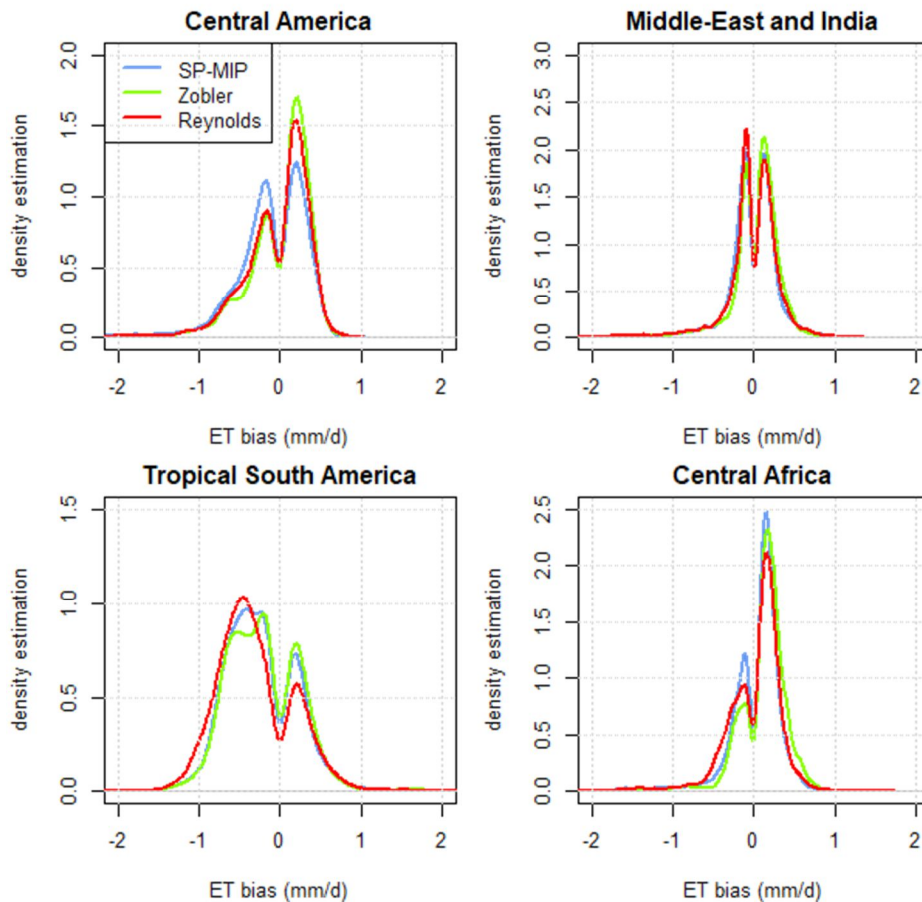


Figure A2 Probability distribution of ET bias in the 4 regions of Fig.A1, for simulations EXP2, EXP3, EXP4 in red, green and blue respectively.

C5: 3. Lastly, at what scales do local differences in soil texture maps and the associated fluxes start to differ substantially? Can the authors define thresholds in these terms?

We agree that the impact of the scale of analysis on the simulated fluxes is an interesting point to look at. To this end, we decided to add a new sub-section 3.5 in the Results, called: "Sensitivity of the simulated water budget to global soil texture maps at different scales". To analyze the scale-related impact of soil texture maps on simulated fluxes, we reproduced Figure 6c of the submitted paper, but upscaled this map of annual mean ET difference (EXP2-EXP4) to coarser resolutions, from 1° to the global scale, by averaging the values of ET (Fig. A3). The resulting probability density functions (pdfs) are shown in Figure A4, and Figure A5 shows the evolution of some metrics characterizing these distributions with the averaging scale. The first noticeable impact of upscaling ET to coarser resolutions is the decrease of extreme ET differences (Fig. A5a,c), leading to a less scattered distribution, also confirmed by the decreasing standard deviation (Fig. A5 b).

These figures (which may be combined in one in the revised manuscript) show that ET follows a nearly normal distribution for the coarse resolutions (above 5°), and starts showing a dissymmetric distribution for the finest resolutions (below 5°), with a prevalence of negative values (Fig A4). This can also be seen in Figure A5c where the median value of the ET difference moves to more negative values as the resolution gets finer. As a consequence, if we wanted to define a threshold at which resolution starts to impact the distribution of annual mean ET, it would be the 5° resolution. We propose to include Figure A3, A4 and A5 as well as the aforementioned analysis in sub-section 3.5, in order to bridge the gap between the point-scale maps at which some strong impacts of the soil texture maps can be found regionally, and the global scale, at which the

terrestrial water budget shows a very weak sensitivity to the soil texture maps, even if they are statistically significant (Fig. 5).

Nonetheless, we would like to point out that this analysis is not exhaustive, as a thorough analysis of the impact of the soil texture map resolution on the simulated fluxes would require performing additional simulations with soil texture maps upscaled to different resolutions. This kind of analysis is out of the original scope of our paper, especially given the general trend in land surface modelling for always higher resolutions (Bierkens et al., 2015; Wood et al., 2011).

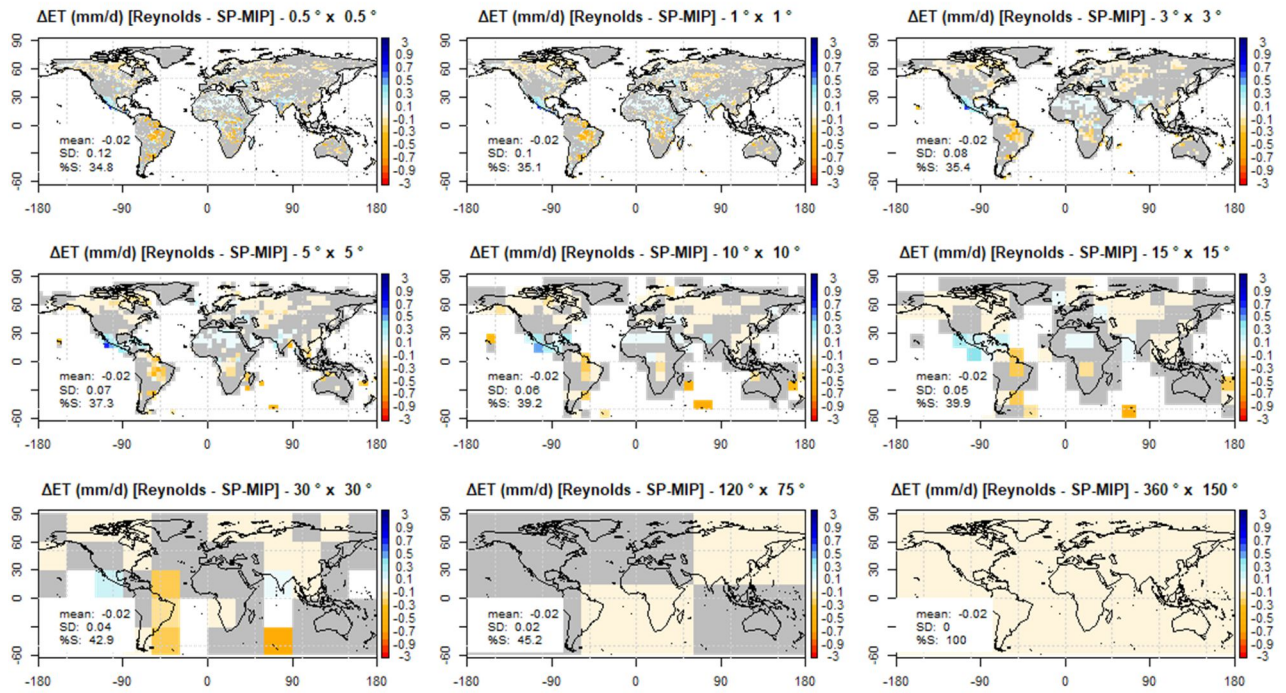


Figure A3 Spatial distribution of simulated annual mean evapotranspiration: difference between EXP2 and EXP4 (Reynolds – SP-MIP), upscaled to different resolutions. Grey color indicates that the difference is not statistically significant at the tested resolution based on Student’s t-test (with a p-value < 0.05). The printed means and standard deviation correspond to the full land area excluding Antarctica. %NS represents the percentage of land with non-significant differences.

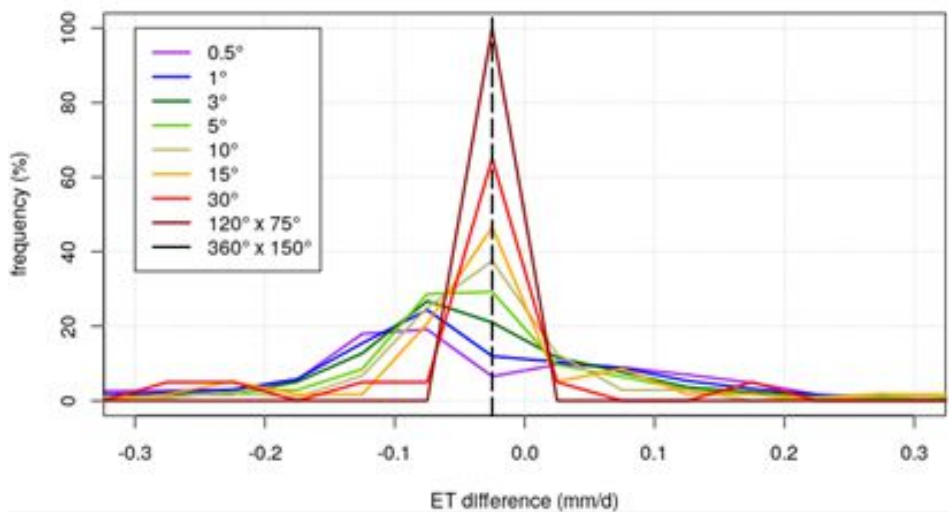


Figure A4 Distribution of annual mean ET difference between EXP2 and EXP4, at different resolutions. These

distributions correspond to the maps of figure A3.

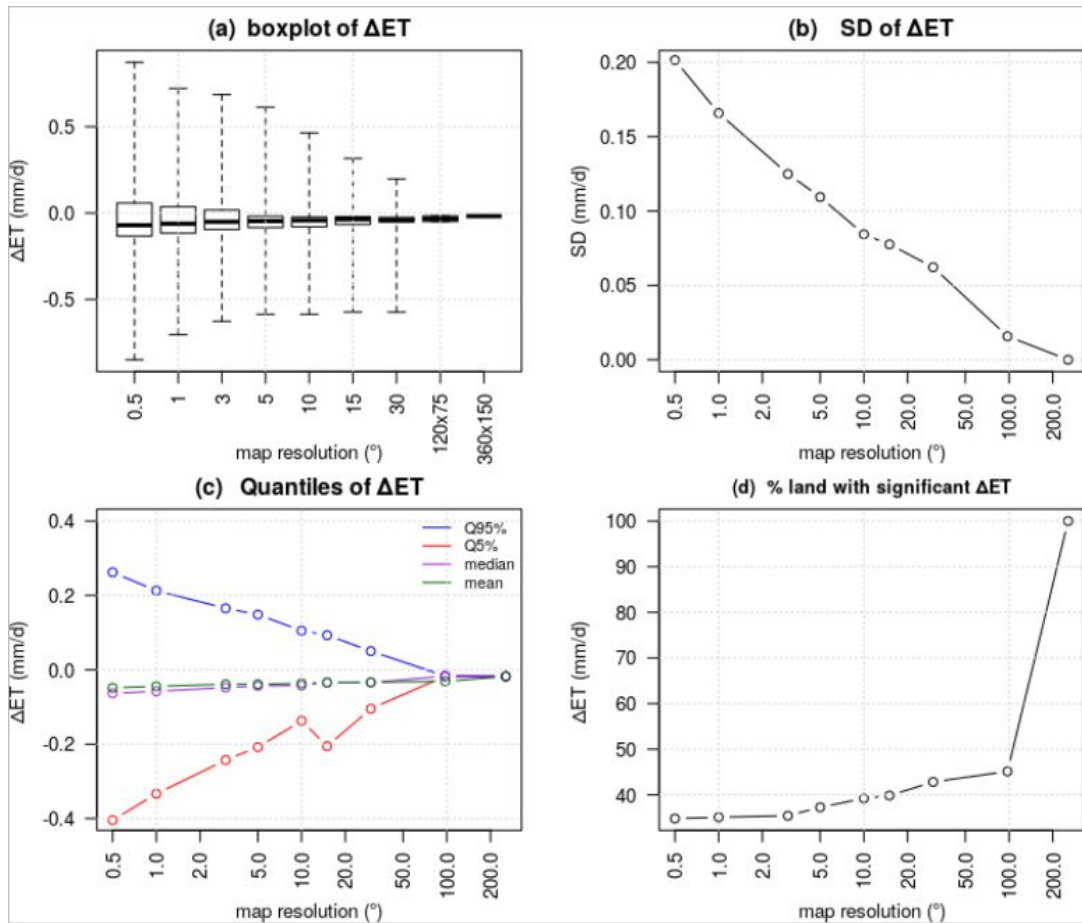


Figure A5 Statistical indicators of distribution of annual mean ET : difference between EXP2 and EXP4, at different resolutions

MINOR COMMENTS:

Abstract:

C6: - Lines 10-11: "Here, we investigate the impact of soil texture on soil water fluxes and storage at global scale". What is the novelty here? The impact of having different soil texture (clay vs. sand) on infiltration/runoff partitioning is well known and a large scale application only seems a modeling exercise without added scientific value. I think the abstract (and paper) would benefit from the definition of a more precise research question/objective.

We agree that our research questions were not well defined, as already discussed in C1. In the revised version of the paper, we will make a clearer description of the research questions in both the abstract and the introduction (cf. C8). The main conclusions will also be updated to match the revised manuscript.

Introduction:

C7: - Line 35: SoilGrids database is available at higher resolution too (250 m).

We will mention the availability of the 250m version of SoilGrids (Hengl et al., 2017) at line 35.

C8: - In general, I think the Introduction lacks some clarity: It is not clear whether the focus here is on testing the LSM at the global scale, or on the effect of PTFs, or on the comparison of different soil texture maps. The paper would largely benefit from a more detailed introduction where the novelty and the goals of the paper are clearly defined in relation to state of the art knowledge on the subject.

The main point of the paper is testing three different soil texture maps, broadly used by LSMs, and comparing their resulting hydrologic variables. In the revised version of our paper, this will be clarified by expanding the last line of the introduction to a more classical paragraph detailing the specific research question of the paper and the structure of the paper:

“Here, we aim at exploring more systematically the impact of soil texture on the water budget from point to global scale, using a state-of-the-art LSM with physically-based soil hydrology, and multiple input soil texture maps. After presenting the model and soil texture maps used in this work, the results are presented as follows. We first provide an analysis of the similarities and differences between the different soil maps, then, we evaluate the point-scale response of the model to different soil textures to make sure it displays a reliable behavior. This point-scale response is then analyzed from a geographic point of view, with a comparison to a distributed observation-based ET product, and a focus is made on areas with a large sensitivity to the soil texture maps. We finally explore how the magnitude and significance of the simulated ET changes with the scale of analysis up to the land scale, defining the terrestrial water budget. The closing section summarizes the main conclusions of the study, and discusses its limitations and perspectives. “

Methods:

C9: - Lines 66-67: at what depth are the soil texture maps? SoilGrids provides, for example, texture properties at different soil depths - why are the authors assuming an exponential decrease of K_s instead of evaluating it from textures at different depths?

We thank the reviewer for pointing out this non-stated information. SoilGrids is available at 7 different depths: 0cm, 5cm, 15cm, 30cm, 60cm, 100cm and 200cm. The SoilGrids map used in this study is the one at 0cm depth, as processed for the SP-MIP project. The Reynolds soil texture map is available at two different depths: 30cm and 100cm, and the first depth is used in this study. The Zobler map is available at one soil depth of 30cm. We will add this information in the introduction of the revised version of the paper.

Although some soil maps provide soil textures for different horizons, this information cannot be used in ORCHIDEE, as will be explained in the model description, in the revised version of the paper (cf. response to comment C6 Referee #3): *“Soil texture is assumed to be uniform over the soil column in ORCHIDEE, which does not permit to distinguish several soil horizons. However, K_s decreases exponentially with depth, to account for the effects of soil compaction and bioturbation, as introduced by d’Orgeval et al. (2008) following Beven & Kirkby (1979).”* We also underline that the simplifying hypothesis of a uniform texture over the whole soil column is discussed in the concluding section of the submitted manuscript (lines 239-240).

C10: - Lines 67-68: please provide a reference for both the exponential decrease with depth and the exponential distribution horizontally.

The following references will be added: Beven & Kirkby (1979) and d’Orgeval et al. (2008) for the

exponential decrease with depth (cf. C9); Entekhabi & Eagleson (1989) and Vereecken et al., (2019) for the horizontal distribution.

C11: - Line 70: please provide references for the evapotranspiration model.

The following references will be added: Krinner et al. (2005) for the modelling of evapotranspiration based on four sub-fluxes (L70-71); d'Orgeval et al. (2008), Campoy et al. (2013) to support the end of the paragraph explaining transpiration and soil evaporation are linked to soil moisture and properties.

C12: - Line 91: what is the error due to selecting only the dominant soil texture? Did the authors investigate the effect of upscaling by using some average (or weighted average) soil properties?

In this study, we did not aim at comparing different upscaling methods; it is out of the scope of this paper. However, in our discussion, we stated some studies which tested different upscaling methods (Samaniego et al., 2010; Montzka et al., 2017).

C13: - Line 113: “network owing to machine learning” – please rephrase.

We thank the reviewer for pointing out this mistake. It is corrected to: “network using machine learning”

Results:

C14: - Lines 133-135: the partitioning of rainfall in infiltration (soil moisture) and runoff differs among soil textures in a way that is well known and studied - I don't see the novelty here. Are the authors simply testing the model?

Yes, the first part of the results in the submitted paper was mostly intended to examine the response of the model to the different soil textures. This provides an additional evaluation of the recent version of ORCHIDEE with physically-based hydrology, which has not been heavily tested, as further explained in C19. However, an important outcome of this analysis is the non-monotonic response of evapotranspiration and total runoff to soil texture, since these two behaviors have not already been underlined, to our knowledge.

C15: - Lines 153-154: “Switching ... variables”. If the maps are similar a priori, why would the authors expect any differences in the global water budget? It would probably be more useful, in my opinion, to focus on those areas where the maps are actually different and discuss the resulting biases in the hydrologic response in those areas.

The sentence following the cited one underlines that points with unchanged texture cover 41.2% of the land surface. It is a lot, but it leaves 58.8% where the soil texture does change from Reynolds to SP-MIP (SoilGrids). That's why the weak sensitivity of the global water budget was not an expected result. Yet, we understand from the reviewers comments that the way we introduced the texture map similarities as an *a priori* explanation to the weak sensitivity of the simulated fluxes is misleading, and as suggested in C22, we will devote a new subsection at the beginning of the Results to gather quantified analyses of the similarities/differences between the tested texture maps.

Regarding the strong effect of soil texture in some local areas, it was already discussed in the conclusion of our submitted manuscript, but the suggestion of the reviewer to put a stronger emphasis on this kind of analysis is a good one. As already written (C1, C2, C4), we therefore

propose to add a new subsection 3.4 in the Results to detail the effect of soil texture map change where the maps are different. A detailed description of this new sub-section is presented in C22.

C16: - Lines 170-177: the results discussed here could have been expected without running massive simulations: the partitioning of rainfall in infiltration and runoff with different soil textures is well known. The exercise here seems more of a reality check for the model than some novel analysis.

We agree that the partitioning of rainfall in infiltration and surface runoff with different soil textures is well known, and the global-scale averages discussed in the commented lines are indeed a reality check. We will shorten this discussion in the revised manuscript. The uniform experiments are more useful to analyze the importance of spatial variability of soil texture, as done in the paper based on Fig S2, to conclude that spatial patterns of simulated hydrologic variables are weakly driven by the soil texture, but rather by the climate forcing (L189-190). An important point, however, is that the largest difference in mean global scale ET between these uniform soil maps (between the uniform clay and silt experiments owing to the non-monotonic response underlined in Figs 3 and 4) is 0.1 mm/d, i.e 8% of the global mean ET using the complex soil texture maps and the same climate forcing. This tells us the maximum range of ET change we can expect from any kind of soil texture map change. This point was not stressed in the submitted manuscript, and will be added in the new version of the paper in sub-section 3.3.

C17: - In general, I think the paper lacks a proper quantification of the differences between the soil texture maps and the related bias in simulated fluxes. If the authors could provide a clear quantitative link between the bias in soil maps and the resulting bias in hydrologic partitioning this would actually allow to extrapolate something from the analysis. As it stands, the analysis only seems a modeling exercise without any useful application. I believe it would be more impactful if the paper could provide answers to questions like: how much does the hydrologic response (e.g., runoff, infiltration, etc) change if the soil texture differs by a certain percentage? How do the probability distributions of the water budget components vary with the distributions of soil texture?

The question is sound, but it is not easy to change soil texture by a certain percentage since it is a qualitative factor. We believe that Fig 4 of the submitted manuscript partially answers the reviewer's demand for quantification, in the special case of the switch from the Reynolds soil map to SP-MIP (SoilGrids).

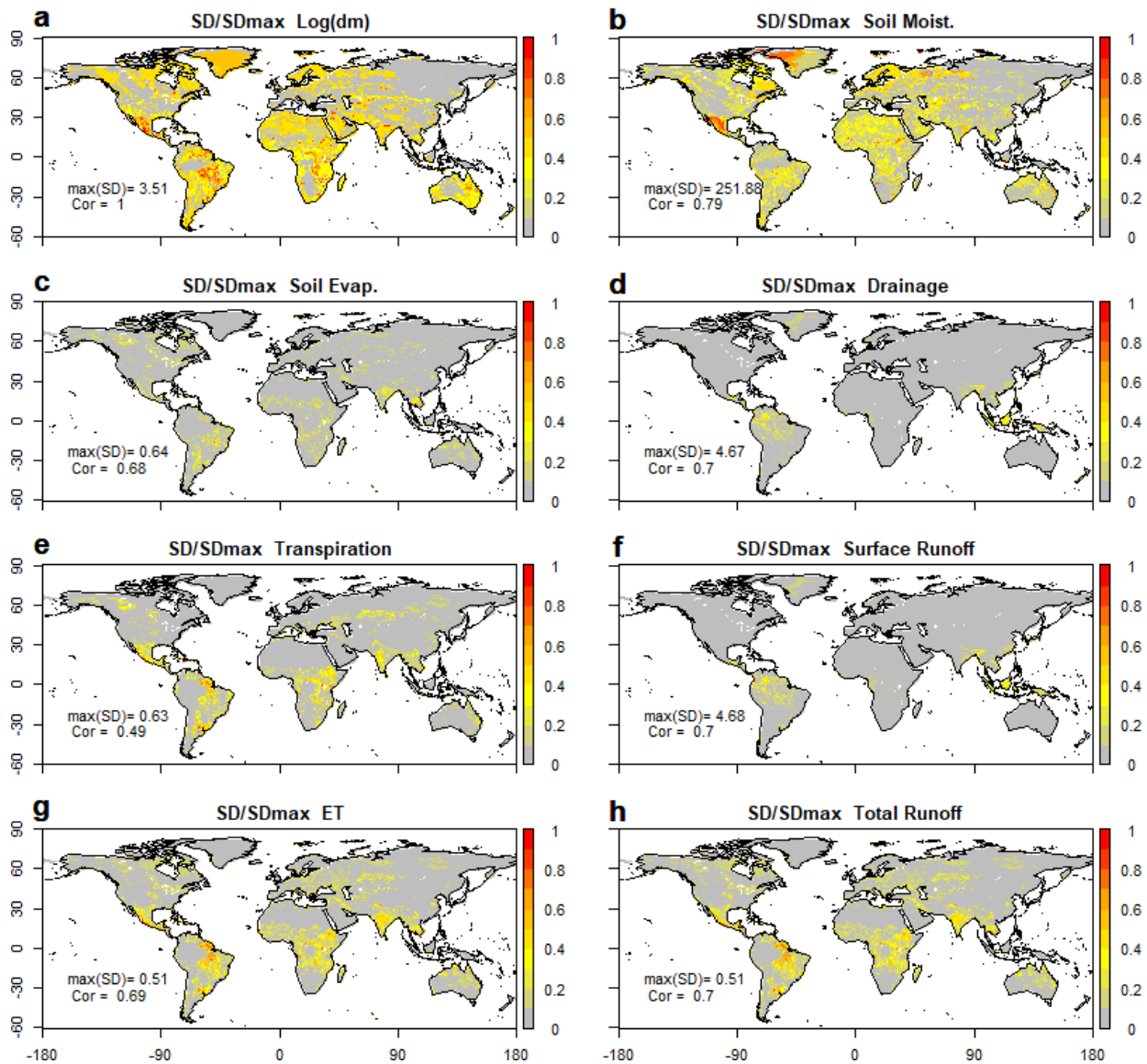


Figure A6 Maps of the standard deviation (SD) of (a) the logarithm of median particle diameter (dm) given by the three complex soil texture maps (Reynolds, Zobler, SP-MIP), and (b-h) the mean annual simulated variables (in mm/d except for soil moisture in mm) using the three different maps. For easier comparison, each SD map is normalized by the maximum standard deviation of the map ($max(SD)$), indicated in each map, with the spatial correlation coefficient (Cor) between the standard deviation of $\log(dm)$ and the standard deviation of each variable.

To go further, we propose to include a new result in section 3.3 “Spatial patterns of simulated fluxes and ET bias”. The goal is to provide a point-scale quantification of the differences between the three complex soil maps on the one hand, and the resulting simulated variables on the other hand. To this end, we mapped the standard deviation of each group of three maps, using the mean diameter (dm) of each texture class to get a quantitative proxy in case of texture (Fig. A6). Although the quantitative meaning of standard deviation can be questioned when calculated from a sample of three values, we used it here as a simple metric of similarity/difference between the three complex maps, and to identify points/regions where the three maps are all consistent (small standard deviation), or where at least one of them is departing (high standard deviation). Compared to the standard deviation of $\log(dm)$, the ones of the simulated fluxes are weak (less than 10 % of the maximum value) over larger fractions of the globe. They are also smaller than the local annual mean values of the variable itself, as shown by comparison to Figure S2 for

evapotranspiration (not shown for the other variables).

Areas which stand out with high standard deviations in all maps are the four regions noted above, where the standard deviation between the three texture maps is very important (Fig. 7a). Aside from these areas, the tropical humid zones (South-East Asia, Indonesia) show rather large standard deviations of surface runoff and drainage (Fig. A6d,f), but without large standard deviation of $\log(dm)$, so this is rather due to the high values of these fluxes in these very humid zones. The overall resemblance between the standard deviation maps of soil texture on the one hand, and the simulated hydrologic variables on the other hand can be quantified at global scale by a spatial correlation coefficient, ranging between 0.49 for transpiration to 0.79 for soil moisture. The latter variable is the most impacted by soil texture change, as supported by this large correlation coefficient, and the large standard deviations on Figure A6b.

C18: - The authors showed that hydrologic fluxes are more sensitive to changes in climatic forcings rather than soil texture maps. But how different are the climatic forcings used compared to soil texture maps? If the bias in the climatic forcing is, a priori, much higher, it is likely that the resulting hydrologic behavior will differ more.

We used two different climate forcings which are both widely used in the LSM community, and expected to be realistic. They both come from climate reanalysis including data assimilation, and are both bias corrected (L80-81). Both were selected for the off-line CMIP6 simulations (van den Hurk et al., 2016), which will be added in the revised version (section 2.2). Thereby, the differences between these two climate datasets are not expected to be higher than ones between the three complex soil maps, also all intended to faithfully capture soil texture patterns. We could have used three state-of-the-art climate forcing datasets, but the resulting spread results would likely have been similar or larger (e.g. Guo et al., 2006; Yin et al., 2018, cited in the paper; Gelati et al., 2018). Thus, we believe it is a valid conclusion that the uncertainty in the climate forcing exceeds the one of the soil texture maps (L189-190).

Conclusions:

C19: - Lines 197-198: the fact that the model has a realistic behavior should not be a main result. The orchidee model has been widely tested, and its ability to reproduce hydrologic fluxes properly in relation to different soil textures is not a novel result.

We agree that the realistic behavior of the model is not the main result, but it serves to support the conclusions regarding the impact of soil texture maps in this model. We would also like to bring the reviewer's attention on the fact that the version of ORCHIDEE used in this study is based on a physical description of water fluxes using Richard's equation, which has not been as widely tested as the first version of ORCHIDEE based on a conceptual description of soil hydrology, especially given the fact that the model is always evolving. Besides, most papers which include an evaluation of the new soil physics from a hydrological perspective (de Rosnay et al., 2002; d'Orgeval et al., 2008; Boone et al., 2009; Campoy et al., 2013; Guimberteau et al., 2014; Barella-Ortiz et al., 2017; Raoult et al., 2018) did not focus on the rightful sensitivity to soil texture.

C20: - Lines 210-212: What is the point of using spatially similar maps to see if they have any discernible effects on the hydrologic fluxes? If, a priori, the maps are similar, what is the point of the entire exercise?

This question is answered earlier in C16.

C21: - Line 214: Did the authors try to test some weighted average SHPs thus accounting for spatial

variability instead of using the dominant soil texture in each cell?

This question is answered earlier in C11.

C22: - Line 225: A detailed analysis of the difference between the various maps should be given upfront. This only appears with Fig. 8 but it would be beneficial to have an in depth analysis of key differences among these maps (as well as of differences resulting from adopting different strategies for upscaling the higher resolution maps) at the beginning of the manuscript.

As suggested by the reviewer, we propose to add, in the revised version, a new sub-section 3.1 in the Results called "*Comparison of the tested soil texture maps*", and dedicated to a quantified analysis of the differences and similarities of the tested texture maps. This sub-section will discuss Figure 8 of the submitted manuscript, which will be updated as follows: Fig. 8a will become Table 3 but remain unchanged (percent overlap between the tested maps), and Fig.8b (to become Table 4; following Table A1 below) will be expanded to show the spatial correlation coefficients between the maps of not only dm , but also of other important hydraulic parameters deduced from the soil texture maps: K_s (as provided by the PTF, thus not including the impact of roots nor soil compaction), soil porosity θ_s , field capacity θ_{fc} , wilting point θ_w , and available water content (AWC, integrated over the the 2m soil column).

Table A1 Statistical descriptors of the soil parameter maps corresponding to the three complex soil texture maps (excluding Antarctica Greenland): mean and standard deviation (SD) of each parameter map; and correlation coefficients between the three pair of maps.

		SP-MIP (SoilGrids)	Reynolds	Zobler
log(<i>dm</i>)	Mean (log μm)	4.48	4.23	4.25
	SD (log μm)	1.51	1.65	1.15
	Cor. SP-MIP	1.00	0.38	0.35
	Cor. Reynolds	0.38	1.00	0.57
K_s	Mean (mm/d)	740	643	428
	SD (mm/d)	1539	1261	376
	Cor. SP-MIP	1.00	0.38	0.36
	Cor. Reynolds	0.38	1.00	0.57
Saturated water content	Mean (m^3/m^3)	0.414	0.416	0.422
	SD (m^3/m^3)	0.017	0.018	0.010
	Cor. SP-MIP	1.00	0.40	0.22
	Cor. Reynolds	0.40	1.0	0.35
Field capacity	Mean (m^3/m^3)	0.177	0.182	0.170
	SD (m^3/m^3)	0.064	0.069	0.046
	Cor. SP-MIP	1.00	0.41	0.36
	Cor. Reynolds	0.41	1.00	0.58
Wilting point	Mean (m^3/m^3)	0.104	0.107	0.092
	SD (m^3/m^3)	0.044	0.054	0.026
	Cor. SP-MIP	1.00	0.42	0.36
	Cor. Reynolds	0.42	1.00	0.58
AWC	Mean (mm)	146.7	150.2	156.5
	SD (mm)	56.9	54.4	39.8
	Cor. SP-MIP	1.00	0.34	0.31
	Cor. Reynolds	0.34	1.00	0.42

This table shows that, whichever the soil parameter, the difference of spatial mean between the three maps is smaller than the difference of spatial standard deviation (SD), even for the least variable map (Zobler). This demonstrates the large similarity of the three complex soil maps tested in our paper, not only regarding soil texture itself (as summarized by *dm*), but also, very logically, for the derived soil hydraulic parameters. This similarity is also confirmed by the spatial correlations between each pair of maps, always positive, the best correlations being found between Zobler and Reynolds for most parameters (always larger than 0.35, and up to 0.58), and the weakest between SP-MIP and Reynolds. Among the different soil parameters, the AWC shows the lowest spatial correlations, which probably comes from the fact that the maximum AWCs are found for medium textures (Fig. S1), which are the dominant textures in all the three maps (Table

1). The above-mentioned results as well as Table A1 will be added in the new section 3.1 of the revised manuscript.

C23: - The clay bias that is only briefly discussed in lines 225-230 seems actually a quite interesting point.

We agree that clay related features were only briefly discussed in the submitted manuscript. In the revised version, we will add a sub-section where we zoom on those areas where clay has a non-negligible impact (details in C4).

C24: If the prevalence of loamy texture in the texture maps is – in part – an artifact due to upscaling procedures and averaging, what would the bias be in the hydrologic partitioning if the actual texture in some grid cell was not as loamy as assumed?

Based on Figures 3 and 4 of the submitted manuscript, we have shown that ET and total runoff show a non-monotonic behavior with respect to soil texture classes (sorted by increasing median diameter); the latter result is a major finding of our manuscript, as highlighted in the abstract. Since the loamy textures correspond to a lower total runoff and higher ET, an overestimation of the loamy textures in a soil texture map would lead to a systematic positive bias in ET and negative bias in total runoff.

C25: - Lines 239-240: Some products (e.g., SoilGrids) have vertically variable information on soil texture – why didn't the authors use this information to relax the hypothesis of vertically homogeneous texture?

We answered this question in C9.

C26: - Lines 236 – 244: most of the paper focused on soil texture, while only two PTFs were tested. Why is the conclusive paragraph of the manuscript on PTFs and inclusion of additional factors in currently used PTFs, while the manuscript only slightly touched this point? Although this is an interesting topic, I wouldn't embark into a discussion on PTFs at this point of the manuscript (as the authors didn't actually do an in depth analysis of the bias induced by different PTFs).

It is true that we only considered two different PTFs in our simulations (EXP4 in and EXP5). The reason is technical, because of the SP-MIP protocol, but we did not focus our analysis on the resulting changes, which will be explored within the SP-MIP project. In this framework, our main conclusions address the impact of the soil texture maps on the simulated land hydrology, and the goal of the last paragraph of the paper is to open the discussion to the impact of other soil properties, such as bulk density and soil structure. Thus, using other sources of information than soil texture to derive the geographic distribution of soil properties may lead to clearer and broader improvements of the simulated water budget than the ones analyzed here owing to soil texture maps alone. We propose to replace the last sentence of the paper by the above one.

References:

- Barella-Ortiz, A., Polcher, J., Rosnay, P. de, Piles, M. and Gelati, E.: Comparison of measured brightness temperatures from SMOS with modelled ones from ORCHIDEE and H-TESEL over the Iberian Peninsula, *Hydrol. Earth Syst. Sci.*, 21(1), 357–375, doi:<https://doi.org/10.5194/hess-21-357-2017>, 2017.
- Beven, K. J. and Kirkby, M. J.: A physically based, variable contributing area model of basin hydrology / Un modèle à base physique de zone d'appel variable de l'hydrologie du bassin versant, *Hydrol. Sci. Bull.*, 24(1), 43–69, doi:10.1080/02626667909491834, 1979.
- Bierkens, M. F. P., Bell, V. A., Burek, P., Chaney, N., Condon, L. E., David, C. H., Roo, A. de, Döll, P., Drost, N., Famiglietti, J. S., Flörke, M., Gochis, D. J., Houser, P., Hut, R., Keune, J., Kollet, S., Maxwell, R. M., Reager, J. T., Samaniego, L., Sudicky, E., Sutanudjaja, E. H., Giesen, N. van de, Winsemius, H. and Wood, E. F.: Hyper-resolution global hydrological modelling: what is next?, *Hydrol. Process.*, 29(2), 310–320, doi:10.1002/hyp.10391, 2015.
- Campoy, A., Ducharne, A., Cheruy, F., Hourdin, F., Polcher, J. and Dupont, J. C.: Response of land surface fluxes and precipitation to different soil bottom hydrological conditions in a general circulation model, *J. Geophys. Res. Atmospheres*, 118(19), 10,725–10,739, doi:10.1002/jgrd.50627, 2013.
- De Lannoy, G. J. M., Koster, R. D., Reichle, R. H., Mahanama, S. P. P. and Liu, Q.: An updated treatment of soil texture and associated hydraulic properties in a global land modeling system, *J. Adv. Model. Earth Syst.*, 6(4), 957–979, doi:10.1002/2014MS000330, 2014.
- D'Orgeval, T., Polcher, J. and Rosnay, P. de: Sensitivity of the West African hydrological cycle in ORCHIDEE to infiltration processes, *Hydrol. Earth Syst. Sci.*, 12(6), 1387–1401, doi:<https://doi.org/10.5194/hess-12-1387-2008>, 2008.
- Ducharne, A., Ghattas, J., Maignan, F., Ottlé, C., Vuichard, N., Guimberteau, M., Krinner, G., Polcher, J., Tafasca, S., Bastrikov, V., Brender, P., Cheruy, F., Guénet, B., Mizuochi, H., Peylin, P., Tootchi, A. and Wang, F.: Soil water processes in the ORCHIDEE-2.0 land surface model: state of the art for CMIP6, *Geosci. Model Dev.*, in prep.
- Entekhabi, D. and Eagleson, P. S.: Land Surface Hydrology Parameterization for Atmospheric General Circulation models Including Subgrid Scale Spatial Variability, *J. Clim.*, 2(8), 816–831, doi:10.1175/1520-0442(1989)002<0816:LSHPFA>2.0.CO;2, 1989.
- Gelati, E., Decharme, B., Calvet, J.-C., Minvielle, M., Polcher, J., Fairbairn, D. and Weedon, G. P.: Hydrological assessment of atmospheric forcing uncertainty in the Euro-Mediterranean area using a land surface model, *Hydrol. Earth Syst. Sci.*, 22(4), 2091–2115, doi:10.5194/hess-22-2091-2018, 2018.
- Guo, Z., Dirmeyer, P. A., Hu, Z.-Z., Gao, X. and Zhao, M.: Evaluation of the Second Global Soil Wetness Project soil moisture simulations: 2. Sensitivity to external meteorological forcing, *J. Geophys. Res. Atmospheres*, 111(D22), doi:10.1029/2006JD007845, 2006.

- Hengl, T., Jesus, J. M. de, Heuvelink, G. B. M., Gonzalez, M. R., Kilibarda, M., Blagotić, A., Shangquan, W., Wright, M. N., Geng, X., Bauer-Marschallinger, B., Guevara, M. A., Vargas, R., MacMillan, R. A., Batjes, N. H., Leenaars, J. G. B., Ribeiro, E., Wheeler, I., Mantel, S. and Kempen, B.: SoilGrids250m: Global gridded soil information based on machine learning, *PLOS ONE*, 12(2), e0169748, doi:10.1371/journal.pone.0169748, 2017.
- Kirkby, M. J. and Beven, K. J.: A physically based, variable contributing area model of basin hydrology, *Hydrol. Sci. J.*, 24, 43–69, 1979.
- Krinner, G., Viovy, N., Noblet-Ducoudré, N. de, Ogée, J., Polcher, J., Friedlingstein, P., Ciais, P., Sitch, S. and Prentice, I. C.: A dynamic global vegetation model for studies of the coupled atmosphere-biosphere system, *Glob. Biogeochem. Cycles*, 19(1), doi:10.1029/2003GB002199, 2005.
- Montzka, C., Herbst, M., Weihermüller, L., Verhoef, A. and Vereecken, H.: A global data set of soil hydraulic properties and sub-grid variability of soil water retention and hydraulic conductivity curves, *Earth Syst. Sci. Data*, 9(2), 529–543, doi:https://doi.org/10.5194/essd-9-529-2017, 2017.
- Raoult, N., Delorme, B., Ottlé, C., Peylin, P., Bastrikov, V., Maugis, P. and Polcher, J.: Confronting Soil Moisture Dynamics from the ORCHIDEE Land Surface Model With the ESA-CCI Product: Perspectives for Data Assimilation, *Remote Sens.*, 10(11), 1786, doi:10.3390/rs10111786, 2018.
- Samaniego, L., Kumar, R. and Attinger, S.: Multiscale parameter regionalization of a grid-based hydrologic model at the mesoscale, *Water Resour. Res.*, 46(5), doi:10.1029/2008WR007327, 2010.
- Van den Hurk, B., Kim, H., Krinner, G., Seneviratne, S. I., Derksen, C., Oki, T., Douville, H., Colin, J., Ducharne, A., Cheruy, F., Viovy, N., Puma, M. J., Wada, Y., Li, W., Jia, B., Alessandri, A., Lawrence, D. M., Weedon, G. P., Ellis, R., Hagemann, S., Mao, J., Flanner, M. G., Zampieri, M., Materia, S., Law, R. M. and Sheffield, J.: LS3MIP (v1.0) contribution to CMIP6: the Land Surface, Snow and Soil moisture Model Intercomparison Project – aims, setup and expected outcome, *Geosci Model Dev*, 9(8), 2809–2832, doi:10.5194/gmd-9-2809-2016, 2016.
- Vereecken, H., Weihermüller, L., Assouline, S., Šimůnek, J., Verhoef, A., Herbst, M., Archer, N., Mohanty, B., Montzka, C., Vanderborght, J., Balsamo, G., Bechtold, M., Boone, A., Chadburn, S., Cuntz, M., Decharme, B., Ducharne, A., Ek, M., Garrigues, S., Goergen, K., Ingwersen, J., Kollet, S., Lawrence, D. M., Li, Q., Or, D., Swenson, S., de Vrese, P., Walko, R., Wu, Y. and Xue, Y.: Infiltration from the Pedon to Global Grid Scales: An Overview and Outlook for Land Surface Modeling, *Vadose Zone J.*, 18(1), doi:10.2136/vzj2018.10.0191, 2019.
- Wood, E. F., Roundy, J. K., Troy, T. J., Beek, L. P. H. van, Bierkens, M. F. P., Blyth, E., Roo, A. de, Döll, P., Ek, M., Famiglietti, J., Gochis, D., Giesen, N. van de, Houser, P., Jaffé, P. R., Kollet, S., Lehner, B., Lettenmaier, D. P., Peters-Lidard, C., Sivapalan, M., Sheffield, J., Wade, A. and Whitehead, P.: Hyperresolution global land surface modeling: Meeting a grand challenge for monitoring Earth's terrestrial water, *Water Resour. Res.*, 47(5), doi:10.1029/2010WR010090, 2011.
- Yin, Z., Otle, C., Ciais, P., Guimberteau, M., Wang, X., Zhu, D., Maignan, F., Peng, S., Piao, S., Polcher, J., Zhou, F. and Kim, H.: Evaluation of ORCHIDEE-MICT-simulated soil moisture over China and impacts of different atmospheric forcing data, *Hydrol. Earth Syst. Sci.*, 22(10), 5463–5484, doi:10.5194/hess-22-5463-2018, 2018.

Weak sensitivity of the terrestrial water budget to global soil texture maps in the ORCHIDEE land surface model

Salma TAFASCA¹, Agnès DUCHARNE¹, Christian VALENTIN²

Reply to anonymous Referee #2

Overall Comment

This study investigates how a land surface model behaves against different global sets of soil parameters in terms of the terrestrial water balance. The experiment configurations follow the protocol of an ongoing international project, Soil Parameter Model Intercomparison Project. It concludes that the choice of the soil texture map is not crucial for large-scale modeling. The manuscript is well-written in a concise form, and their findings are important to our community. I encourage the HESS journal to host this study, but the current version of the manuscript would not be at level to be accepted because of some hasty explanations and not enough interpretation and discussion.

We would like to thank the reviewer for taking the time to go through the paper, and for the relevant comments. According to all the three reviews that we received, we decided to make some substantial changes to the paper, in particular, the scientific question of the paper will be more clarified and new sub-sections will be added. A detailed presentation of the new structure of the paper is presented in the answer to Referee #1. In the following, we will provide a response to every point raised by Referee #2.

Specific Comments

13 : “medium texture” is not a clear term here.

Medium textures are the loamy textures, with medium dm (median diameter). To clarify this in the abstract, we will use the term loamy texture, which is clearer

16 : Please provide reason or speculation why it “is not crucial”. If not, it could mislead readers to consider soil parameters are not important, which is not true.

The referred sentence relates to the soil texture maps and the not to the soil parameters. The specific reason is given by the previous sentence: “The three tested complex soil texture maps [...] result in similar water budgets at all scales, compared to the uncertainties of observation-based products and meteorological forcing datasets”. But this conclusion will be refined by underlining the areas where the choice of the soil texture map makes a significant difference, as detailed in a new subsection 3.4 “Regional zooms on greatly impacted areas”, following the suggestion by Referee #1.

81 : Please add data citation for GSWP3-v1 H. Kim. (2017). Global Soil Wetness Project Phase 3 Atmospheric Boundary Conditions (Experiment 1) [Data set]. Data Integration and Analysis System (DIAS). <https://doi.org/10.20783/DIAS.501>

We will add this reference to the description of GSWP3-v1.

93 : Rather “coarse and fine” than “medium and extreme”?

Lines 92 and 93 will be changed to: “In addition, we tested four spatially uniform texture maps, corresponding to the Loam, Loamy Sand, Silt, and Clay texture classes (EXP6 to EXP9), to analyze the importance of spatial variability of soil texture on the global water budget.”

133 : Please add the definition of “soil-moisture” which is sampled from each soil texture class which has a similar range of precipitation. Also, specify the sampling depth; top-soil, rootzone, full-column or any specific depth?

The simulated soil moisture corresponds here to the whole soil column (2m depth), as will be specified in the revised manuscript. As for the clustering by soil texture and normalization by mean precipitation, the latter is only used for the fluxes (see line 125), and not for soil moisture. We will add that this normalization is performed at point scale, using the pluri-annual mean of precipitation.

142 – 145 : Please provide additional information how the model treats the root uptake and root-zone soil-moisture. Also, speculations on the role of groundwater capillary action would be a very important aspect, too.

In ORCHIDEE, a root uptake function (describing the water extraction ability of roots) is used to calculate transpiration; it is a function of both the soil moisture profile and root density profile. The latter one follows an exponential decrease with depth at a rate depending on the plant functional type. We will add this in the model description, in section 2.1 of the new version of the paper.

Regarding capillary rise, the standard version of ORCHIDEE used here considers free drainage at the soil bottom, which corresponds to the assumption of uniform soil moisture profile below the soil bottom, i.e. groundwater does not impact soil moisture through capillary rise. This will also be added in the model description section.

149 : How does leaf area index affect soil evaporation; interception loss, radiative transfer in canopy? Citing previous research would be helpful to show soil evaporation “strongly depends on other factors”.

In ORCHIDEE, LAI has an important influence on the partition between soil evaporation and transpiration, via the fraction that is effectively covered by foliage, which increases exponentially with LAI with a coefficient of 0.5, also controlling light extinction through the canopy (Krinner et al. 2005). This fraction contributes to transpiration and interception loss, while the complementary fraction is assumed to be bare of vegetation, and only contributes to soil evaporation. This explanation will be added to the description of the ORCHIDEE LSM (section 2.1), thus complying with a request by Referee #3.

To support the sentence of lines 148-149, we will also add the following references: Martens et al. (2017) and Wang et al (2018) regarding the anti-correlation between LAI and soil evaporation (further supported by the spatial correlation of -0.32 between these two variables in our simulation EXP2); the negative impact of vegetation on soil evaporation can also develop owing to the litter, which exerts a resistance to this flux (Ogée & Brunet, 2002; Sakaguchi & Zeng, 2009). However, the dependence of soil evaporation on climatic variables (temperature, potential ET) and soil moisture will not be expanded, as it is very well established.

158 – 163 : Only a part of Figure 4 has been touched. I suggest the authors to add in-depth interpretation of this figure. For example, the change of evaporation could be compared with of soil-moisture – (transpiration + total runoff). It is not recommended, but to discard this paragraph and Fig. 4 would be another option.

We agree with Referee #2 that Figure 4 was too briefly discussed. This figure is intended to show how the simulated variables change when only soil texture changes, to better analyze the model's response to the different soil textures. We propose to expand the last paragraph of section 3.1 addressing this Figure:

“By focusing this time on the point-scale changes induced by changing the soil texture map (from Reynolds to SoilGrids), Figure 4 highlights that the simulated soil evaporation decreases from fine to coarse textures, so that capillary retention, which is the main limiting factor to soil evaporation in ORCHIDEE, depends more strongly on soil moisture (higher for fine soils) than on intrinsic capillary forces (stronger for fine soils). We fail to see this behavior in Figure 3, which is likely due to the greater impact of diverse climatic conditions and vegetation associated with every soil texture. Figure 4 also confirms the results of Figure 3 for the other variables, including the decrease of soil moisture with coarser soils and the greater impact of soil texture on runoff variables (surface runoff and drainage). In particular, we find that replacing fine textures with coarse textures (above the first diagonal of the matrices) results in higher drainage (due to the higher permeability of coarse-textured soils) and lower surface runoff, with changes that can exceed 1mm/d in absolute value for some textural changes (all involving medium texture classes). As a result, less water is available in the soil, which leads to less soil evaporation, further leading to more transpiration (Fig. 4bc).

The convex behavior of total runoff with soil texture can also be seen in Figure 4h, which is antisymmetric along the two diagonals, thus defining four different kinds of total runoff change to soil texture change. This behavior results from the fact that total runoff sums up two variables of opposite response to soil texture change (surface runoff and drainage), the net response depending on the dominant component. Hence, changes to medium textures from either coarse or fine textures (left and right red triangles in Fig. 4h) lead to reduced total runoff, owing to reduced surface runoff in the first case, and reduced drainage in the second. In contrast, changes from medium texture to either coarse or fine textures lead to increased runoff (bottom and top blue triangles in Fig. 4h), owing to increased surface runoff or drainage, respectively. This pattern thus means that the medium textures correspond to the smallest total runoff. By means of long-term water conservation, the opposite patterns are found for total evapotranspiration changes (Figure 4d), because of the opposite responses of soil evaporation and transpiration to soil texture, and supporting the concave response of this flux to soil texture found in Figure 3.”

175 : “coarse or clay” would be “coarse or fine” or “loamy sand or clay”.
“coarse or clay” will be replaced by “coarse or fine”.

175 – 177 : To me, evapotranspiration of EXP6 and EXP7 also seem out of the observed range.

It is true that land mean evapotranspiration of EXP6 is out of the observed range, but the one of EXP7 seems acceptable if we accept that the three estimates have an error margin, as shown for the estimates of Rodell et al (2015) for both total ET and total runoff, for which EXP6 and EXP7 fall within the confidence interval. Thus, when confronting the estimates of both mean total ET and total runoff over land, only EXP8 and EXP9 are clearly out of the

observed range. We will make this point clearer in the revised version of the paper.

182 – 183 : Please specify regions.

As explained in the response to Referee #1, the structure of the paper will be changed and a new sub-section dedicated to regional zooms on greatly impacted regions will be added, these regions include: Central America, Middle-East and India, Tropical South America and Central Africa. Lines 182 -183 will be changed accordingly.

185 – 186 : To me, it does not seem to have a larger variability to the other fluxes (e.g., total runoff), particularly.

We agree with the referee, but we are not comparing here the variability of evapotranspiration to the one of other variables. What we try to explain at lines 185-186 is the orange pocket in Fig 6a, with a decrease of ET when changing the soil texture to a uniform Loam, while we have previously shown that the medium textures correspond to the largest ET (cf. Figs 3 and 4, with the concave response of ET to soil texture). This region corresponds to a Clay Loam in SoilGrids (Fig. 1c), which is also found in many other regions (e.g. extensively in South America), without any significant change in ET when changing SoilGrids to the uniform Loam map. The underlying reason is thought to be the large variability of evapotranspiration within the Clay loam and Loam texture classes (Figure 3b), which makes it possible to have a local decrease of ET when changing soil texture from Clay loam to Loam despite the opposite relationship between the central values of these classes in Figure 3. The incriminated sentence will be rephrased based on the previous one, and moved to the new section of the revised version of the paper 3.4, as explained in answer to Referee #1.

209 : Please add “at the global scale”

It will be added in the new version of the paper.

References:

Krinner, G., Viovy, N., Noblet-Ducoudré, N. de, Ogée, J., Polcher, J., Friedlingstein, P., Ciais, P., Sitch, S. and Prentice, I. C.: A dynamic global vegetation model for studies of the coupled atmosphere-biosphere system, *Glob. Biogeochem. Cycles*, 19(1), doi:10.1029/2003GB002199, 2005.

Martens, B., Miralles, D. G., Lievens, H., Schalie, R. van der, Jeu, R. A. M. de, Fernández-Prieto, D., Beck, H. E., Dorigo, W. A. and Verhoest, N. E. C.: GLEAM v3: satellite-based land evaporation and root-zone soil moisture, *Geosci. Model Dev.*, 10(5), 1903–1925, doi:https://doi.org/10.5194/gmd-10-1903-2017, 2017.

Ogée, J. and Brunet, Y.: A forest floor model for heat and moisture including a litter layer, *J. Hydrol.*, 255(1), 212–233, doi:10.1016/S0022-1694(01)00515-7, 2002.

Rodell, M., Beaudoing, H. K., L'Ecuyer, T. S., Olson, W. S., Famiglietti, J. S., Houser, P. R., Adler, R., Bosilovich, M. G., Clayson, C. A., Chambers, D., Clark, E., Fetzer, E. J., Gao, X., Gu, G., Hilburn, K., Huffman, G. J., Lettenmaier, D. P., Liu, W. T., Robertson, F. R., Schlosser, C. A., Sheffield, J. and Wood, E. F.: The Observed State of the Water Cycle in the Early Twenty-First Century, *J. Clim.*, 28(21), 8289–8318, doi:10.1175/JCLI-D-14-00555.1, 2015.

Sakaguchi, K. and Zeng, X.: Effects of soil wetness, plant litter, and under-canopy atmospheric stability on ground evaporation in the Community Land Model (CLM3.5), *J. Geophys. Res. Atmospheres*, 114(D1), doi:10.1029/2008JD010834, 2009.

Wang, F., Ducharne, A., Cheruy, F., Lo, M.-H. and Grandpeix, J.-Y.: Impact of a shallow groundwater table on the global water cycle in the IPSL land–atmosphere coupled model, *Clim. Dyn.*, 50(9), 3505–3522, doi:10.1007/s00382-017-3820-9, 2018.

Weak sensitivity of the terrestrial water budget to global soil texture maps in the ORCHIDEE land surface model

Salma TAFASCA¹, Agnès DUCHARNE¹, Christian VALENTIN²

Correspondence to: Salma Tafasca (salma.tafasca@upmc.fr)

Reply to anonymous Referee #3

General

C1: This paper explores the impact of soil texture on the simulated water budget by the ORCHIDEE LSM at the global scale at 0.5 degree resolution. The authors conclude that the use of three different soil texture maps result in very similar terrestrial water budgets, and that the choice of the input soil texture map is not crucial for large scale modelling. While the study topic is very relevant and deserves publication, the manuscript needs to be revised.

We would like to thank the reviewer for taking the time to go through the paper, and for the relevant comments. According to all the three reviews that we received, we decided to make some substantial changes to the paper, in particular, the scientific question of the paper will be more clarified and new sub-sections will be added. A detailed presentation of the new structure of the paper is presented in the answer to Referee #1. In the following, we will provide a response to every point raised by Referee #3, these points are numbered from C1 to C21 for convenience.

C2: First, I think the authors should make in the Introduction their research question(s) clearer, in my opinion lines 52-53 are not sufficient, and it is also not quite clear why this research is different from earlier studies.

This comment was already raised by Referee #1, and we agree that the scientific question of the paper was too briefly stated in the introduction of the submitted paper. In the revised version of our paper, this will be clarified by expanding the last line of the introduction to a more classical paragraph detailing the specific research question of the paper and the structure of the paper: *“Here, we aim at exploring more systematically the impact of soil texture on the water budget from point to global scale, using a state-of-the-art LSM with physically-based soil hydrology, and multiple input soil texture maps. After presenting the model and soil texture maps used in this work, the results are presented as follows. We first provide an analysis of the similarities and differences between the different soil maps, then, we evaluate the point-scale response of the model to different soil textures to make sure it displays a reliable behavior. This point-scale response is then analyzed from a geographic point of view, with a comparison to a distributed observation-based ET product, and a focus is made on areas with a large sensitivity to the soil texture maps. We finally explore how the magnitude and significance of the simulated ET changes with the scale of analysis up to the land scale, defining the terrestrial water budget. The closing section summarizes the main conclusions of the study, and discusses its limitations and perspectives.”*

C3: The authors mention the use a physically based soil hydrological modelling component (including Richards equation) in these lines (line 53), but do not follow up in the Discussion and conclusions section.

This is a good point, and we propose to add the following sentences in the closing section, at the end of L210, after discussing the SP-MIP project: *“As mentioned in Introduction, much stronger responses to soil properties have been reported from bucket-type LSMs. It must be underlined, however, that these papers considered much larger changes of soil properties, which reduces in bucket-type models to available water holding capacity (AWC), combining information on porosity, soil depth, and the difference between field capacity and wilting point. As an example, the main changes discussed in Stamm et al. (1994), Ducharne & Laval (2000), de Rosnay & Polcher (1998), and Milly & Dunne (1994), correspond respectively to AWC changes of +75%, +110%, +200%, and +1400%, while the AWC changes when switching among the three soil texture maps used in the present paper range between +1 and +7%.”* These percentages will be supported by citing the updated Figure 8, to be moved to the new section 3.1, cf response to comment C22 Referee#1.

C4: Furthermore, I believe the manuscript could benefit from a more detailed analysis and description on the differences between hydrological variables from different soil texture inputs (and PTFs), also focused on a regional/local scale.

We agree with the reviewer, and as detailed in the answer to Referee #1, we will add a dedicated sub-section in the results (3.4) where we look into the impacts of soil texture in the most impacted regions.

C5: Finally, I am wondering why the authors did choose to scale up the high resolution soil texture dataset to the model resolution as a function of the dominant USDA soil texture class. Why not, when applicable, calculate the soil hydraulic parameters at high resolution, and then scale up (with appropriate scaling operators (for example in the line with Samaniego et al., 2010))?

By default, ORCHIDEE upscales the input soil texture map to the model resolution (0.5°) by selecting the dominant USDA soil texture. This choice is hard-coded, and it is not in the purpose of our study to test different upscaling methods. However, we would like to point out that only the Reynolds map was upscaled by the model; the Zobler soil map is available at 1° resolution, so no upscaling was performed for this map, and the used SoilGrids map was provided by the SP-MIP team at the 0.5° resolution.

Specific comments

C6: A detailed description of the ORCHIDEE LSM would be helpful.

Based on this comment, and the ones from Referee #2 regarding root uptake and the effect of LAI on evapotranspiration, we will expand the description of ORCHIDEE in section 2.1. To this end, lines 61-74 will be changed to the following text (changes in bold):

*“The physically-based soil hydrology scheme solves the vertical soil moisture redistribution based on a multi-layer solution of saturation-based Richards equation, using a 2-m soil discretized into 11 soil layers **of increasing thickness with depth** (de Rosnay et al., 2002). **Infiltration is processed before soil moisture redistribution, owing to a time-splitting procedure inspired by the model of Green and Ampt (1911), with a sharp wetting front***

propagating like a piston (d'Orgeval et al., 2008; Vereecken et al., 2019). The unsaturated values of hydraulic conductivity and diffusivity are given by the model of Mualem (1976) - Van Genuchten (1980).

In each grid cell, the corresponding parameters (saturated hydraulic conductivity K_s , inverse of air entry suction α , shape parameter m , porosity, and residual moisture) are taken from Carsel and Parrish (1988), as a function of the dominant USDA soil texture class, itself derived from an input soil texture map. **The tabulated values of the different soil parameters are given for each USDA class in Figure S1. Soil texture is assumed to be uniform over the soil column in ORCHIDEE, which does not permit to distinguish several soil horizons. However, K_s decreases exponentially with depth, to account for the effects of soil compaction and bioturbation, as introduced by d'Orgeval et al. (2008) following Beven & Kirkby (1979). It must also be noted that the horizontal variations of K_s are taken into account by an exponential probability distribution, but only for calculating infiltration and surface runoff (Entekhabi & Eagleson, 1989; Vereecken et al., 2019). The soil texture also influences heat capacity and conductivity, and heat diffusion is calculated with the same vertical discretization as water diffusion in the top 2m, but extended to 10 m (Wang et al., 2016).**

Evapotranspiration is described by a classical bulk aerodynamic approach, distinguishing four sub-fluxes: sublimation, interception loss, soil evaporation, and transpiration (Krinner et al., 2005). The latter two are **directly coupled to soil water redistribution, and depend on soil moisture and soil properties**, which control how the corresponding rates are reduced compared to the potential rate: transpiration is limited by a stomatal resistance, increasing when soil moisture drops from field capacity to wilting point (which both depend on soil texture as detailed in Supplementary S1); soil evaporation is not limited by a resistance, but only by upward capillary fluxes, which control the soil propensity to meet the evaporation demand (d'Orgeval et al., 2008; Campoy et al., 2013). **Evapotranspiration also depends on the vegetation of each grid-cell, described here as a mosaic of up to 15 Plant Functional Types (PFTs), based on the global land cover map used in the IPSL simulations for CMIP6 (Boucher et al., 2019). In each PFT, root density is assumed to decrease exponentially with depth, with a PFT-dependent decay factor. The resulting root density profile is combined to the soil moisture profile and a water stress function depending of field capacity and wilting point to define the integrated water stress factor of each PFT to transpiration.**

This flux is also coupled to photosynthesis, which depends on soil moisture, light availability, CO₂ concentration, and air temperature, following Farquhar et al. (1980) and Collatz et al. (1992) for C₃ and C₄ plants, respectively. The resulting carbon assimilation is allocated to several vegetation pools, including leaf mass thus leaf area index (LAI), owing to a dynamic phenology module called STOMATE (Krinner et al., 2005). It must be underlined that LAI has an important influence on the partition between soil evaporation and transpiration, via the fraction that is effectively covered by foliage, which increases exponentially with LAI with a coefficient of 0.5, also controlling light extinction through the canopy (Krinner et al. 2005). This fraction contributes to transpiration and interception loss, while the complementary fraction is assumed to be bare of vegetation, and only contributes to soil evaporation."

C7: Line 13: explain "medium texture", I think not every reader knows what medium means Medium textures are the loamy textures, with medium dm (median diameter). To clarify this

in the abstract, we will use the term loamy texture, which is clearer.

C8: Line 13-14: “The three tested complex soil texture maps being rather similar by construction...”. Do the authors mean that the soil texture maps are similar because of the way how they were constructed (taking the dominant USDA soil texture class)?

The soil texture maps are similar because of the way they are upscaled but also, and more importantly, because of their common origins (FAO/UNESCO soil map). Based on Referee #1 comments, we think that these lines are misleading, since they suggest that the similarity between the soil texture maps is *a priori* knowledge of this study, while it is a result. These lines will be replaced by a new sub-section, inserted in the beginning of the Results, and gathering quantified analyses of the similarities/differences between the tested texture maps (cf. answer to Referee #1).

C9: As mentioned in the General comments, why not calculate soil hydraulic parameters at the high resolution scale?

As mentioned earlier, testing different upscaling methods is out of the scope of this paper.

C10: Indeed the soil texture maps are quite similar. Why then not focus more on sensitivity of PTFs (now two are used in this study)?

The sensitivity to various PTFs has been the scope of many studies, as recently reviewed by van Looy et al. (2017). In contrast, the main objective of our study is to examine the hydrological response to different soil texture maps. We consider two different PTFs in our simulations (EXP4 and EXP5) because of the SP-MIP protocol, but we don't focus our analysis on the resulting changes, which will be explored within the SP-MIP project, and are very weak based on land averages, but for soil moisture, noted by the Referee in comment C15.

C11: Line 35: 1-km SoilGrids database. A 250 m version is also available. Were the different soil layers also included in the analysis? And if yes, how? Also for example to calculate the exponential decline of K_s ?

We will mention the availability of the 250m version of SoilGrids (Hengl et al., 2017) at line 35. As said in the paper, the SoilGrids map used in this study was processed at 0.5° for the SP-MIP project, and we will add it is based on the texture at 0cm depth (section 2.2). But even if SP-MIP had provided soil textures for different horizons, this information cannot be used in ORCHIDEE, as explained in the description of the model, in the revised version of the paper (cf. response to C6): “Soil texture is assumed to be uniform over the soil column in ORCHIDEE, which does not permit to distinguish several soil horizons. However, K_s decreases exponentially with depth, to account for the effects of soil compaction and bioturbation, as introduced by d’Orgeval et al. (2008) following Beven & Kirkby (1979).” We also underline that the simplifying hypothesis of a uniform texture over the whole soil column is discussed in the concluding section of the submitted manuscript (lines 239-240).

C12: Lines 144-145: “Rather surprisingly, we find here...”, Could you explain this in more detail? If drainage and transpiration decrease you would expect higher soil moisture values, right? The transpiration decrease is perhaps controlled by dominant vegetation type?

We agree with the reviewer, and will thus remove “Rather surprisingly”. As for the transpiration decrease for fine-textured soils, it is not controlled by dominant vegetation types, as supported by Figure 4c where each pixel of the matrix corresponds to a unique set

of grid-points undergoing a soil texture change, thus with unchanged climate and vegetation cover. This implies that the decrease of transpiration found in Figure 3 when soil texture gets finer is effectively due to soil texture. A likely reason is the increase of matric potential, thus soil moisture retention, when the texture gets finer, as shown in Figure S1 for particular values of the potential, defining the wilting point, field capacity and air entry suction point ($1/\alpha$). This analysis leads to a more complex explanation of the response of transpiration to soil texture, and we propose to replace lines 142-147 by the following paragraph:

“Transpiration, however, increases as soil gets coarser (Fig. 3c), with two explanations probably acting together. Firstly, the increase of matric potential when the texture gets finer, as shown in Figure S1 for particular values of the potential, defining the wilting point, field capacity and air entry suction point ($1/\alpha$), makes root uptake thus transpiration more difficult for a given soil moisture if the soil texture is finer. Secondly, the high conductivity of coarse soils enhances water infiltration at the soil surface, quickly available for plant uptake. The increase of K_s for coarse textures also explains the associated drainage increase when its dependence on mean precipitation is filtered (Fig. 3f). The fact that soil moisture decreases when drainage and transpiration get higher indicates that annual mean soil moisture is the result more than the cause of these fluxes”.

C13: Lines 148-149: Could you elaborate more (also include references)? These factors should also affect evapotranspiration...

To support this sentence, focused on the response of soil evaporation, we propose to add the following references: Martens et al. (2017) and Wang et al (2018) regarding the anti-correlation between LAI and soil evaporation (further supported by the spatial correlation of -0.32 between these two variables in our simulation EXP2); the negative impact of vegetation on soil evaporation can also develop owing to the litter, which exerts a resistance to this flux (Ogée & Brunet, 2002; Sakaguchi & Zeng, 2009). However, the dependence of soil evaporation on climatic variable (temperature, potential ET) and soil moisture will not be expanded, as it is very well established. Then, the referee is right that this dispersion transfers to evapotranspiration (Figure 3d), but to a weaker extent since soil evaporation is not the main component of total ET.

C14: Line 158: Please describe Figure 4 in more detail.

We agree with Referee #3 (and Referee #2) that Figure 4 was too briefly discussed. This figure is intended to show how the simulated variables change when only soil texture changes, to better analyze the model's response to the different soil textures. We propose to expand the last paragraph of section 3.1 addressing this Figure:

“By focusing this time on the point-scale changes induced by changing the soil texture map (from Reynolds to SoilGrids), Figure 4 highlights that the simulated soil evaporation decreases from fine to coarse textures, so that capillary retention, which is the main limiting factor to soil evaporation in ORCHIDEE, depends more strongly on soil moisture (higher for fine soils) than on intrinsic capillary forces (stronger for fine soils). We fail to see this behavior in Figure 3, which is likely due to the greater impact of diverse climatic conditions and vegetation associated with every soil texture. Figure 4 also confirms the results of Figure 3 for the other variables, including the decrease of soil moisture with coarser soils and the greater impact of soil texture on runoff variables (surface runoff and drainage). In particular, we find that replacing fine textures with coarse textures (above the first diagonal of the matrices) results in higher drainage (due to the higher permeability of coarse-textured soils) and lower

surface runoff, with changes that can exceed 1mm/d in absolute value for some textural changes (all involving medium texture classes). As a result, less water is available in the soil, which leads to less soil evaporation, further leading to more transpiration (Fig. 4bc).

The convex behavior of total runoff with soil texture can also be seen in Figure 4h, which is antisymmetric along the two diagonals, thus defining four different kinds of total runoff change to soil texture change. This behavior results from the fact that total runoff sums up two variables of opposite response to soil texture change (surface runoff and drainage), the net response depending on the dominant component. Hence, changes to medium textures from either coarse or fine textures (left and right red triangles in Fig. 4h) lead to reduced total runoff, owing to reduced surface runoff in the first case, and reduced drainage in the second. In contrast, changes from medium texture to either coarse or fine textures lead to increased runoff (bottom and top blue triangles in Fig. 4h), owing to increased surface runoff or drainage, respectively. This pattern thus means that the medium textures correspond the smallest total runoff. By means of long-term water conservation, the opposite patterns are found for total evapotranspiration changes (Figure 4d), because of the opposite responses of soil evaporation and transpiration to soil texture, and supporting the concave response of this flux to soil texture found in Figure 3."

C15: Figure 5: EXP5 seems to show a large difference in soil moisture with EXP4. In my opinion an interesting result, but not mentioned in the text and explained.

While both EXP4 and EXP5 use the same soil texture map, the PTF used in each experiment is different. Moreover, in EXP5 (as well as EXP6-EXP9), K_s is constant with depth, unlike the experiments EXP1-EXP4. We will add this clarification when describing the different simulations (section 2.2, L 1109): *"It must be noted that the five simulations based on the soil parameters of Schaap et al. (2001) also differ from the four others (EXP1 to EXP4) because the decrease of K_s with depth is relaxed, to comply with the SP-MIP protocol."*

As a consequence, the decrease of soil moisture between EXP4 and EXP5 is not only due to PTF change but also the increase of K_s at the bottom of the soil column in EXP5, because K_s does not decrease with depth. This favors drainage, thus reduces soil moisture, and we propose to add this explanation when discussing Fig. 5, at line 172.

C16: Line 187-188 and Figure 7: Ok, indeed transpiration and soil evaporation show weak sensitivity, but other variables like drainage, surface runoff and soil moisture show a stronger sensitivity. For example, when you focus on Scandinavia, drainage decreases, surface runoff increases, and soil moisture increases. I believe the manuscript should also focus on these variables, in specific regions. Why is transpiration not affected here by the soil texture maps, and the water balance components as drainage, surface runoff and soil moisture do change?

As stated earlier, a new subsection dedicated to regional zooms on the most impacted regions by soil texture change will be added in the Results (3.4). In Figure 7, the Scandinavian soils were changed from Sandy Loam (in Reynolds map) to Loam (in Zobler map). According to Figure 4, the consequence of this change is an increase in surface runoff (by 0.1-0.5 mm/d) and soil moisture (by 100-200 kg/m²), and a decrease in drainage (by -0.1 to -0.05 mm/d). The change in transpiration is much lower than the one of surface runoff and drainage, and does not exceed 0.05 mm/d (in absolute value). The latter results are well in agreement with Figure 7, and the non-significant changes in transpiration pointed by the Referee are in fact due to the weak impact of soil texture change on transpiration.

C17: Lines 208-209: what about other variables (water balance components) than evapotranspiration?

Up to now, only preliminary results were communicated by the SP-MIP team. No information about other variables was revealed.

C18: Lines 214-215: why not calculate hydraulic parameters at high resolution to remove some of that bias?

As explained earlier, it is out of the purpose of the paper to test different upscaling methods.

C19: Lines 218-219: yes, the authors could have used these upscaling method of Samaniego. In this paper, we do not aim at testing different upscaling methods.

C20: Lines 226-235: again the focus on evapotranspiration. What about other water balance components?

In our paper, we mapped the impact of soil texture on different hydrologic variables (Figure 7 of the submitted paper and Figure S3 of the supplementary), but we chose to map the biases of the ET variable since the distributed observation-based products are only available for this variable.

C21: Line 236-244: To include and end with this paragraph the authors should focus more on PTFs (methods and results) and describe these in more detail (methods).

It must be underlined that we don't claim here that our paper demonstrates the need for more complex PTFs. On the contrary, it massively cites other studies supporting this conclusion, and we do so because the need for more complex PTFs is related to the specific conclusion of our paper, i.e. the weak sensitivity to soil texture maps except in some very specific areas where the USDA class for Clay is not precise enough. Thus, using other sources of information than soil texture to derive the geographic distribution of soil properties may lead to clearer and broader improvements of the simulated water budget than the ones analyzed here owing to soil texture maps alone. We propose to replace the last sentence of the paper by the above one.

References

- Beven, K. J. and Kirkby, M. J.: A physically based, variable contributing area model of basin hydrology / Un modèle à base physique de zone d'appel variable de l'hydrologie du bassin versant, *Hydrol. Sci. Bull.*, 24(1), 43–69, doi:10.1080/02626667909491834, 1979.
- Boucher, O., Servonnat, J., and 76 others: Presentation and evaluation of the IPSL-CM6A-LR climate model, JAMES, submitted, 2019.
- Carsel, R. F. and Parrish, R. S.: Developing joint probability distributions of soil water retention characteristics, *Water Resour. Res.*, 24(5), 755–769, doi:10.1029/WR024i005p00755, 1988.
- Collatz, G. J., Ribas-Carbo, M. and Berry, J. A.: Coupled photosynthesis stomatal conductance model for leaves of C4 plants. *Aust. J. Plant Physiol.*, 19, 519-539. doi: 10.1071/PP9920519, 1992.
- De Rosnay, P., and Polcher, J.: Modelling root water uptake in a complex land surface scheme coupled to a GCM, *Hydrol. Earth Syst. Sci.*, 2, 239–255, doi:10.5194/hess-2-239-1998, 1998.
- De Rosnay, P., Polcher, J., Bruen, M. and Laval, K.: Impact of a physically based soil water flow and soil-plant interaction representation for modeling large-scale land surface processes, *J. Geophys. Res. Atmospheres*, 107(D11), ACL 3-1-ACL 3-19, doi:10.1029/2001JD000634, 2002.
- D'Orgeval, T., Polcher, J. and Rosnay, P. de: Sensitivity of the West African hydrological cycle in ORCHIDEE to infiltration processes, *Hydrol. Earth Syst. Sci.*, 12(6), 1387–1401, doi:https://doi.org/10.5194/hess-12-1387-2008, 2008.
- Entekhabi, D. and Eagleson, P. S.: Land Surface Hydrology Parameterization for Atmospheric General Circulation models Including Subgrid Scale Spatial Variability, *J. Clim.*, 2(8), 816–831, doi:10.1175/1520-0442(1989)002<0816:LSHPFA>2.0.CO;2, 1989.
- Farquhar, G. D., Von Caemmerer, S., and Berry, J. A.: A biochemical model of photosynthetic CO₂ assimilation in leaves of C₃ species. *Planta*, 149, 78-90, doi: 10.1007/BF00386231, 1980.
- Green, W. H. and Ampt, G.: Studies on soil physics, 1. The flow of air and water through soils, *J. Agric. Sci*, 4, 1–24, 1911.
- Hengl, T., Jesus, J. M. de, Heuvelink, G. B. M., Gonzalez, M. R., Kilibarda, M., Blagotić, A., Shangquan, W., Wright, M. N., Geng, X., Bauer-Marschallinger, B., Guevara, M. A., Vargas, R., MacMillan, R. A., Batjes, N. H., Leenaars, J. G. B., Ribeiro, E., Wheeler, I., Mantel, S. and Kempen, B.: SoilGrids250m: Global gridded soil information based on machine learning, *PLOS ONE*, 12(2), e0169748, doi:10.1371/journal.pone.0169748, 2017.

Looy, K. V., Bouma, J., Herbst, M., Koestel, J., Minasny, B., Mishra, U., Montzka, C., Nemes, A., Pachepsky, Y. A., Padarian, J., Schaap, M. G., Tóth, B., Verhoef, A., Vanderborght, J., Ploeg, M. J. van der, Weihermüller, L., Zacharias, S., Zhang, Y. and Vereecken, H.: Pedotransfer Functions in Earth System Science: Challenges and Perspectives, *Rev. Geophys.*, 55(4), 1199–1256, doi:10.1002/2017RG000581, 2017.

Mualem, Y.: A new model for predicting the hydraulic conductivity of unsaturated porous media, *Water Resour. Res.*, 12(3), 513–522, doi:10.1029/WR012i003p00513, 1976.

Ogée, J. and Brunet, Y.: A forest floor model for heat and moisture including a litter layer, *J. Hydrol.*, 255(1), 212–233, doi:10.1016/S0022-1694(01)00515-7, 2002.

Sakaguchi, K. and Zeng, X.: Effects of soil wetness, plant litter, and under-canopy atmospheric stability on ground evaporation in the Community Land Model (CLM3.5), *J. Geophys. Res. Atmospheres*, 114(D1), doi:10.1029/2008JD010834, 2009.

Samaniego, L., Kumar, R. and Attinger, S.: Multiscale parameter regionalization of a grid-based hydrologic model at the mesoscale, *Water Resour. Res.*, 46(5), doi:10.1029/2008WR007327, 2010.

Schaap, M. G., Leij, F. J. and van Genuchten, M. T.: rosetta: a computer program for estimating soil hydraulic parameters with hierarchical pedotransfer functions, *J. Hydrol.*, 251(3), 163–176, doi:10.1016/S0022-1694(01)00466-8, 2001.

Stamm, J.F., Wood, E.F. and Lettenmaier, D.P.: Sensitivity of a GCM Simulation of Global Climate to the Representation of Land-Surface Hydrology. *J. Climate*, 7, 1218–1239, doi:10.1175/1520-0442(1994)007<1218:SOAGSO>2.0.CO;2, 1994

Van Genuchten, M.: A Closed-form Equation for Predicting the Hydraulic Conductivity of Unsaturated Soils 1, *Soil Sci. Soc. Am. J.*, 44(5), 892–898, doi:10.2136/sssaj1980.03615995004400050002x, 1980.

Vereecken, H., Weihermüller, L., Assouline, S., Šimůnek, J., Verhoef, A., Herbst, M., Archer, N., Mohanty, B., Montzka, C., Vanderborght, J., Balsamo, G., Bechtold, M., Boone, A., Chadburn, S., Cuntz, M., Decharme, B., Ducharne, A., Ek, M., Garrigues, S., Goergen, K., Ingwersen, J., Kollet, S., Lawrence, D. M., Li, Q., Or, D., Swenson, S., de Vrese, P., Walko, R., Wu, Y. and Xue, Y.: Infiltration from the Pedon to Global Grid Scales: An Overview and Outlook for Land Surface Modeling, *Vadose Zone J.*, 18(1), doi:10.2136/vzj2018.10.0191, 2019.

Wang, F., Cheruy, F. and Dufresne, J.-L.: The improvement of soil thermodynamics and its effects on land surface meteorology in the IPSL climate model, *Geosci. Model Dev.*, 9(1), 363–381, doi:https://doi.org/10.5194/gmd-9-363-2016, 2016.

Weak sensitivity of the terrestrial water budget to global soil texture maps in the ORCHIDEE land surface model

Salma TAFASCA¹, Agnès DUCHARNE¹, Christian VALENTIN²

¹ METIS (Milieux Environnementaux, Transferts et Interactions dans les Hydrosystèmes et les Sols), Institut Pierre Simon Laplace (IPSL), Sorbonne Université, CNRS, EPHE, Paris, France

² iEES-Paris (Institut d'Ecologie et des Sciences de l'Environnement de Paris), Sorbonne Université, CNRS, INRA, IRD, Paris, France

Correspondence to: Salma Tafasca (salma.tafasca@upmc.fr)

Abstract

10 Soil physical properties play an important role for estimating soil water and energy fluxes. Many hydrological and land surface models (LSMs) use soil texture maps to infer these properties. Here, we investigate the impact of soil texture on soil water fluxes and storage at different global-scales using the ORCHIDEE LSM, forced by several complex or globally-uniform soil texture maps. At point scale, ~~t~~the model shows a realistic sensitivity of runoff processes and soil moisture to soil texture, and reveals that loamy-medium textures give the highest evapotranspiration and lowest total runoff rates. The three tested complex soil texture maps ~~being rather similar by construction, especially when upscaled at the 0.5° resolution used here, they~~ result in similar water budgets at all scales, compared to the uncertainties of observation-based products and meteorological forcing datasets, although important differences are observed can be found at the regional scale, particularly in areas where the different maps disagree on the prevalence of clay soils. The three tested soil texture maps are also found to be similar by construction, with a shared prevalence of loamy textures, and have a spatial overlap over 40% between each pair of maps, which explains
15 the overall weak impact of soil texture map change. A useful outcome is that the choice of the input soil texture map is not crucial for large-scale modelling: but tthe added-value of more detailed soil information (horizontal and vertical resolution, soil composition) deserves further studies.

1. Introduction

Land surface models (LSMs) simulate water and energy fluxes at the interface between the land surface and the atmosphere. They were developed for continental to global scales to provide realistic land boundary conditions to climate models (Remaud et al., 2018), and to investigate the water, energy and carbon cycles at the Earth surface, and the related natural resources and risks (Guimberteau et al., 2017; Haddeland et al., 2011; Sterling et al., 2013; Zhao et al., 2017). By lack of sufficient spatial coverage for detailed soil properties, LSMs, like many physically-based hydrological models, rely on pedotransfer functions (PTF), which relate available soil information to the required soil properties (Looy et al., 2017; De Lannoy et al., 2014). The simplest approach, still used by most LSMs, relies on soil texture, as classified by the US Department of Agriculture (USDA) into 12 soil classes based on the percent of sand, silt and clay particles (USDA Soil Survey Staff et al., 1951). Look-up tables

relate these broad texture classes to multiple soil properties, usually with one single central value for each class and property, as found in Cosby et al. (1984) and Carsel and Parrish (1988) for the Clapp and Hornberger (1978) and Van Genuchten (1980) soil water models, respectively. In this framework, several global soil texture maps are used by LSMs, with different resolutions and soil texture distributions: based on the 1:5,000,000 FAO/UNESCO Soil Map of the World (FAO/UNESCO, 1971-1981), itself based on soil surveys defining 106 soil units, Zobler (1986) and Reynolds et al. (2000) provided soil texture maps at a resolution of 1° and 5 arc-min respectively, for depths of 30 and 100 cm for Reynolds et al. (2000), and 30 cm for Zobler (1986) ~~respectively, both based on the 1:5,000,000 FAO/UNESCO Soil Map of the World (FAO/UNESCO, 1971-1981), itself based on soil surveys defining 106 soil units~~; the FAO/UNESCO Soil Map of the World ~~latter map~~ was updated as the Harmonized World Soil Database (HSWD), produced at 30 arc-sec by including new regional and national soil information (Nachtergaele et al., 2010; Batjes, 2016); the soil texture map of the 1-km SoilGrids database (Hengl et al., 2014), recently updated at 250 m (Hengl et al., 2017), ~~is although~~ not independent from the above FAO/UNESCO global soil maps, but also relies on large number of national and international soil profile databases, combined with automated spatial prediction models (Hengl et al., 2014). Both HSWD and SoilGrids soil texture maps are available at seven depths ranging from 0 cm to
45 2 m.

Most studies concluding that soil texture exerts an important impact on soil hydrology were conducted at small to medium scales, either through site measurements (e.g. An et al., 2018; Song et al., 2010), or regional-scale and multi-site data analysis (Lehmann et al., 2018; Wang et al., 2009) and model sensitivity analyses. Using a mesoscale hydrologic model over the Mississippi river basin, Livneh et al. (2015) compared two different soil texture maps, and the more spatially detailed one
50 better reproduced hydrologic variability and extreme events. With the Noah LSM over China, Zheng and Yang (2016) found that the sensitivity of the simulated water budget to soil texture was dependent on climate, soil moisture being less sensitive to soil texture in arid areas, while evapotranspiration and runoff showed the highest sensitivity in the transitional zones. Li et al. (2018) confirmed these results over the Tibetan Plateau but showed additional influence of the vegetation cover on the sensitivity to soil texture, as also found over the US (Xia et al., 2015). At a global scale, De Lannoy et al. (2014) developed an
55 improved soil texture map for the Catchment LSM, by merging several texture and organic material maps. Combined with updated PTF, this new map offered modest yet significant improvements of the simulated hydrology compared to various point-scale measurements. Related studies revealed a strong impact of soil water-holding capacity and its spatial patterns using the first generations of LSMs, but with bucket-type soil hydrology instead of Richards equation (Milly & Dunne 1994; Ducharne & Laval, 2000).

60 Here, we aim at exploring more systematically the impact of soil texture on the water budget at a global scale, using a state-of-the-art LSM with physically based soil hydrology, and multiple input soil texture maps. ~~Here, we aim at exploring more systematically the impact of soil texture on the water budget from point to global scale, using a state-of-the-art LSM with physically-based soil hydrology, and multiple input soil texture maps. After presenting the model and soil texture maps used~~

in this work, the results are presented as follows. We first provide an analysis of the similarities and differences between the
65 different soil maps, then, we evaluate the point-scale response of the model to different soil textures to make sure it displays a
reliable behaviour. This point-scale response is then analysed from a geographic point of view, with a comparison to a
distributed observation-based evapotranspiration product, and a focus is made on areas with a large sensitivity to the soil
texture maps. We finally explore how the magnitude and significance of the simulated evapotranspiration response changes
with the scale of analysis up to the land scale, defining the terrestrial water budget. The closing section summarizes the main
70 conclusions of the study, and discusses its limitations and perspectives.

2. Materials and Methods

2.1. Soil texture in the ORCHIDEE LSM

ORCHIDEE (ORganizing Carbon and Hydrology in Dynamic EcosystEms) is the land component of the IPSL (Institut Pierre-Simon Laplace) climate model, and describes the complex links between vegetation phenology and the water, energy and
75 carbon exchanges at the land surface (Krinner et al., 2005). We use here the version of ORCHIDEE developed for CMIP6
(Eyring et al., 2016) and detailed in forthcoming papers (Boucher et al., 2019; Cheruy et al., 2019; Ducharme et al., in prep);
but we deactivated the soil freezing option for simplicity.

The physically-based soil hydrology scheme solves the vertical soil moisture redistribution based on a multi-layer
solution of the saturation-based Richards equation, using a 2-m soil discretized into 11 soil layers of increasing thickness with
80 depth (de Rosnay et al., 2002), and a special processing for infiltration. Infiltration is processed before soil moisture
redistribution, owing to a time-splitting procedure inspired by the model of Green and Ampt (1911), with a sharp wetting front
propagating like a piston (d'Orgeval et al., 2008; Vereecken et al., 2019). The unsaturated values of hydraulic conductivity
and diffusivity are given by the model of Mualem (1976) - Van Genuchten (1980).

In each grid cell, the corresponding parameters (saturated hydraulic conductivity K_s , inverse of air entry suction α ,
85 shape parameter m , porosity, and residual moisture) are taken from Carsel and Parrish (1988), as a function of the dominant
USDA soil texture class, itself derived from an input soil texture map. The tabulated values of the different soil parameters are
displayed in Figure S1 for each USDA class. Soil texture is assumed to be uniform over the soil column in ORCHIDEE, which
does not permit to distinguish several soil horizons. However, K_s decreases exponentially with depth, to account for the effects
of soil compaction and bioturbation, as introduced by d'Orgeval et al. (2008) following Beven & Kirkby (1979). It must also
90 be noted that the horizontal variations of K_s are taken into account by an exponential probability distribution, but only for
calculating infiltration and surface runoff (Entekhabi & Eagleson, 1989; Vereecken et al., 2019). The soil texture also
influences heat capacity and conductivity, and heat diffusion is calculated with the same vertical discretization as water
diffusion in the top 2m, but extended to 10 m (Wang et al., 2016). To account for the effects soil compaction and bioturbation,

95 K_s decreases exponentially with depth, while the effect of horizontally variable K_s on infiltration is described by an exponential distribution. Finally, soil texture also influences heat capacity and conductivity (Wang et al., 2016).

Evapotranspiration is described by a classical bulk aerodynamic approach, distinguishing four sub-fluxes: sublimation, interception loss, soil evaporation, and transpiration. The latter two are directly coupled to soil water redistribution, and depend on soil moisture and properties, which control how the corresponding rates are reduced compared to the potential rate: transpiration is limited by a stomatal resistance, increasing when soil moisture drops from field capacity to wilting point (which both depend on soil texture as detailed in Supplementary S1); soil evaporation is not limited by a resistance, but only by upward capillary fluxes, which control the soil propensity to meet the evaporation demand (d'Orgeval et al., 2008; Campoy et al., 2013). Evapotranspiration also depends on the vegetation of each grid-cell, described here as a mosaic of up to 15 plant functional types (PFTs), based on the global land cover map used in the IPSL simulations for CMIP6 (Boucher et al., 2019). In each PFT, root density is assumed to decrease exponentially with depth, with a PFT-dependent decay factor. The resulting root density profile is combined to the soil moisture profile and a water stress function depending of field capacity and wilting point to define the integrated water stress factor of each PFT on transpiration.

This flux is also coupled to photosynthesis, which depends on soil moisture, light availability, CO₂ concentration, and air temperature, following Farquhar et al. (1980) and Collatz et al. (1992) for C3 and C4 plants, respectively. The resulting carbon assimilation is allocated to several vegetation pools, including leaf mass thus leaf area index (LAI), owing to a dynamic phenology module called STOMATE (Krinner et al., 2005). It must be underlined that LAI has an important influence on the partition between soil evaporation and transpiration, via the fraction that is effectively covered by foliage, which increases exponentially with LAI with a coefficient of 0.5, also controlling light extinction through the canopy (Krinner et al. 2005). This fraction contributes to transpiration and interception loss, while the complementary fraction is assumed to be bare of vegetation, and only contributes to soil evaporation.

115 **2.2. Simulation protocol**

We performed nine global-scale simulations with ORCHIDEE (tag 2.0), using different soil texture maps and climatic forcing datasets (Table 1). The analysed period is 1980-2010, following a 20-year warm-up since 1960 to provide accurate initial conditions. Atmospheric forcing datasets being known to exert a first-order influence on LSM results (Guo et al., 2006; Yin et al., 2018), we used two different datasets to drive our simulations, to compare the related uncertainties to the ones coming from the different soil texture maps. Both datasets were constructed at a 0.5° resolution by downscaling and bias-correcting an atmospheric reanalysis. All simulations but one use the GSWP3-v1 meteorological dataset (Kim, 2017)(van den Hurk et al., 2016), with a 3-hourly time step, and based on the 20th Century Reanalysis (20CR; Compo et al., 2011). In contrast, simulation EXP1 uses the 6-hourly CRU-NCEP-v7 meteorological dataset (Wei et al., 2014), based on the NCEP/NCAR reanalysis (Kalnay et al., 1996), and extended beyond 1957-1996 in near real-time. Both meteorological datasets were selected for the off-line CMIP6 simulations (van den Hurk et al., 2016).

The three simulations EXP2 to EXP4 rely on complex soil texture maps to define the dominant texture class of each 0.5° grid cell (Figure 1): the 1° map of Zobler (1986) originally contains 5 soil textural classes, but is simplified by ORCHIDEE into three USDA texture classes (Sandy Loam, Loam, and Clay Loam); the 5-arc-min map of Reynolds et al. (2000) uses the USDA classification and we used directly the 30-cm map; the third map was upscaled from the original 1km SoilGrids map of Hengl et al. (2014) at the 0 cm depth (Hengl et al., 2014) by selecting the dominant soil texture in every 0.5° pixel. This map was provided at a 0.5° resolution by the Soil Parameter Model Intercomparison Project (SP-MIP, Gudmundsson & Cuntz, 2017), which aims at quantifying to which degree the differences between LSMs result from soil parameter specification, and will thus be referred to as the SP-MIP map in the following. It was upscaled from the original 1km map of Hengl et al. (2014) at the 0cm depth by selecting the dominant soil texture in every 0.5° pixel.

In addition, we tested four spatially uniform texture maps, corresponding to the Loam, Loamy Sand, Silt, and Clay classes (EXP6 to EXP9), to analyse the importance of the spatial variability of soil texture assess the effects of medium and extreme soil texture on the global terrestrial water budget. These simulations were defined by SP-MIP, and rely on hydraulic parameter values given by Schaap et al. (2001) for each USDA class. We ran an additional simulation (EXP 5) with the SP-MIP map SoilGrids and the soil parameters of Schaap et al. (2001) to quantify the difference induced by this PTF compared to the default PTF of ORCHIDEE (Carsel & Parrish, 1988) used with the SP-MIP map SoilGrids in EXP4. It must be noted that the five simulations based on the soil parameters of Schaap et al. (2001) also differ from the four others (EXP1 to EXP4) because the decrease of K_s with depth is relaxed, to comply with the SP-MIP protocol.

2.3. Calculation of median diameter dm for each of the 12 USDA soil texture classes

Every texture class is represented by a polygon in the USDA textural triangle (Fig. 1d). For each texture class, we located the centroid of the corresponding polygon to obtain a central value of the composition in clay, silt and sand particles (Table 2). These clay, silt and sand particles have various diameters, respectively ranging in [0, 2 μ m], [2 μ m, 50 μ m] and [50 μ m, 2000 μ m] (USDA; Staff, 1951). To construct the particle-size distribution curve of each texture class (Fig. 2), we further assumed that clay, silt and sand particle diameters are uniformly distributed in the latter intervals. The median diameter of each texture class is then obtained by intersecting the corresponding curve with a cumulative value of 50%, such that half of soil particles reside above this point, and half reside below this point. The resulting median diameters are listed in Table 2. Carsel and Parrish (1988) provide the mean content of sand, silt and clay for each soil texture, but their estimations are based on American soil surveys, which might not be representative of the whole globe, so we preferred to use the composition of the of the polygon centroids. Note that using the mean composition of by Carsel and Parrish (1988) leads to very similar results.

2.4. Evaluation datasets

To assess the realism of our simulations, we use three different datasets. Jung et al. (2010) constructed a series of global 1° evapotranspiration maps at the monthly time step from 1982 to 2008, by interpolating in situ eddy-covariance measurements

from the FLUXNET network ~~using~~ machine learning algorithms and ancillary geospatial information (land surface remote sensing and meteorology). GLEAM (Martens et al., 2017) is another series of global evapotranspiration maps, provided by at the 0.25° resolution and the daily time step over 1980-2015. They strongly rely on remote-sensing datasets (radiation, precipitation, temperatures, surface soil moisture, vegetation optical depth, snow water equivalents), used as input to an evapotranspiration model based on Priestley and Taylor (1972). Finally, Rodell et al. (2015) quantified the mean annual fluxes of the water cycle at the beginning of the 21st century, at a coarser scale (continents and major ocean basins) but with the aim of providing consistent estimates of precipitation, evaporation, and runoff, by combining in situ and satellite measurements, data assimilation systems, and multiple energy and water budget closure constraints.

3. Results

3.1. Comparison of the tested soil texture maps

Whichever the complex soil texture map, Loam is by far the most dominant texture (Table 1), covering between 44 to 64 % of the land surface. Other important soil textures in all maps are Sandy Loam, Clay Loam and Sandy Clay Loam, and these four medium textures alone cover 81, 86 and 100 % of land based on Reynolds, SP-MIP, and the simplified Zobler map, respectively. The Silty Clay, Silty Clay Loam and Sandy Clay classes are poorly present in all three maps: altogether, they cover 0.9, 0.2 and 0 % of land based on SP-MIP, Reynolds and the simplified Zobler map, respectively. The Silt texture class is absent from Reynolds and Zobler maps, while it found in the SP-MIP map, but only to fill the no-data land points (3.3%). To better document the differences and similarities between the three soil texture maps, we also quantified the spatial overlap between each pair of complex maps (Table 3). It is always more than 41%, and the best agreement is found between the Reynolds and Zobler maps (52%). Nonetheless, this leaves 48 % of the grid cells (in the best case) where the soil texture does change.

To explore if it changes for similar or very different soil textures, we compared several groups of three maps derived from the tested soil texture maps: the maps of the corresponding particle diameter dm (section 2.3), of K_s (as provided by the PTF, thus not including the impact of roots nor soil compaction), soil porosity θ_s , field capacity θ_{fc} , wilting point θ_w , and available water content (AWC, integrated over the 2-m soil column). The values of these soil parameters for the 12 USDA soil texture classes are detailed in Supplementary S1 and depicted in Figure S1. Table 4 shows that, whichever the soil parameter, the difference of spatial mean between the three maps is smaller than the mean spatial standard deviation, even for the least variable map (Zobler). This demonstrates the large similarity of the three complex soil maps tested in our paper, not only regarding soil texture itself (as summarized by dm), but also, very logically, for the derived soil hydraulic parameters. This similarity is also confirmed by the spatial correlations between each pair of maps, always positive, the best correlations being found between Zobler and Reynolds for most parameters (always larger than 0.35, and up to 0.58), and the weakest between the SP-MIP map and Reynolds.

3.1.3.2. Point scale sensitivity to the 12 USDA texture classes

190 To check if the ORCHIDEE model displays a realistic response to soil texture, we examined how the pluri-annual means of the main water budget variables relate to soil texture (Fig. 3). We clustered all the points with a similar texture, and sorted the texture classes based on their median particles diameter (section 2.3). The mean fluxes were also divided by mean precipitation to reduce the effect of misleading texture-climate associations, as between sandy classes and arid climates. We focused on EXP2, ~~since the because the~~ Reynolds map exhibits the largest range of soil textures (11 different classes).

195 The simulated total soil moisture (over the 2-m soil depth), drainage and surface runoff exhibit a clear monotonic response to soil texture (sorted by median diameter). Increasing soil moisture for finer textures is explained by their higher water retention and field capacity. The opposite responses of drainage and surface runoff (Fig. 3f-g) both result from higher permeability in coarser soils, enhancing drainage and infiltration at the soil surface, thus reducing surface runoff. These responses to soil texture are coherent with experimental results (e.g. An et al., 2018; Song et al., 2010).

200 As it sums up two opposite responses, total runoff shows a larger spread and a non-monotonic (convex) behaviour, with smaller total runoff for medium textures. The opposite response (concave) is found for evapotranspiration (Fig. 3d), because precipitation is partitioned between evapotranspiration and total runoff in every grid cell. The highest evapotranspiration rates found for medium textures is consistent with the high available water capacity for these loamy textures (Fig. S1). Transpiration, however, increases as soil gets coarser (Fig. 3c), with two explanations probably acting together.
205 Firstly, the increase of matric potential when the texture gets finer, as shown in Figure S1 for particular values of the potential, defining the wilting point, field capacity and air entry suction point ($1/\alpha$), makes root uptake thus transpiration more difficult for a given soil moisture if the soil texture is finer. Secondly, and the most likely explanation is that the high conductivity of coarse soils enhances water infiltration at the soil surface, quickly available for plant uptake. The increase of K_s for coarse textures also explains the associated drainage increase when its dependence on mean precipitation is filtered (Fig. 3f). The
210 fact ~~Rather surprisingly, we find here~~ that soil moisture decreases when drainage and transpiration get higher ~~decrease when soil moisture gets higher~~. This indicates that annual mean soil moisture is the result more than the cause of these fluxes, ~~which are strongly driven by hydraulic conductivity when their dependence on mean precipitation is filtered~~.

Soil evaporation shows more variability within a soil texture class than between the different soil texture classes (Fig. 3b), showing this flux strongly depends on other factors, ~~{like~~ temperature, leaf area index, etc. (Martens et al., 2017; Wang et al., 2018) etc.). To ~~exclude-filter~~ their spurious effects, we also analysed in Figure 4 the effect of changing soil texture (~~from EXP2 to EXP4~~) at the point-scale, thus under similar climatic and land cover conditions. Figure 4 shows the changes occurring ~~when~~ a soil texture class in the Reynolds map is replaced by another in the SP-MIP SoilGrids map. The Zobler map was excluded from this analysis since it contains only three soil texture classes. Switching maps from Reynolds to the SP-MIP map SoilGrids (i.e. from EXP2 to EXP4) results in a majority of land points with unchanged texture, and thus, similar-identical

220 simulated variables. These land points are represented by the diagonal pixels of the matrices and ~~ecorrespond~~nsist of to 41.2% of the land surface. Land points with coarser texture in the SP-MIP map~~SoilGrids~~ represent 34.1% of the land surface (upper side of the diagonal line in the matrices) against 24.7% for finer textures (lower side of the diagonal line in the matrices).

Figure 4 highlights that simulated soil evaporation decreases from fine to coarse textures, so that capillary retention, which is the main limiting factor to soil evaporation in ORCHIDEE, depends more strongly on soil moisture (higher for fine soils; Fig. 4e) than on intrinsic capillary forces (stronger for fine soils). We fail to see this behaviour in Figure 3, which is likely due to the greater impact of diverse climatic conditions and vegetation associated with every soil texture. ~~This point-scale analysis also confirms the results of Figure 3 for the other variables, including the decrease of soil moisture with coarser soils and the greater impact of soil texture on runoff variables (surface runoff and drainage).~~ Figure 4 also confirms the results of Figure 3 for the other variables, including the decrease of soil moisture with coarser soils and the larger impact of soil texture on surface runoff and drainage than on transpiration and soil evaporation. In particular, we find that replacing fine textures with coarse textures (above the first diagonal of the matrices) results in higher drainage (due to the higher permeability of coarse-textured soils) and lower surface runoff, with changes that can exceed 1 mm/d in absolute value for some textural changes (all involving medium texture classes).

The convex behaviour of total runoff with soil texture can also be seen in Figure 4h, which is antisymmetric along the two diagonals, thus defining four different kinds of total runoff response to soil texture change. This behaviour results from the fact that total runoff sums up two variables with ane~~f~~ opposite response to soil texture change (surface runoff and drainage), the net response depending on the dominant component. Hence, changes to medium textures from either coarse or fine textures (left and right red triangles in Fig. 4h) lead to reduced total runoff, owing to reduced surface runoff in the first case, and reduced drainage in the second. In contrast, changes from medium texture to either coarse or fine textures lead to increased runoff (bottom and top blue triangles in Fig. 4h), owing to increased surface runoff or drainage, respectively. This pattern thus means that the medium textures correspond to the smallest total runoff. By means of long-term water conservation, the opposite patterns are found for total evapotranspiration changes (Figure 4d), because of the opposite responses of soil evaporation and transpiration to soil texture, and supporting the concave response of this flux to soil texture found in Figure 3.

245 3.2.3.3. Spatial patterns of simulated fluxes and evapotranspiration bias ~~Sensitivity to different soil texture maps~~

Although ORCHIDEE exhibits a clear and physically-based response to soil texture at point-scale, the use of three different realistic soil texture maps (EXP2, EXP3, and EXP4) results in rather similar spatial distributions of the simulated fluxes. ~~We~~ mostly focus on evapotranspiration (Fig. 56, Fig. S2), since comparison is possible with a spatially-distributed observation-based product (GLEAM). At a grid cell scale, changing the soil texture map (Fig. 56a-c) results in weak changes in simulated evapotranspiration, which are statistically significant over less than 35% of the land surface, against 77% when switching the climate forcing (Fig. 56d). The very weak changes in evapotranspiration maps when switching from a uniform to a complex

soil texture maps (Fig. 5a)– show that the spatial variability of soil texture is a weak driver of the spatial variability of evapotranspiration (Fig. S2). In agreement with the concave response of evapotranspiration to soil texture (section 3.2), the largest increases are found when switching from very coarse or very fine textures to medium ones. This explains the dominance of evapotranspiration increase in the example cases of Figures 56a-b, since the Zobler and uniform Loam maps have the largest areal fractions of Loam (Table 1).

~~Although the other simulated hydrologic variables display a stronger sensitivity to soil texture maps, in agreement with section 3.12, it remains weak and predominantly insignificant in front of internal variability (Fig. 7, S3).~~

Consistently, the evapotranspiration biases are overall similar whichever the soil texture map (Fig. 56e-g, Fig S2), while climate forcing uncertainty ~~is confirmed~~ appears as a first order driving factor of the bias patterns (with visible differences between Figs. 56g and 56h). We find that the simulated evapotranspiration better matches GLEAM with CRU-NCEP in equatorial rain belts, and with GSWP3 in the mid-latitudes. In a few spots, however, the different soil maps induce large changes of ean lead to strongly different evapotranspiration biases, especially in Central Africa, Central America, India and the Amazon basin, which are discussed in the following subsection. In particular, the Zobler and Reynolds maps respectively produce a strong positive bias in Sudan and western India (Fig. 6f), and a strong negative bias in the eastern Amazon basin (Fig. 6g), further confirmed by an overestimation of simulated river discharge in this area (not shown). These biases are all related to the Clay texture, as discussed below. The other simulated hydrologic variables display a stronger sensitivity to soil texture maps, in agreement with section 3.2, but it remains weak and predominantly insignificant in front of inter-annual variability (Fig. 6, S3).

To provide a point-scale quantification of the differences between the three complex soil maps and the resulting simulated variables, we mapped the standard deviation of each group of three maps, using the mean diameter (dm) of each texture class to get a quantitative proxy in case of texture (Fig. 75). Although the quantitative meaning of standard deviation can be questioned when calculated from a sample of three values, we used it here as a simple lumped metric of similarity/difference between the three complex maps, and to identify points/regions where the three maps are all consistent (small standard deviation), or where at least one of them is departing (high standard deviation). Compared to the standard deviation of $\log(dm)$, the ones of the simulated fluxes are weak (less than 10 % of the maximum value) over larger fractions of the globe. They are also smaller than the local annual mean values of the variable itself, as shown by comparison to Figure S2 for evapotranspiration (not shown for the other variables).

Areas which stand out with high standard deviations in all maps are the four regions noted above, where the standard deviation between the three texture maps is very important (Fig. 7a). Aside from these areas, the tropical humid zones (South-East Asia, Indonesia) show rather large standard deviations of surface runoff and drainage (Fig. 7d,f), but without large standard deviation of $\log(dm)$, so this is rather due to the high values of these fluxes in these very humid zones. The overall resemblance between the standard deviation maps of soil texture on the one hand, and the simulated hydrologic variables on

the other hand can be quantified at global scale by a spatial correlation coefficient, ranging between 0.49 for transpiration to 0.79 for soil moisture. The latter variable is the most impacted by soil texture change, as supported by this large correlation coefficient, and the large standard deviations on Figure 7b.

3.4. Regional zooms on greatly impacted areas

Figure 8 displays the four 40° x 60° areas where the different soil maps can lead to strongly different evapotranspiration biases, with a strong link to the (mis)representation of Clay soils, since the largest changes in evapotranspiration and total runoff are expected where soil texture changes between medium (loamy) and extreme (Clay or Sand) textures (Figs. 3 and 4). The Sand soil texture, however, does not induce a large impact on the simulated hydrological fluxes, as it is mostly found in arid areas where water is a limiting factor. This is the case in the Arabian Peninsula (Fig. 8b) and the Sahara, where the sandy soils mapped in the SP-MIP map are absent in Zobler and only weakly present in Reynolds, but the evapotranspiration bias hardly changes and remains negative.

In Tropical South America and Central Africa (Fig. 8c,d), the Reynolds map shows a larger presence of Clay compared to the other two maps, part of which results in an important negative evapotranspiration bias. When compared to the FAO soil order map (Fig. S4), it is found that the Clay class of the Reynolds map gathers different soil orders, including (i) Vertisols, which consist of swelling clay (smectites) with low permeability, and mostly found in dry regions like Sudan, Deccan (India), or eastern Australia (Deckers et al., 2003), and (ii) Oxisols, which are found in humid Tropics, exhibit a large textural variability, and contain non-swelling clay (kaolinite) with much higher permeability than Vertisols (Spaargaren and Deckers, 1998). The Oxisols mapped as Clay in the Reynolds map and inducing a large negative evapotranspiration bias call for a better representation of the Clay texture, with a soil texture map that distinguishes the two types of clays with different hydrologic behaviours. In contrast, neglecting Vertisols leads to overestimate evapotranspiration which is the case with the Zobler map in Deccan and Sudan (Fig. 8b,d), so the corresponding biases switch sign from negative to positive in Deccan, and become more positive in Sudan. These problems come from the simplification of the Zobler map in the ORCHIDEE model, which converts the original “very fine” soils to Clay Loam (section 2.2). Vertisols are also overlooked in Australia by the simplified Zobler map and by the SP-MIP map (Fig. 1), but with insignificant impact on evapotranspiration in this strongly water-stressed area (Fig. 6). Finally, in Central America, the SP-MIP soil map shows a much higher presence of Clay compared to the Zobler and Reynolds soil maps. It should be underlined that the original 1km SoilGrids from which the SP-MIP map was derived does not show this dominance of Clay in this area, and we think that this feature is an error in the SP-MIP map. This over-representation of Clay turned the evapotranspiration bias from null/positive (with the Reynolds and Zobler maps) to negative.

3.5. Sensitivity of the simulated water budget to global soil texture maps at different scales

315 ~~Although ORCHIDEE exhibits a clear and physically based response to soil texture at point scale, the use of three different realistic~~ At the global scale like at the point-scale, the three complex soil texture maps (~~EXP2, EXP3 and EXP4~~) results in very similar terrestrial water budgets (Fig. 105). Whichever the hydrologic variable, the global mean differences induced by these three maps (~~EXP2, EXP3 and EXP4~~) are smaller than the ones induced by different meteorological forcing (EXP1 vs EXP2), which are comparable to the uncertainty range between several observation-based estimates of the terrestrial water budget (Section 2.43). Compared to these estimates, it is also worth noting that ORCHIDEE simulates fairly well the mean
320 partition between evapotranspiration and total runoff with any of the complex texture maps.

In contrast, the use of spatially uniform soil texture maps (EXP6 to EXP9) induces major differences in surface runoff, drainage and soil moisture. The strong decrease of soil moisture from EXP4 to EXP5 is not only due to the PTF change between these simulation, but more importantly to the relaxation of the decrease of K_s with depth, which leads to larger K_s at the bottom of the soil column, favouring drainage, thus reducing soil moisture. The ~~different-global~~ water budgets resulting from these
325 uniform maps are in agreement with the response of the model to soil texture (section 3.42). In particular, the uniform clay map (EXP9) induces high soil moisture and surface runoff, and low drainage, compared to the other uniform maps, while the uniform coarse map (Loamy Sand in EXP8, but Sand would give similar results based on Fig. 3) shows the opposite behaviour. Eventually, using a uniform coarse or fineclay texture (EXP8 or EXP9) brings the simulated global mean evapotranspiration and runoff considerably out of the observed range, contrarily to the uniform medium texture maps (EXP6, EXP7). Overall,
330 these uniform experiments tell us the maximum range of change we can expect from any kind of soil texture map change. For instance, the largest difference in mean global scale evapotranspiration (between the uniform clay and silt experiments owing to the non-monotonic response underlined in Figs. 3 and 4) is 0.1 mm/d, i.e. 8% of the global mean evapotranspiration using the complex soil texture maps and the same climate forcing.

To analyse the scale-related impact of soil texture maps on simulated fluxes, we upscaled the map of annual mean
335 evapotranspiration difference (EXP2-EXP4) to coarser resolutions, from 1° to the global scale, by averaging the values of the difference (Fig. 11). The resulting probability density functions are shown in Figure 12a, and Figure 12b-e shows how some metrics characterizing these distributions evolve with the averaging scale. The first noticeable impact of upscaling to coarser resolutions is the decrease of extreme evapotranspiration differences (Fig. 12b,d), leading to a less scattered distribution, also confirmed by the decreasing standard deviation (Fig. 12c). This figure shows that evapotranspiration difference follows a
340 symmetrical distribution for the coarsest resolutions (above 5°), and starts showing a dissymmetric distribution below 5°, with a prevalence of negative values. This can also be seen in Figure 12d where the median of the evapotranspiration difference is all the more negative as the resolution gets finer. Thus, the strong impact of the soil texture map change that can be found locally (section 3.4) is mitigated at larger scales, and particularly at the global scale at which the terrestrial water budget shows a very weak sensitivity to the soil texture maps, even if it is statistically significant (Figs. 10 & 11).

Using the ORCHIDEE LSM and different soil texture maps, we found that the model shows a realistic sensitivity of surface runoff, drainage and soil moisture to soil texture compared to experimental and field studies (Rawls et al., 1993; Osman, 2013). These sensitivities lead to higher simulated evapotranspiration and lower total runoff for medium textures, which are discernable against other sources of variability when sorting the twelve USDA texture classes based on their median diameter.

350 Apart in some areas which exhibit important differences in evapotranspiration, often attributed to the Clay texture class, The three complex soil texture maps tested here lead to similar water budgets at all scales, and the large uncertainties in observation-based products and climate forcing datasets make it impossible to conclude which map gives the best simulation.

These numerical results are specific to the ORCHIDEE model and the selected maps, but this model and these maps are representative examples of most state-of-the-art LSM applications (Vereecken et al., 2019), and comparable results were

355 obtained with another LSM and other maps (De Lannoy et al., 2014). Besides, preliminary analyses of the LSM simulations conducted for the SP-MIP project (Gudmundsson & Cuntz, 2017) seem to confirm that varying soil parameters (resulting from different soil texture maps and different PTFs) have a small impact on long-term mean simulated evapotranspiration at the global scale, compared to other relevant uncertainties, including inter-model differences.

As mentioned in Introduction, much stronger responses to soil properties have been reported from bucket-type LSMs.

360 It must be underlined, however, that these papers considered much larger changes of soil properties, which reduces in bucket-type models to available water holding capacity (AWC), combining information on porosity, soil depth, and the difference between field capacity and wilting point. As an example, the main changes discussed in Stamm et al. (1994), Ducharme & Laval (2000), de Rosnay & Polcher (1998), and Milly & Dunne (1994), correspond respectively to AWC changes of +75%, +110%, +200%, and +1400%, while the AWC changes when switching among the three soil texture maps used in the present

365 paper does not exceed 5% (Table 2).

The weak sensitivity of the model to the three complex soil maps but in very specific areas at the global scale is probably largely explained by their spatial similarity, which can be primarily ~~comes attributed from~~ to their shared dependence on the FAO/UNESCO Soil Map, although weaker in SoilGrids ~~(and thus, in the SP-MIP map)~~. Another reason is the coarse spatial resolution at which soil texture is used in ORCHIDEE and most LSMs, since selecting the dominant soil texture in

370 every grid cell (here with 0.5° side, ca. 50 km) statistically enhances medium textures. As the latter lead to higher evapotranspiration and smaller total runoff than more extreme textures (with larger percent of sand or clay particles), an important consequence, from a water budget point of view, is that dominant soil textures should favor excessive evapotranspiration and insufficient total runoff.

Many alternative parameter upscaling methods were proposed to better preserve high resolution soil information,

375 often based on averaging operators (usefully optimized to match coarse-scale observed streamflow in Samaniego et al., 2010), while Montzka et al. (2017) deduce upscaled parameters from theoretically upscaled hydraulic conductivity and diffusivity

curves. More invasive approaches would consist in describing the effects of high resolution soil information directly in the model equations, as frequently done for the effect of K_s on infiltration owing to tractable statistical distributions (Vereecken et al., 2019). We lack similar developments for the full range of simulated water fluxes, apart from the partitioning of each grid cell into three soil columns with different soil textures, tested by de Rosnay et al. (2002) in ORCHIDEE but now abandoned.

The soil texture maps themselves can also be questioned. When compared to the FAO soil order map (Fig. S4), the SP-MIP map (following SoilGrids) SoilGrids tends to amplify the extent of sandy soils in Sahara and Saudi Arabia but ignores most sandy soils in Asia (e.g. Taklamakan desert). The largest evapotranspiration changes in our simulations were found in areas where the three soil texture maps disagree in their representation of clay soils, which calls for a better representation of this class in the soil texture maps. Of particular relevance is the distinction between Vertisols and Oxisols because of their very different hydrological properties. More generally, the use of simple PTFs based on soil texture classes only is increasingly questioned. Firstly, they overlook the first-order influence of bulk density and soil structure, which require information on organic matter content (Smettem, 1987; Rahmati et al., 2018; Sun et al., 2018) and coarse fragments exceeding 2 mm, frequent in many soils (Brakensiek and Rawls, 1994; Valentin, 1994). Secondly, the simplifying assumption that soil texture is homogeneous vertically throughout the soil column should be revised. A particular attention should be paid on surface soil properties in areas prone to soil crusting (Valentin et al., 2008; Gal et al., 2017), which mainly include loamy soils (Rawls et al., 1990) and also arid and semi-arid soils (Valentin and Bresson, 1992), producing high total runoff (Yair, 1990; Casenave and Valentin, 1992; Karambiri et al., 2003; Bouvier et al., 2018). Thus, using other sources of information than soil texture to derive the geographic distribution of soil properties may lead to clearer and broader improvements of the simulated water budget than the ones analysed here owing to mineral soil texture maps alone. All these factors should be incorporated in PTFs and LSMs to improve the simulated hydrology.

Code availability

The version of the ORCHIDEE model used for this study is based on tag 2.0, freely available from http://forge.ipsl.jussieu.fr/orchidee/browser/tags/ORCHIDEE_2_0/ORCHIDEE/

Small modifications were coded to read new maps of soil texture or soil parameters, and the corresponding code can be obtained upon request to first author.

Data availability

The GLEAM dataset used in this study can be freely accessed from www.GLEAM.eu. Primary data used in the analysis and other supplementary information that may be useful in reproducing the author's work can be obtained by contacting the corresponding author.

Author contribution

ST, AD and CV designed the research. ST performed the simulations, analysed the data and prepared a draft of the manuscript. All authors contributed to interpreting results, discussing findings and improving the manuscript.

Competing interests

410 The authors declare that they have no conflict of interest.

Acknowledgments

The ORCHIDEE simulations were performed using the IDRIS computational facilities (Institut du Développement et des Ressources en Informatique Scientifique, CNRS, France). Some of them were designed by Lukas Gudmundsson and Matthias Cuntz for the SP-MIP project.

415 References

- Al-Yaari, A., Ducharne, A., Cheruy, F., Crow, W. T. and Wigneron, J.-P.: Satellite-based soil moisture provides missing link between summertime precipitation and surface temperature biases in CMIP5 simulations over conterminous United States, *Sci. Rep.*, 9(1), 1657, doi:10.1038/s41598-018-38309-5, 2019.
- An, N., Tang, C.-S., Xu, S.-K., Gong, X.-P., Shi, B. and Inyang, H. I.: Effects of soil characteristics on moisture evaporation, *Eng. Geol.*, 239, 126–135, doi:10.1016/j.enggeo.2018.03.028, 2018.
- 420 Batjes, N. H.: Harmonized soil property values for broad-scale modelling (WISE30sec) with estimates of global soil carbon stocks, *Geoderma*, 269, 61–68, doi:10.1016/j.geoderma.2016.01.034, 2016.
- [Beven, K. J. and Kirkby, M. J.: A physically based, variable contributing area model of basin hydrology / Un modèle à base physique de zone d'appel variable de l'hydrologie du bassin versant, *Hydrol. Sci. Bull.*, 24\(1\), 43–69, doi:10.1080/02626667909491834, 1979.](#)
- 425 [Boucher, O., Servonnat, J., Albright, A. L., Aumont, O., Balkanski, Y., Bastrikov, V., Bekki, S., Bonnet, R., Bony, S., Bopp, L., Braconnot, P., Brockmann, P., Cadule, P., Caubel, A., Cheruy, F., Cozic, A., ugnet, D., D'Andrea, F., Davini, P., de Lavergne, C., Denvil, S., Dupont, E., 360 Deshayes, J., Devilliers, M., Ducharne, A., Dufresne, J.-L., Ethé, C., Fairhead, L., Falletti, L., Foujols, M.-A., Gardoll, S., Gastineau, G., Ghattas, J., Grandpeix, J.-Y., Guenet, B., Guez, L., Guilyardi, E., Guimberteau, M., Hauglustaine, D., Hourdin, F., Idelkadi, A., Joussaume, S., Kageyama, M., Khadre-Traoré, A., Khodri, M., Krinner, G., Lebas, N., Levvasseur, G., Lévy, C., Lott, F., Lurton, T., Luysaert, S., Madec, G., Madeleine, J.-B., Maignan, F., Marchand, M., Marti, O., Mellul, L., Meurdesoif, Y., Mignot, J., Musat, I., Ottlé, C., Peylin, P., Planton, Y., Polcher, J., Rio, C., Rousset, C., Sepulchre, P., Sima, A., Swingedouw, D., Thiéblemont, R., Vancoppenolle, M., Vial, 365 J., Vialard, J., Viovy, N., and Vuichard, N.: Presentation and evaluation of the IPSL-CM6A-LR climate model, *J. Adv. Model. Earth Syst.*, submitted, 2019.](#)
- 430 [Bouvier, C., Bouchenaki, L. and Trambly, Y.: Comparison of SCS and Green-Ampt Distributed Models for Flood Modelling in a Small Cultivated Catchment in Senegal, *Geosciences*, 8\(4\), 122, doi:10.3390/geosciences8040122, 2018.](#)
- Brakensiek, D. L. and Rawls, W. J.: Soil containing rock fragments: effects on infiltration, *CATENA*, 23(1), 99–110, doi:10.1016/0341-8162(94)90056-6, 1994.
- 440 [Bughici, T. and Wallach, R.: Formation of soil–water repellency in olive orchards and its influence on infiltration pattern, *Geoderma*, 262, 1–11, doi:10.1016/j.geoderma.2015.08.002, 2016.](#) [Campoy, A., Ducharne, A., Cheruy, F., Hourdin, F., Polcher, J. and Dupont, J. C.: Response of land surface fluxes and precipitation to different soil bottom hydrological conditions in a general circulation model, *J. Geophys. Res. Atmospheres*, 118\(19\), 10,725–10,739, doi:10.1002/jgrd.50627, 2013.](#)

- 445 Carsel, R. F. and Parrish, R. S.: Developing joint probability distributions of soil water retention characteristics, *Water Resour. Res.*, 24(5), 755–769, doi:10.1029/WR024i005p00755, 1988.
- Casenave, A. and Valentin, C.: A runoff capability classification system based on surface features criteria in semi-arid areas of West Africa, *J. Hydrol.*, 130(1), 231–249, doi:10.1016/0022-1694(92)90112-9, 1992.
- 450 Cheng, F.-Y. and Chen, Y.: Variations in soil moisture and their impact on land–air interactions during a 6-month drought period in Taiwan, *Geosci. Lett.*, 5(1), 26, doi:10.1186/s40562-018-0125-8, 2018.
- [Cheruy, F., Ducharne, A., Hourdin, F., Musat, I., Vignon, E., Gastineau, G., Bastrikov, V., Vuichard, V., Diallo, B., Dufresne, J.-L., Ghattas, J., Grandpeix, J.-Y., Idelkadi, A., Mellul, L., Maignan, F., Menegoz, M., Ottlé, C., Peylin, P., Wang, F., Zhao, Y.: Improved near surface continental climate in IPSL-CM6 by combined evolutions of atmospheric and land surface physics. *J. Adv. Model. Earth Syst.*, submitted, 2019.](#)
- 455 Clapp, R. B. and Hornberger, G. M.: Empirical equations for some soil hydraulic properties, *Water Resour. Res.*, 14(4), 601–604, doi:10.1029/WR014i004p00601, 1978.
- [Collatz, G. J., Ribas-Carbo, M. and Berry, J. A.: Coupled Photosynthesis-Stomatal Conductance Model for Leaves of C4 Plants, *Funct. Plant Biol.*, 19\(5\), 519–538, doi:10.1071/pp9920519, 1992.](#)
- 460 Compo, G. P., Whitaker, J. S., Sardeshmukh, P. D., Matsui, N., Allan, R. J., Yin, X., Gleason, B. E., Vose, R. S., Rutledge, G., Bessemoulin, P., Brönnimann, S., Brunet, M., Crouthamel, R. I., Grant, A. N., Groisman, P. Y., Jones, P. D., Kruk, M. C., Kruger, A. C., Marshall, G. J., Mauerer, M., Mok, H. Y., Nordli, Ø., Ross, T. F., Trigo, R. M., Wang, X. L., Woodruff, S. D. and Worley, S. J.: The Twentieth Century Reanalysis Project, *Q. J. R. Meteorol. Soc.*, 137(654), 1–28, doi:10.1002/qj.776, 2011.
- 465 Cosby, B. J., Hornberger, G. M., Clapp, R. B. and Ginn, T. R.: A Statistical Exploration of the Relationships of Soil Moisture Characteristics to the Physical Properties of Soils, *Water Resour. Res.*, 20(6), 682–690, doi:10.1029/WR020i006p00682, 1984.
- De Lannoy, G. J. M., Koster, R. D., Reichle, R. H., Mahanama, S. P. P. and Liu, Q.: An updated treatment of soil texture and associated hydraulic properties in a global land modeling system, *J. Adv. Model. Earth Syst.*, 6(4), 957–979, doi:10.1002/2014MS000330, 2014.
- [Deckers, J., Nachtergaele, F., & Spaargaren, O.: Tropical soils in the classification systems of USDA, FAO and WRB, *Evolution of Tropical Soil Science, Past and Future*, 79. Brussels, Royal Academy of Overseas Sciences pp. 79-94, 2003.](#)
- 470 [De Rosnay, P. and Polcher, J.: Modelling root water uptake in a complex land surface scheme coupled to a GCM, *Hydrol. Earth Syst. Sci. Discuss.*, 2\(2/3\), 239–255, 1998.](#)
- De Rosnay, P., Polcher, J., Bruen, M. and Laval, K.: Impact of a physically based soil water flow and soil-plant interaction representation for modeling large-scale land surface processes, *J. Geophys. Res. Atmospheres*, 107(D11), ACL 3-1-ACL 3-19, doi:10.1029/2001JD000634, 2002.
- 475 Dong, J. and Ochsner, T. E.: Soil Texture Often Exerts a Stronger Influence Than Precipitation on Mesoscale Soil Moisture Patterns, *Water Resour. Res.*, 54(3), 2199–2211, doi:10.1002/2017WR021692, 2018.
- D’Orgeval, T., Polcher, J. and Rosnay, P. de: Sensitivity of the West African hydrological cycle in ORCHIDEE to infiltration processes, *Hydrol. Earth Syst. Sci.*, 12(6), 1387–1401, doi:https://doi.org/10.5194/hess-12-1387-2008, 2008.
- 480 [Ducharne, A., Ghattas, J., Maignan, F., Ottlé, C., Vuichard, N., Guimberteau, M., Krinner, G., Polcher, J., Tafasca, S., Bastrikov, V., Brender, P., Cheruy, F., Guénet, B., Mizuochi, H., Peylin, P., Tootchi, A. and Wang, F.: Soil water processes in the ORCHIDEE 2.0 land surface model: state of the art for CMIP6, *Geosci. Model Dev.*, in prep.](#)
- Ducharne, A. and Laval, K.: Influence of the Realistic Description of Soil Water-Holding Capacity on the Global Water Cycle in a GCM, *J. Clim.*, 13(24), 4393–4413, doi:10.1175/1520-0442(2000)013<4393:IOTRDO>2.0.CO;2, 2000.
- 485 [Entekhabi, D. and Eagleson, P. S.: Land Surface Hydrology Parameterization for Atmospheric General Circulation models Including Subgrid Scale Spatial Variability, *J. Clim.*, 2\(8\), 816–831, doi:10.1175/1520-0442\(1989\)002<0816:LSHPFA>2.0.CO;2, 1989.](#)
- Eswaran, H., Reich, P. and Padmanabhan, E.: World soil resources: Opportunities and challenges, in *World Soil Resources and Food Security*, pp. 29–51, CRC Press., 2012.
- 490 Eyring, V., Bony, S., Meehl, G. A., Senior, C. A., Stevens, B., Stouffer, R. J. and Taylor, K. E.: Overview of the Coupled Model Intercomparison Project Phase 6 (CMIP6) experimental design and organization, *Geosci. Model Dev.*, 9(5), 1937–1958, doi:10.5194/gmd-9-1937-2016, 2016.

FAO and UNESCO: FAO-UNESCO Soil Map of the World, 1971-1981.

[Farquhar, G. D., von Caemmerer, S. and Berry, J. A.: A biochemical model of photosynthetic CO₂ assimilation in leaves of C₃ species, *Planta*, 149\(1\), 78–90, doi:10.1007/BF00386231, 1980.](#)

495 Gal, L., Grippa, M., Hiernaux, P., Pons, L. and Kergoat, L.: The paradoxical evolution of runoff in the pastoral Sahel: analysis of the hydrological changes over the Agoufou watershed (Mali) using the KINEROS-2 model, *Hydrol. Earth Syst. Sci.*, 21(9), 4591–4613, doi:https://doi.org/10.5194/hess-21-4591-2017, 2017.

[Green, W. H. and Ampt, G. A.: Studies on Soil Physics., *J. Agric. Sci.*, 4\(1\), 1–24, doi:10.1017/S0021859600001441, 1911.](#)

500 Guimberteau, M., Ducharne, A., Ciais, P., Boisier, J.-P., Peng, S., De Weirtdt, M. and Verbeeck, H.: Testing conceptual and physically based soil hydrology schemes against observations for the Amazon Basin, *Geosci. Model Dev.*, 7, 1115–1136, doi:10.5194/gmd-7-1115-2014, 2014.

505 Guimberteau, M., Ciais, P., Ducharne, A., Boisier, J. P., Dutra Aguiar, A. P., Biemans, H., De Deurwaerder, H., Galbraith, D., Kruijt, B., Langerwisch, F., Poveda, G., Rammig, A., Rodriguez, D. A., Tejada, G., Thonicke, K., Von Randow, C., Von Randow, R. C., Zhang, K. and Verbeeck, H.: Impacts of future deforestation and climate change on the hydrology of the Amazon Basin : a multi-model analysis with a new set of land-cover change scenarios, *Hydrol. EARTH Syst. Sci.*, 21(3), 1455–1475, doi:http://dx.doi.org/10.5194/hess-21-1455-2017, 2017.

Gundmundsson, L. and Cuntz, M.: Soil Parameter Model Intercomparison Project (SP-MIP): Assessing the influence of soil parameters on the variability of Land Surface Models, [online] Available from: https://www.gewexevents.org/wp-content/uploads/GLASS2017_SP-MIP_Protocol.pdf (Accessed 4 April 2019), 2017.

510 Guo, Z., Dirmeyer, P. A., Hu, Z.-Z., Gao, X. and Zhao, M.: Evaluation of the Second Global Soil Wetness Project soil moisture simulations: 2. Sensitivity to external meteorological forcing, *J. Geophys. Res. Atmospheres*, 111(D22), doi:10.1029/2006JD007845, 2006.

515 Haddeland, I., Clark, D. B., Franssen, W., Ludwig, F., Voß, F., Arnell, N. W., Bertrand, N., Best, M., Folwell, S., Gerten, D., Gomes, S., Gosling, S. N., Hagemann, S., Hanasaki, N., Harding, R., Heinke, J., Kabat, P., Koirala, S., Oki, T., Polcher, J., Stacke, T., Viterbo, P., Weedon, G. P. and Yeh, P.: Multimodel Estimate of the Global Terrestrial Water Balance: Setup and First Results, *J. Hydrometeorol.*, 12(5), 869–884, doi:10.1175/2011JHM1324.1, 2011.

Hengl, T., Jesus, J. M. de, MacMillan, R. A., Batjes, N. H., Heuvelink, G. B. M., Ribeiro, E., Samuel-Rosa, A., Kempen, B., Leenaars, J. G. B., Walsh, M. G. and Gonzalez, M. R.: SoilGrids1km — Global Soil Information Based on Automated Mapping, *PLOS ONE*, 9(8), e105992, doi:10.1371/journal.pone.0105992, 2014.

520 [Hengl, T., Jesus, J. M. de, Heuvelink, G. B. M., Gonzalez, M. R., Kilibarda, M., Blagotić, A., Shangguan, W., Wright, M. N., Geng, X., Bauer-Marschallinger, B., Guevara, M. A., Vargas, R., MacMillan, R. A., Batjes, N. H., Leenaars, J. G. B., Ribeiro, E., Wheeler, I., Mantel, S. and Kempen, B.: SoilGrids250m: Global gridded soil information based on machine learning, *PLOS ONE*, 12\(2\), e0169748, doi:10.1371/journal.pone.0169748, 2017.](#)

525 Jung, M., Reichstein, M., Ciais, P., Seneviratne, S. I., Sheffield, J., Goulden, M. L., Bonan, G., Cescatti, A., Chen, J., de Jeu, R., Dolman, A. J., Eugster, W., Gerten, D., Gianelle, D., Gobron, N., Heinke, J., Kimball, J., Law, B. E., Montagnani, L., Mu, Q., Mueller, B., Oleson, K., Papale, D., Richardson, A. D., Rouspard, O., Running, S., Tomelleri, E., Viovy, N., Weber, U., Williams, C., Wood, E., Zaehle, S. and Zhang, K.: Recent decline in the global land evapotranspiration trend due to limited moisture supply, *Nature*, 467(7318), 951–954, doi:10.1038/nature09396, 2010.

530 Kalnay, E., Kanamitsu, M., Kistler, R., Collins, W., Deaven, D., Gandin, L., Iredell, M., Saha, S., White, G., Woollen, J., Zhu, Y., Chelliah, M., Ebisuzaki, W., Higgins, W., Janowiak, J., Mo, K. C., Ropelewski, C., Wang, J., Leetmaa, A., Reynolds, R., Jenne, R. and Joseph, D.: The NCEP/NCAR 40-Year Reanalysis Project, *Bull. Am. Meteorol. Soc.*, 77(3), 437–472, doi:10.1175/1520-0477(1996)077<0437:TNYRP>2.0.CO;2, 1996.

535 Karambiri, H., Ribolzi, O., Delhoume, J. P., Ducloux, J., Coudrain-Ribstein, A. and Casenave, A.: Importance of soil surface characteristics on water erosion in a small grazed Sahelian catchment, *Hydrol. Process.*, 17(8), 1495–1507, doi:10.1002/hyp.1195, 2003.

[Kim, H.: Global Soil Wetness Project Phase 3 Atmospheric Boundary Conditions \(Experiment 1\), \[online\] Available from: https://doi.org/10.20783/DIAS.501, 2017.](#)

540 Kishné, A. S., Yimam, Y. T., Morgan, C. L. S. and Dornblaser, B. C.: Evaluation and improvement of the default soil hydraulic parameters for the Noah Land Surface Model, *Geoderma*, 285, 247–259, doi:10.1016/j.geoderma.2016.09.022, 2017.

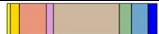
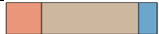
- Krinner, G., Viovy, N., Noblet-Ducoudré, N. de, Ogée, J., Polcher, J., Friedlingstein, P., Ciais, P., Sitch, S. and Prentice, I. C.: A dynamic global vegetation model for studies of the coupled atmosphere-biosphere system, *Glob. Biogeochem. Cycles*, 19(1), doi:10.1029/2003GB002199, 2005.
- 545 Lehmann, P., Merlin, O., Gentine, P. and Or, D.: Soil Texture Effects on Surface Resistance to Bare-Soil Evaporation, *Geophys. Res. Lett.*, 45(19), 10,398–10,405, doi:10.1029/2018GL078803, 2018.
- Li, J., Chen, F., Zhang, G., Barlage, M., Gan, Y., Xin, Y. and Wang, C.: Impacts of Land Cover and Soil Texture Uncertainty on Land Model Simulations Over the Central Tibetan Plateau, *J. Adv. Model. Earth Syst.*, 10(9), 2121–2146, doi:10.1029/2018MS001377, 2018.
- 550 ~~Lipiec, J., Kuś, J., Słowińska-Jurkiewicz, A. and Nosalewicz, A.: Soil porosity and water infiltration as influenced by tillage methods, *Soil Tillage Res.*, 89(2), 210–220, doi:10.1016/j.still.2005.07.012, 2006.~~
- Livneh, B., Kumar, R. and Samaniego, L.: Influence of soil textural properties on hydrologic fluxes in the Mississippi river basin, *Hydrol. Process.*, 29(21), 4638–4655, doi:10.1002/hyp.10601, 2015.
- 555 Looy, K. V., Bouma, J., Herbst, M., Koestel, J., Minasny, B., Mishra, U., Montzka, C., Nemes, A., Pachepsky, Y. A., Padarian, J., Schaap, M. G., Tóth, B., Verhoef, A., Vanderborght, J., Ploeg, M. J. van der, Weihermüller, L., Zacharias, S., Zhang, Y. and Vereecken, H.: Pedotransfer Functions in Earth System Science: Challenges and Perspectives, *Rev. Geophys.*, 55(4), 1199–1256, doi:10.1002/2017RG000581, 2017.
- Martens, B., Miralles, D. G., Lievens, H., Schalie, R. van der, Jeu, R. A. M. de, Fernández-Prieto, D., Beck, H. E., Dorigo, W. A. and Verhoest, N. E. C.: GLEAM v3: satellite-based land evaporation and root-zone soil moisture, *Geosci. Model Dev.*, 10(5), 1903–1925, doi:https://doi.org/10.5194/gmd-10-1903-2017, 2017.
- 560 Milly, P. C. D. and Dunne, K. A.: Sensitivity of the Global Water Cycle to the Water-Holding Capacity of Land, *J. Clim.*, 7(4), 506–526, doi:10.1175/1520-0442(1994)007<0506:SOTGWC>2.0.CO;2, 1994.
- Montzka, C., Herbst, M., Weihermüller, L., Verhoef, A. and Vereecken, H.: A global data set of soil hydraulic properties and sub-grid variability of soil water retention and hydraulic conductivity curves, *Earth Syst. Sci. Data*, 9(2), 529–543, doi:https://doi.org/10.5194/essd-9-529-2017, 2017.
- 565 Mostovoy, G. V. and Anantharaj, V. G.: Observed and Simulated Soil Moisture Variability over the Lower Mississippi Delta Region, *J. Hydrometeorol.*, 9(6), 1125–1150, doi:10.1175/2008JHM999.1, 2008.
- Mualem, Y.: A new model for predicting the hydraulic conductivity of unsaturated porous media, *Water Resour. Res.*, 12(3), 513–522, doi:10.1029/WR012i003p00513, 1976.
- 570 Nachtergaele, F. O., Velthuisen, H. van, Verelst, L., Batjes, N. H., Dijkshoorn, J. A., Engelen, V. W. P. van, Fischer, G., Jones, A., Montanarella, L., Petri, M., Prieler, S., Shi, X., Teixeira, E. and Wiberg, D.: The Harmonized World Soil Database, 2010.
- Osman, K. T.: *Soils: Principles, Properties and Management*, Springer Netherlands. [online] Available from: <https://www.springer.com/gp/book/9789400756625> (Accessed 22 May 2019), 2013.
- 575 Priestley, C. H. B. and Taylor, R. J.: On the Assessment of Surface Heat Flux and Evaporation Using Large-Scale Parameters, *Mon. Weather Rev.*, 100(2), 81–92, doi:10.1175/1520-0493(1972)100<0081:OTAOSH>2.3.CO;2, 1972.
- 580 Rahmati, M., Weihermüller, L., Vanderborght, J., Pachepsky, Y. A., Mao, L., Sadeghi, S. H., Moosavi, N., Kheirfam, H., Montzka, C., Looy, K. V., Toth, B., Hazbavi, Z., Yamani, W. A., Albalasmeh, A. A., Alghzawi, M. Z., Angulo-Jaramillo, R., Antonino, A. C. D., Arampatzis, G., Armindo, R. A., Asadi, H., Bamutaze, Y., Batlle-Aguilar, J., Béchet, B., Becker, F., Blöschl, G., Bohne, K., Braud, I., Castellano, C., Cerdà, A., Chalhoub, M., Cichota, R., Císlarová, M., Clothier, B., Coquet, Y., Cornelis, W., Corradini, C., Coutinho, A. P., Oliveira, M. B. de, Macedo, J. R. de, Durães, M. F., Emami, H., Eskandari, I., Farajnia, A., Flammini, A., Fodor, N., Gharaibeh, M., Ghavimippanah, M. H., Ghezzehei, T. A., Giertz, S., Hatzigiannakis, E. G., Horn, R., Jiménez, J. J., Jacques, D., Keesstra, S. D., Kelishadi, H., Kiani-Harchegani, M., Kouselou, M., Kumar Jha, M., Lassabatere, L., Li, X., Liebig, M. A., Lichner, L., López, M. V., Machiwal, D., Mallants, D., Mallmann, M. S., Marques, O., De, J. D., Marshall, M. R., Mertens, J., Meunier, F., Mohammadi, M. H., Mohanty, B. P., Pulido-Moncada, M., 585 Montenegro, S., Morbidelli, R., Moret-Fernández, D., Moosavi, A. A., Mosaddeghi, M. R., Mousavi, S. B., Mozaffari, H., Nabiollahi, K., Neyshabouri, M. R., Ottoni, M. V., Filho, O., Benedicto, T., Pahlavan-Rad, M. R., Panagopoulos, A., Peth, S., Peyneau, P.-E., Picciafuoco, T., Poesen, J., Pulido, M., Reinert, D. J., Reinsch, S., Rezaei, M., Roberts, F. P., Robinson, D., Rodrigo-Comino, J., et al.: Development and analysis of the Soil Water Infiltration Global database, *Earth Syst. Sci. Data*, 10(3), 1237–1263, doi:https://doi.org/10.5194/essd-10-1237-2018, 2018.

- 590 Rawls, W. J., Brakensiek, D. L., Simanton, J. R. and Kohl, K. D.: Development of a crust factor for a Green-Ampt model, *Trans. ASAE*, 33(4), 1224–1228, 1990.
- Rawls, W. J., Ahuja, L. R., Brakensiek, D. L. and Shirmohammadi, A.: Infiltration and soil water movement, in: *Handbook of Hydrology*, New York. Available from: <https://ci.nii.ac.jp/naid/10018251877/> (Accessed 23 May 2019), 1993.
- 595 Remaud, M., Chevallier, F., Cozic, A., Lin, X. and Bousquet, P.: On the impact of recent developments of the LMDz atmospheric general circulation model on the simulation of CO₂ transport, *Geosci. Model Dev.*, 11(11), 4489–4513, doi:10.5194/gmd-11-4489-2018, 2018.
- Reynolds, C. A., Jackson, T. J. and Rawls, W. J.: Estimating soil water-holding capacities by linking the Food and Agriculture Organization Soil map of the world with global pedon databases and continuous pedotransfer functions, *Water Resour. Res.*, 36(12), 3653–3662, doi:10.1029/2000WR900130, 2000.
- 600 Rodell, M., Beaudoin, H. K., L'Ecuyer, T. S., Olson, W. S., Famiglietti, J. S., Houser, P. R., Adler, R., Bosilovich, M. G., Clayson, C. A., Chambers, D., Clark, E., Fetzer, E. J., Gao, X., Gu, G., Hilburn, K., Huffman, G. J., Lettenmaier, D. P., Liu, W. T., Robertson, F. R., Schlosser, C. A., Sheffield, J. and Wood, E. F.: The Observed State of the Water Cycle in the Early Twenty-First Century, *J. Clim.*, 28(21), 8289–8318, doi:10.1175/JCLI-D-14-00555.1, 2015.
- 605 [Samaniego, L., Kumar, R. and Attinger, S.: Multiscale parameter regionalization of a grid-based hydrologic model at the mesoscale. *Water Resour. Res.*, 46\(5\), doi:10.1029/2008WR007327, 2010.](#)
- Schaap, M. G., Leij, F. J. and van Genuchten, M. T.: rosetta: a computer program for estimating soil hydraulic parameters with hierarchical pedotransfer functions, *J. Hydrol.*, 251(3), 163–176, doi:10.1016/S0022-1694(01)00466-8, 2001.
- Smettem, K. R. J.: Characterization of water entry into a soil with a contrasting textural class: spatial variability of infiltration parameters and influence of macroporosity, *Soil Sci.*, 144(3), 167–174, 1987.
- 610 Song, R., Chu, G., Ye, J., Bai, L., Zhang, R. and Yang, J.: Effects of surface soil mixed with sand on water infiltration and evaporation in laboratory, *Editor. Off. Trans. Chin. Soc. Agric. Eng.*, 26(1), 109–114, 2010.
- [Spaargaren, O. C. and Deckers, J.: The World Reference Base for Soil Resources, in *Soils of Tropical Forest Ecosystems*, edited by A. Schulte and D. Ruhiyat, pp. 21–28, Springer, Berlin, Heidelberg., 1998.](#)
- 615 [Stamm, J. F., Wood, E. F. and Lettenmaier, D. P.: Sensitivity of a GCM Simulation of Global Climate to the Representation of Land-Surface Hydrology, *J. Clim.*, 7\(8\), 1218–1239, doi:10.1175/1520-0442\(1994\)007<1218:SOAGSO>2.0.CO;2, 1994.](#)
- Sterling, S. M., Ducharne, A. and Polcher, J.: The impact of global land-cover change on the terrestrial water cycle, *Nat. Clim. Change*, 3(4), 385–390, doi:10.1038/nclimate1690, 2013.
- Sun, D., Yang, H., Guan, D., Yang, M., Wu, J., Yuan, F., Jin, C., Wang, A. and Zhang, Y.: The effects of land use change on soil infiltration capacity in China: A meta-analysis, *Sci. Total Environ.*, 626, 1394–1401, doi:10.1016/j.scitotenv.2018.01.104, 2018.
- 620 USDA Soil Survey Staff and Bureau of Plant Industry, Soils and agricultural Engineering: Soil survey manual, Agricultural Research Administration, U.S. Dept. of Agriculture, Washington, D.C., 1951.
- Valentin, C.: Surface sealing as affected by various rock fragment covers in West Africa, *CATENA*, 23(1), 87–97, doi:10.1016/0341-8162(94)90055-8, 1994.
- 625 Valentin, C. and Bresson, L.-M.: Morphology, genesis and classification of surface crusts in loamy and sandy soils, *Geoderma*, 55(3), 225–245, doi:10.1016/0016-7061(92)90085-L, 1992.
- Valentin, C., Agus, F., Alamban, R., Boosaner, A., Bricquet, J. P., Chaplot, V., de Guzman, T., de Rouw, A., Janeau, J. L., Orange, D., Phachomphonh, K., Do Duy Phai, Podwojewski, P., Ribolzi, O., Silvera, N., Subagyono, K., Thiébaux, J. P., Tran Duc Toan and Vadari, T.: Runoff and sediment losses from 27 upland catchments in Southeast Asia: Impact of rapid land use changes and conservation practices, *Agric. Ecosyst. Environ.*, 128(4), 225–238, doi:10.1016/j.agee.2008.06.004, 2008.
- 630 Van den Hurk, B., Kim, H., Krinner, G., Seneviratne, S. I., Derksen, C., Oki, T., Douville, H., Colin, J., Ducharne, A., Cheruy, F., Viovy, N., Puma, M. J., Wada, Y., Li, W., Jia, B., Alessandri, A., Lawrence, D. M., Weedon, G. P., Ellis, R., Hagemann, S., Mao, J., Flanner, M. G., Zampieri, M., Matera, S., Law, R. M. and Sheffield, J.: LS3MIP (v1.0) contribution

- 635 to CMIP6: the Land Surface, Snow and Soil moisture Model Intercomparison Project – aims, setup and expected outcome, *Geosci Model Dev*, 9(8), 2809–2832, doi:10.5194/gmd-9-2809-2016, 2016.
- Van Genuchten, M.: A Closed-form Equation for Predicting the Hydraulic Conductivity of Unsaturated Soils 1, *Soil Sci. Soc. Am. J.*, 44(5), 892–898, doi:10.2136/sssaj1980.03615995004400050002x, 1980.
- 640 Vereecken, H., Pachepsky, Y., Bogaen, H. and Montzka, C.: Upscaling Issues in Ecohydrological Observations, in *Observation and Measurement of Ecohydrological Processes*, edited by X. Li and H. Vereecken, pp. 435–454, Springer Berlin Heidelberg, Berlin, Heidelberg., 2019.
- Wang, F., Cheruy, F. and Dufresne, J.-L.: The improvement of soil thermodynamics and its effects on land surface meteorology in the IPSL climate model, *Geosci. Model Dev.*, 9(1), 363–381, doi:https://doi.org/10.5194/gmd-9-363-2016, 2016.
- 645 [Wang, F., Ducharne, A., Cheruy, F., Lo, M.-H. and Grandpeix, J.-Y.: Impact of a shallow groundwater table on the global water cycle in the IPSL land–atmosphere coupled model, *Clim. Dyn.*, 50\(9\), 3505–3522, doi:10.1007/s00382-017-3820-9, 2018.](#)
- Wang, T., Istanbuluoglu, E., Lenters, J. and Scott, D.: On the role of groundwater and soil texture in the regional water balance: An investigation of the Nebraska Sand Hills, USA, *Water Resour. Res.*, 45(10), W10413, doi:10.1029/2009WR007733, 2009.
- 650 Wei, Y., Liu, S., Huntzinger, D. N., Michalak, A. M., Viovy, N., Post, W. M., Schwalm, C. R., Schaefer, K., Jacobson, A. R., Lu, C., Tian, H., Ricciuto, D. M., Cook, R. B., Mao, J. and Shi, X.: The North American carbon program multi-scale synthesis and terrestrial model intercomparison project – Part 2: Environmental driver data, *Geosci. Model Dev. Discuss.*, 7, 2875–2893, 2014.
- 655 Xia, Y., Ek, M. B., Wu, Y., Ford, T. and Quiring, S. M.: Comparison of NLDAS-2 Simulated and NASMD Observed Daily Soil Moisture. Part II: Impact of Soil Texture Classification and Vegetation Type Mismatches, *J. Hydrometeorol.*, 16(5), 1981–2000, doi:10.1175/JHM-D-14-0097.1, 2015.
- Yair, A.: Runoff generation in a sandy area—the nizzana sands, Western Negev, Israel, *Earth Surf. Process. Landf.*, 15(7), 597–609, doi:10.1002/esp.3290150703, 1990.
- 660 Yin, Z., Otle, C., Ciais, P., Guimberteau, M., Wang, X., Zhu, D., Maignan, F., Peng, S., Piao, S., Polcher, J., Zhou, F. and Kim, H.: Evaluation of ORCHIDEE-MICT-simulated soil moisture over China and impacts of different atmospheric forcing data, *Hydrol. Earth Syst. Sci.*, 22(10), 5463–5484, doi:10.5194/hess-22-5463-2018, 2018.
- 665 Zhao, F., Veldkamp, T. I. E., Frieler, K., Schewe, J., Ostberg, S., Willner, S., Schauburger, B., Gosling, S. N., Schmied, H. M., Portmann, F. T., Leng, G., Huang, M., Liu, X., Tang, Q., Hanasaki, N., Biemans, H., Gerten, D., Satoh, Y., Pokhrel, Y., Stacke, T., Ciais, P., Chang, J., Ducharne, A., Guimberteau, M., Wada, Y., Kim, H. and Yamazaki, D.: The critical role of the routing scheme in simulating peak river discharge in global hydrological models, *Environ. Res. Lett.*, 12(7), 075003, doi:10.1088/1748-9326/aa7250, 2017.
- Zheng, H. and Yang, Z.-L.: Effects of soil-type datasets on regional terrestrial water cycle simulations under different climatic regimes, *J. Geophys. Res. Atmospheres*, 121(24), 14387–14402, doi:10.1002/2016JD025187, 2016.
- 670 Zobler, L.: A world soil hydrology file for global climate modeling. National Aeronautics and Space Administration, Technical memorandum 87802, 1986.

675 **Tables and Figures**

Table 1. Summary of the experiments used in this study. Texture distribution displays the percentage of each soil texture in the used soil map.* Indicates the experiments used in the SP-MIP. [See Figure 1 for color codes.](#)

Experiment	Soil map	Climate Forcing	PTF	Text.Distrib
EXP1	Reynolds	CRU-NCEP	Carsel & Parrish (1988)	
EXP2	Reynolds	GSWP3	Carsel & Parrish (1988)	
EXP3*	Zobler	GSWP3	Carsel & Parrish (1988)	
EXP4*	SP-MIPoilGrids	GSWP3	Carsel & Parrish (1988)	
EXP5*	SP-MIPoilGrids	GSWP3	Schaap et al. (2001)	
EXP6*	Loam	GSWP3	Schaap et al. (2001)	
EXP7*	Silt	GSWP3	Schaap et al. (2001)	
EXP8*	Loamy Sand	GSWP3	Schaap et al. (2001)	
EXP9*	Clay	GSWP3	Schaap et al. (2001)	

680

Table 2. Percent sand, silt and clay contents of the geometric centroids of the 12 USDA soil texture classes. *dm*: the computed median diameter.

Texture class	Label	% Clay	% Silt	% Sand	<i>dm</i> (μm)
Clay	C	62.9	17.5	19.5	1.6
Silty Clay	SiC	46.7	46.7	6.7	5.4
Silty Clay Loam	SiCL	33.8	56.3	10.0	15.9
Clay Loam	CL	33.8	33.8	32.5	25.1
Silt	Si	5.3	87.3	7.3	26.6
Silt Loam	SiL	13.4	65.2	21.4	29.0
Loam	L	18.7	40.2	41.0	39.3
Sandy Clay	SaC	41.7	6.7	51.7	112.9
Sandy Clay Loam	SaCL	27.1	12.9	59.9	373.3
Sandy Loam	SaL	10.4	25.1	64.6	490.7
Loamy Sand	LSa	5.8	12.5	81.7	806.1
Sand	Sa	3.3	5.0	91.7	936.4

685 [Table 3. Percent overlap between the three tested soil texture maps.](#)

	SP-MIP	Reynolds	Zobler
SP-MIP	100.0	-	-
Reynolds	41.2	100.0	-
Zobler	46.0	52.0	100.0
Unif. Loam	48.5	43.9	64.3
Unif. Silt	3.3	0.0	0.0
Unif. Loamy Sand	2.1	6.0	0.0
Unif. Clay	2.7	5.8	0.0

Table 4. Statistical descriptors of the soil parameter maps corresponding to the three complex soil texture maps (excluding Antarctica Greenland): mean and standard deviation (SD) of each parameter map; and correlation coefficients between the three pair of maps.

		<u>SP-MIP</u>	<u>Reynolds</u>	<u>Zobler</u>
<u>log(dm)</u>	<u>Mean (log μm)</u>	<u>4.48</u>	<u>4.23</u>	<u>4.25</u>
	<u>SD (log μm)</u>	<u>1.51</u>	<u>1.65</u>	<u>1.15</u>
	<u>Cor. SP-MIP</u>	<u>1.00</u>	<u>0.38</u>	<u>0.35</u>
	<u>Cor. Reynolds</u>	<u>0.38</u>	<u>1.00</u>	<u>0.57</u>
<u>K_s</u>	<u>Mean (mm/d)</u>	<u>740</u>	<u>643</u>	<u>428</u>
	<u>SD (mm/d)</u>	<u>1539</u>	<u>1261</u>	<u>376</u>
	<u>Cor. SP-MIP</u>	<u>1.00</u>	<u>0.38</u>	<u>0.36</u>
	<u>Cor. Reynolds</u>	<u>0.38</u>	<u>1.00</u>	<u>0.57</u>
<u>Saturated water content</u>	<u>Mean (m³/m³)</u>	<u>0.414</u>	<u>0.416</u>	<u>0.422</u>
	<u>SD (m³/m³)</u>	<u>0.017</u>	<u>0.018</u>	<u>0.010</u>
	<u>Cor. SP-MIP</u>	<u>1.00</u>	<u>0.40</u>	<u>0.22</u>
	<u>Cor. Reynolds</u>	<u>0.40</u>	<u>1.0</u>	<u>0.35</u>
<u>Field capacity</u>	<u>Mean (m³/m³)</u>	<u>0.177</u>	<u>0.182</u>	<u>0.170</u>
	<u>SD (m³/m³)</u>	<u>0.064</u>	<u>0.069</u>	<u>0.046</u>
	<u>Cor. SP-MIP</u>	<u>1.00</u>	<u>0.41</u>	<u>0.36</u>
	<u>Cor. Reynolds</u>	<u>0.41</u>	<u>1.00</u>	<u>0.58</u>
<u>Wilting point</u>	<u>Mean (m³/m³)</u>	<u>0.104</u>	<u>0.107</u>	<u>0.092</u>
	<u>SD (m³/m³)</u>	<u>0.044</u>	<u>0.054</u>	<u>0.026</u>
	<u>Cor. SP-MIP</u>	<u>1.00</u>	<u>0.42</u>	<u>0.36</u>
	<u>Cor. Reynolds</u>	<u>0.42</u>	<u>1.00</u>	<u>0.58</u>
<u>AWC</u>	<u>Mean (mm)</u>	<u>146.7</u>	<u>150.2</u>	<u>156.5</u>
	<u>SD (mm)</u>	<u>56.9</u>	<u>54.4</u>	<u>39.8</u>
	<u>Cor. SP-MIP</u>	<u>1.00</u>	<u>0.34</u>	<u>0.31</u>
	<u>Cor. Reynolds</u>	<u>0.34</u>	<u>1.00</u>	<u>0.42</u>

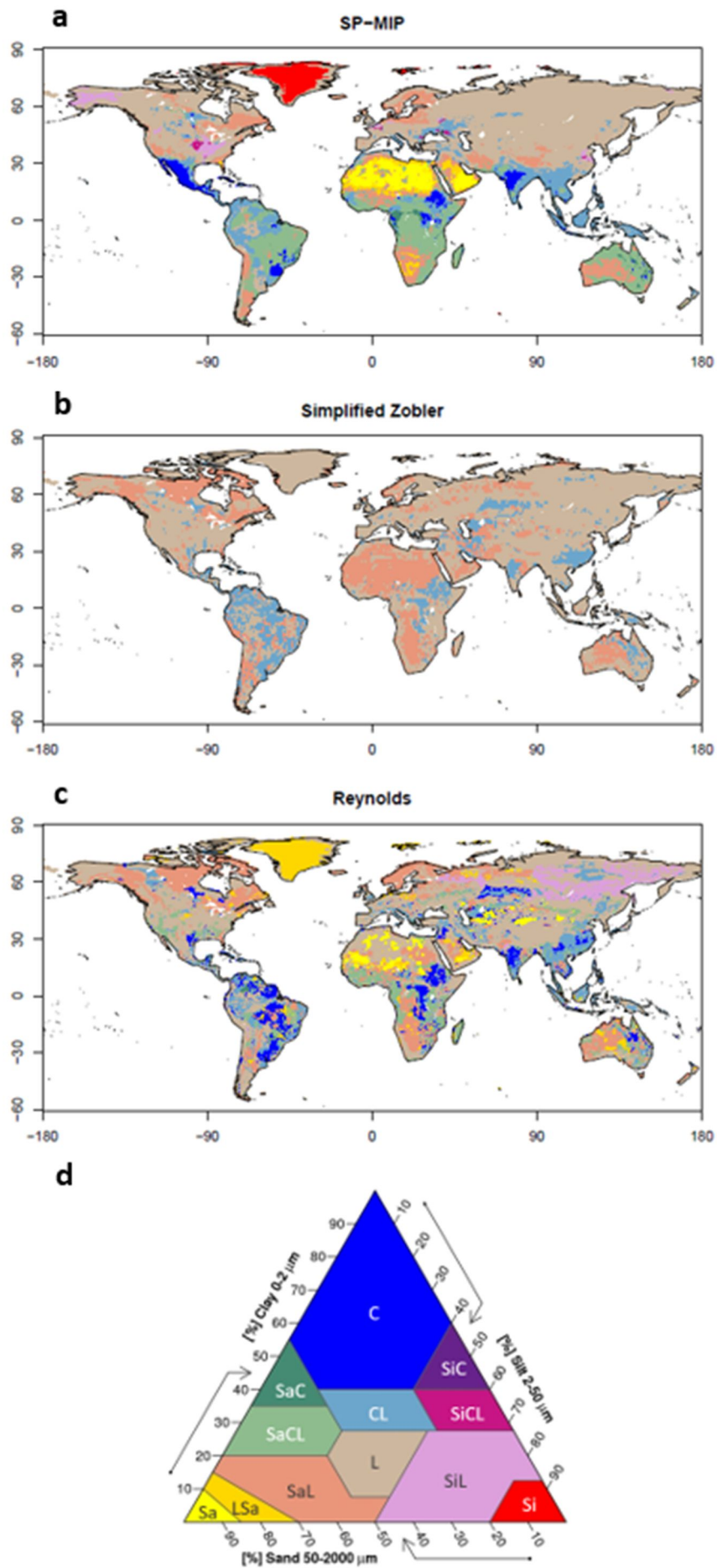


Figure 1. (a-c) Global maps of soil texture classes used in this study. (d) Soil texture triangle of the 12 textural classes as defined by the USDA. For texture labels see Table 2.

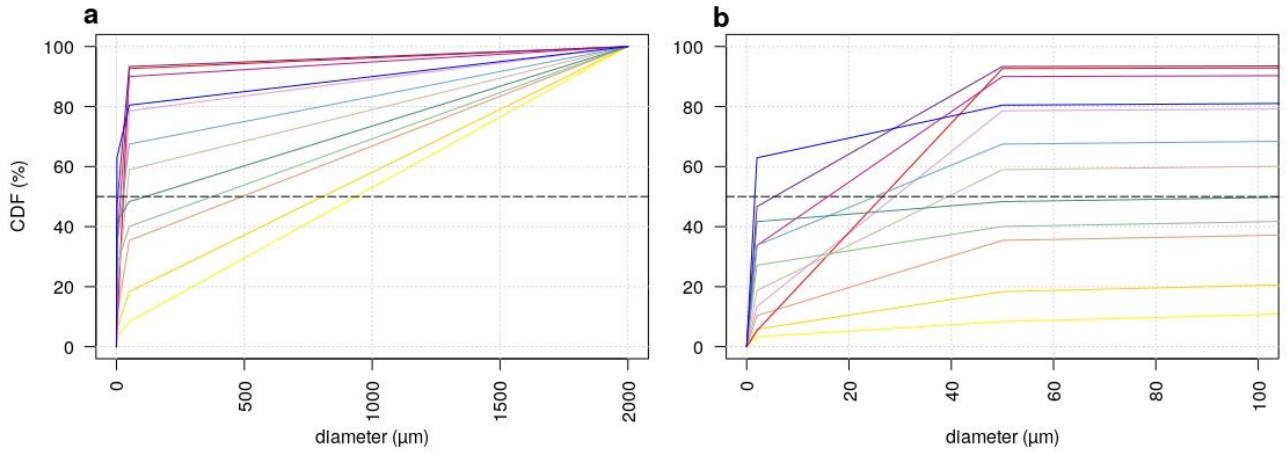


Figure 2. (a) Cumulative grain size distribution curves of the 12 USDA soil texture classes and (b) zoom over diameter interval [0,100 μm]. The dashed line defines the 50% cumulative value.

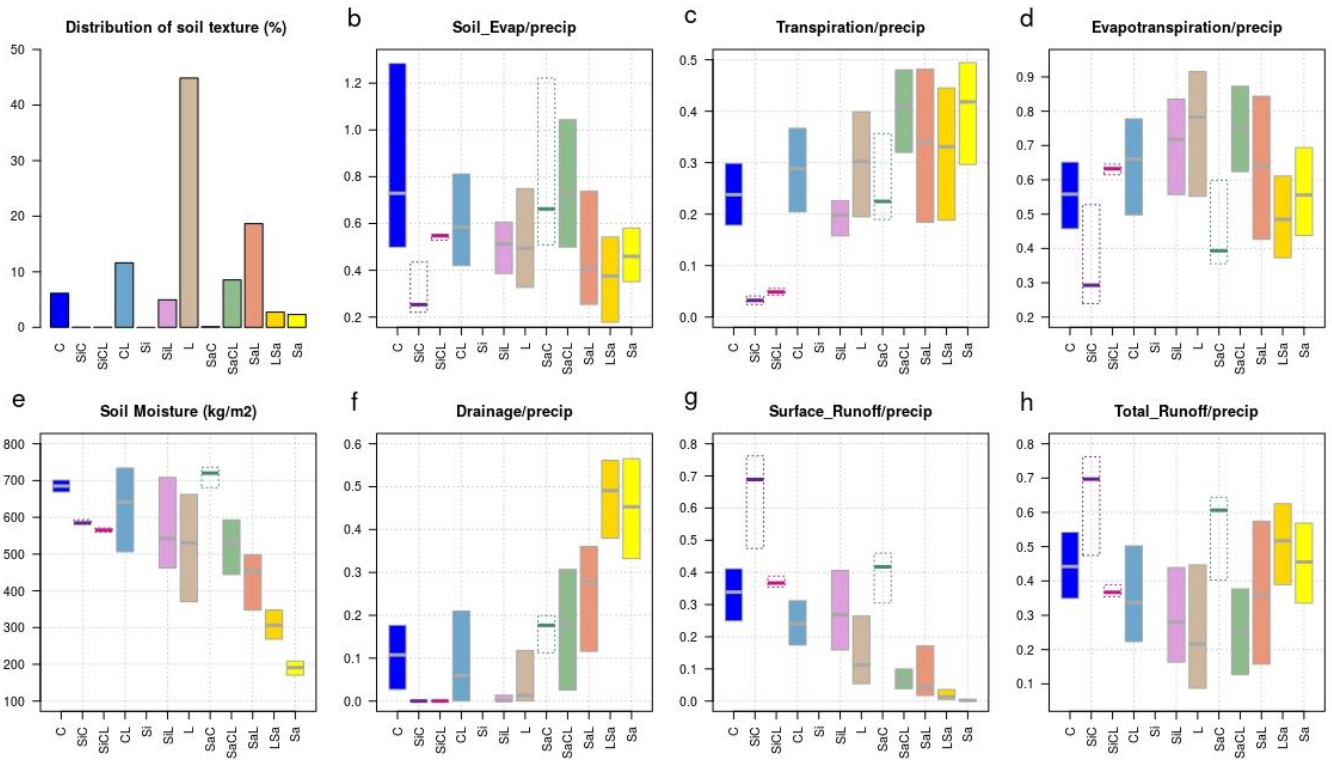


Figure 3. Variability of simulated variables of EXP2 over the land surface excluding Antarctica and Greenland, over the period 1980-2010, within each soil texture class. Soil texture classes are sorted from the finest to the coarsest based on dm (from left to right). See Figure 1 for color codes. Note that the Silt class is absent from Reynolds map. Dashed boxes correspond to texture classes covering less than 0.2% of the land area. Water fluxes are expressed as percent of mean precipitation. Soil moisture is averaged over areas with similar annual precipitation (between 1 and 2 mm/d), to remove impact of precipitation variation. Transpiration and soil evaporation fluxes are averaged over vegetated and bare soil fractions of the grid cells respectively.

710

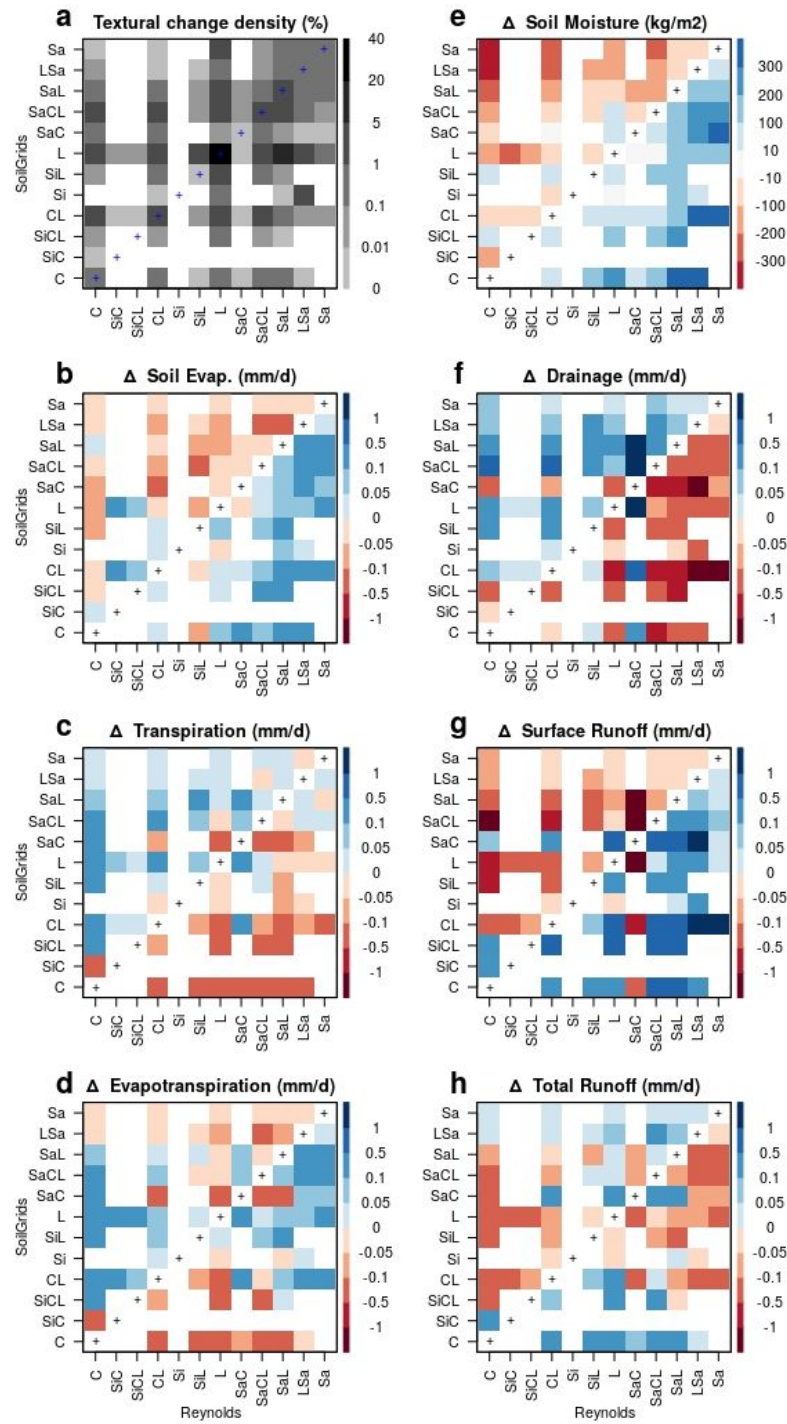
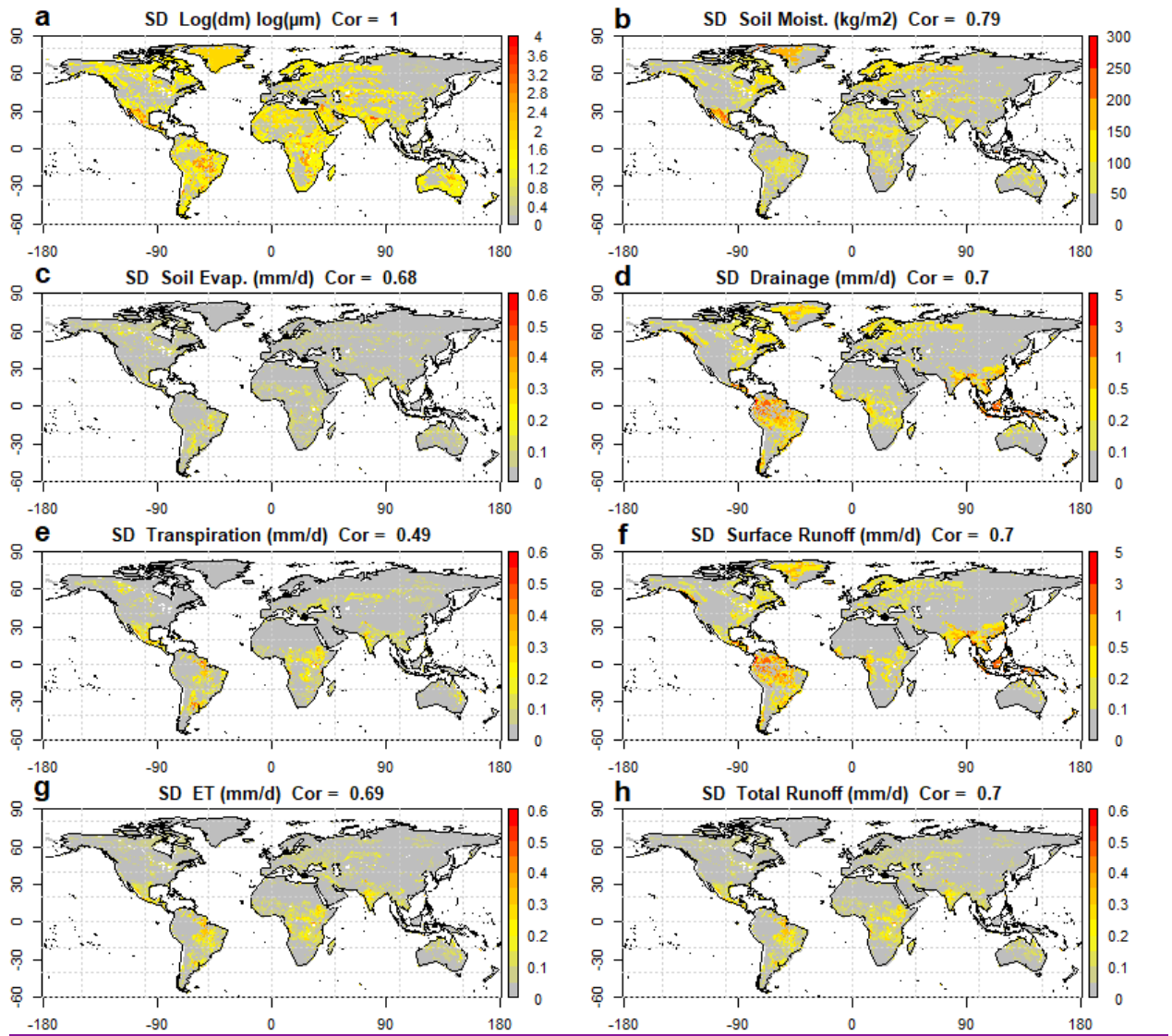


Figure 4. Change in mean simulated variables over the globe land surface excluding Antarctica, averaged over the period 1980-2010, caused by changing the soil texture map from Reynolds to SP-MIPsoilGrids (EXP2 to EXP4). Soil texture classes are sorted from the finest (clay) to the coarsest (sand), in the x and y axis. The first plot illustrates the percentage of each textural change.

715

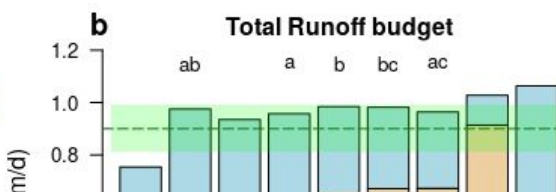
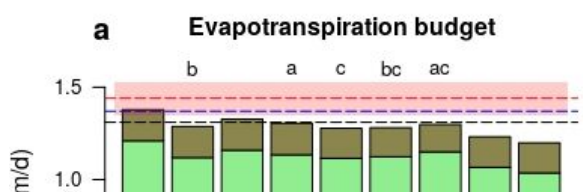
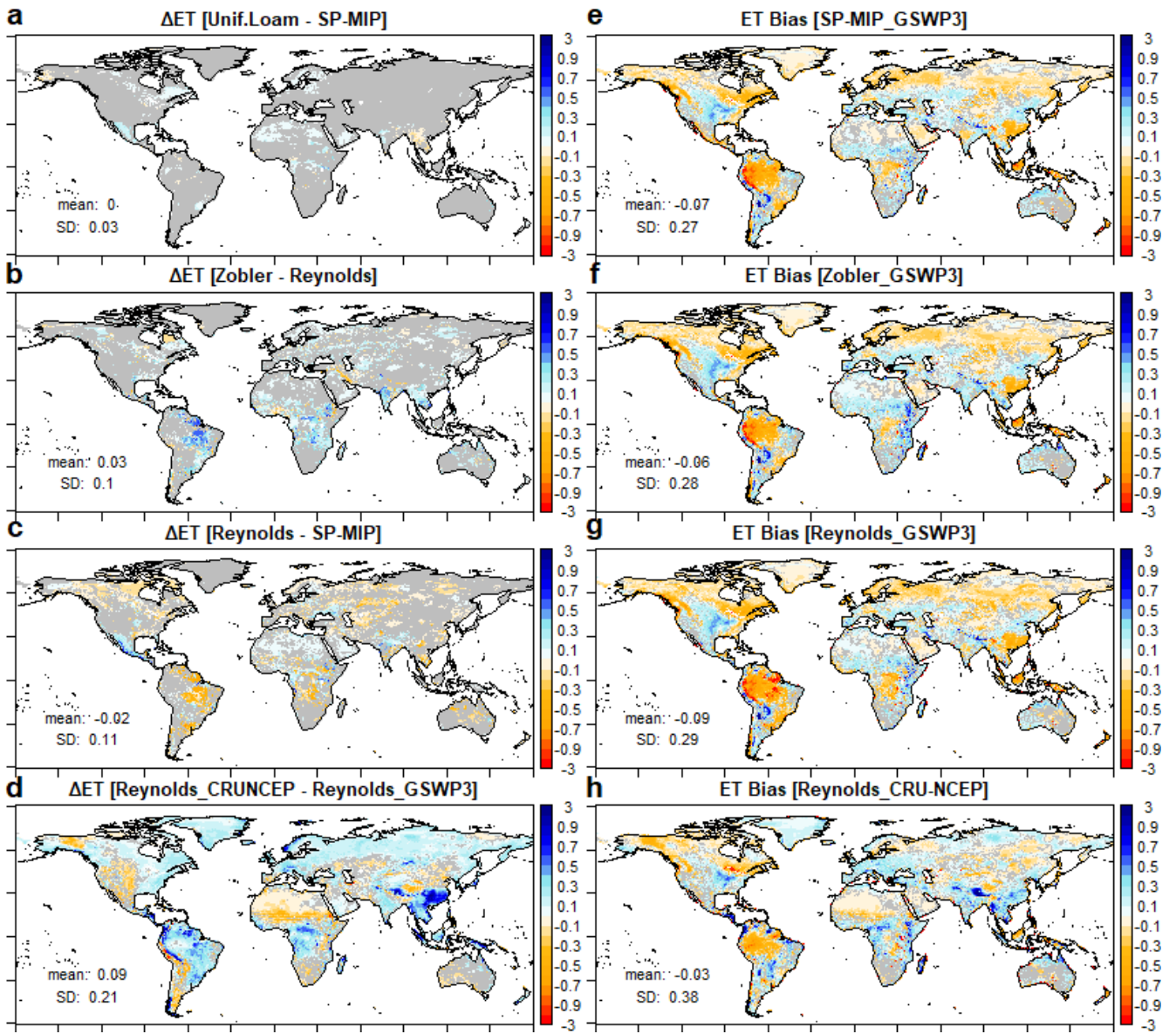
720



725

Figure 5 Maps of the standard deviation (SD) of (a) the logarithm of median particle diameter (d_m) given by the three complex soil texture maps (Reynolds, Zobler, SP-MIP), and (b-h) the mean annual simulated variables (in mm/d except for soil moisture in mm) using the three different maps. The Spearman rank correlation between the standard deviation of $\log(d_m)$ and the standard deviation of each variable is indicated above each map (Cor). The range of the color bar on each map extends from 0 to the rounded maximum value in the map. [AD1]

730



740

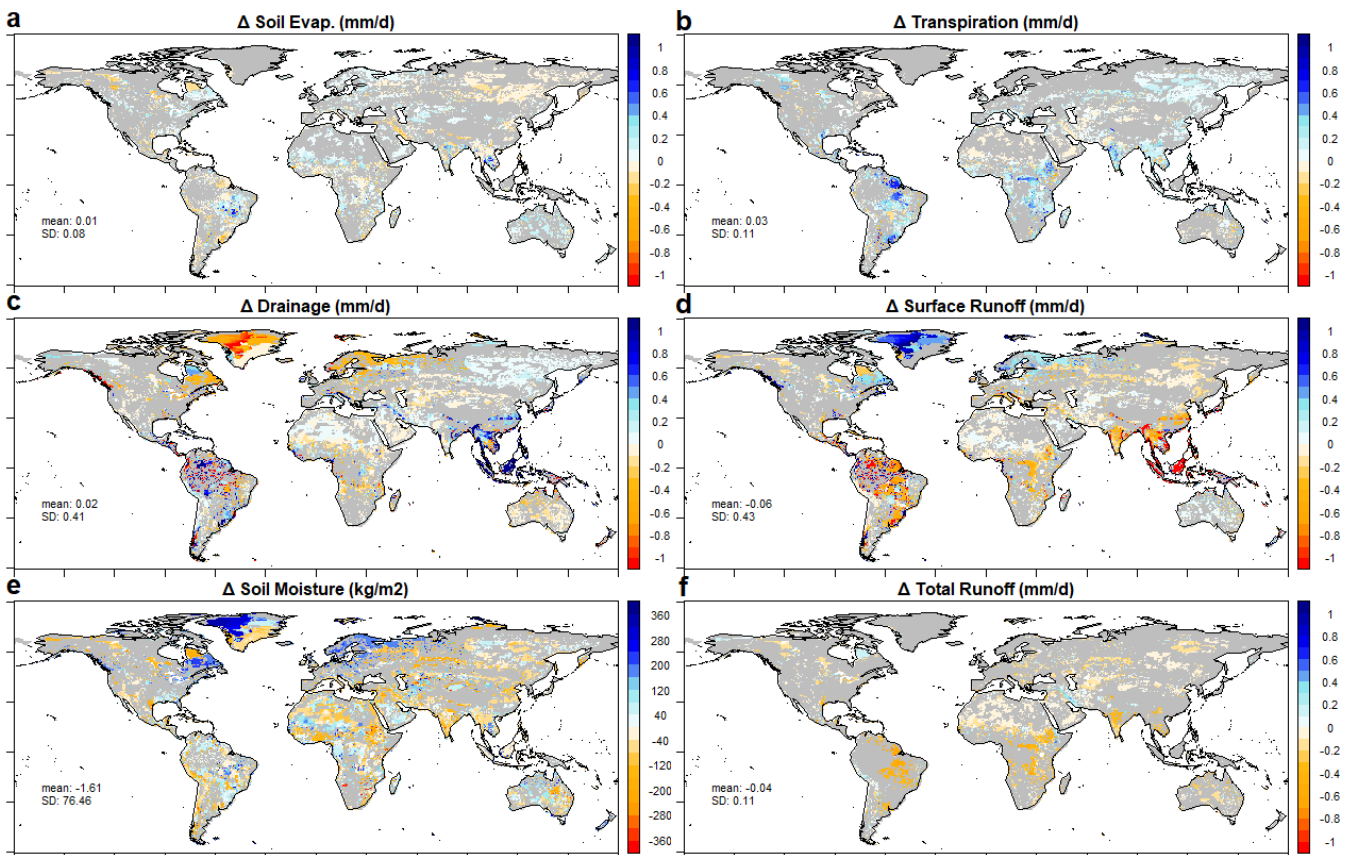
Figure 5. Terrestrial water budget components for the nine simulations of Table 1, on average over 1980-2010 and over all land areas but Antarctica: (a) Evapotranspiration budget, (b) Total runoff budget, (c) Soil moisture. Letters above bars describe statistical significance; the mean difference between bars with the same letter is not statistically significant based on Student's t-test (with a p-value of 5%). Red and green semi-transparent bands show the uncertainty range in the estimates of Rodell et al. (2015), for evapotranspiration and total runoff respectively. The estimated values of evapotranspiration and total runoff used for evaluation are described in section 2.3.

745

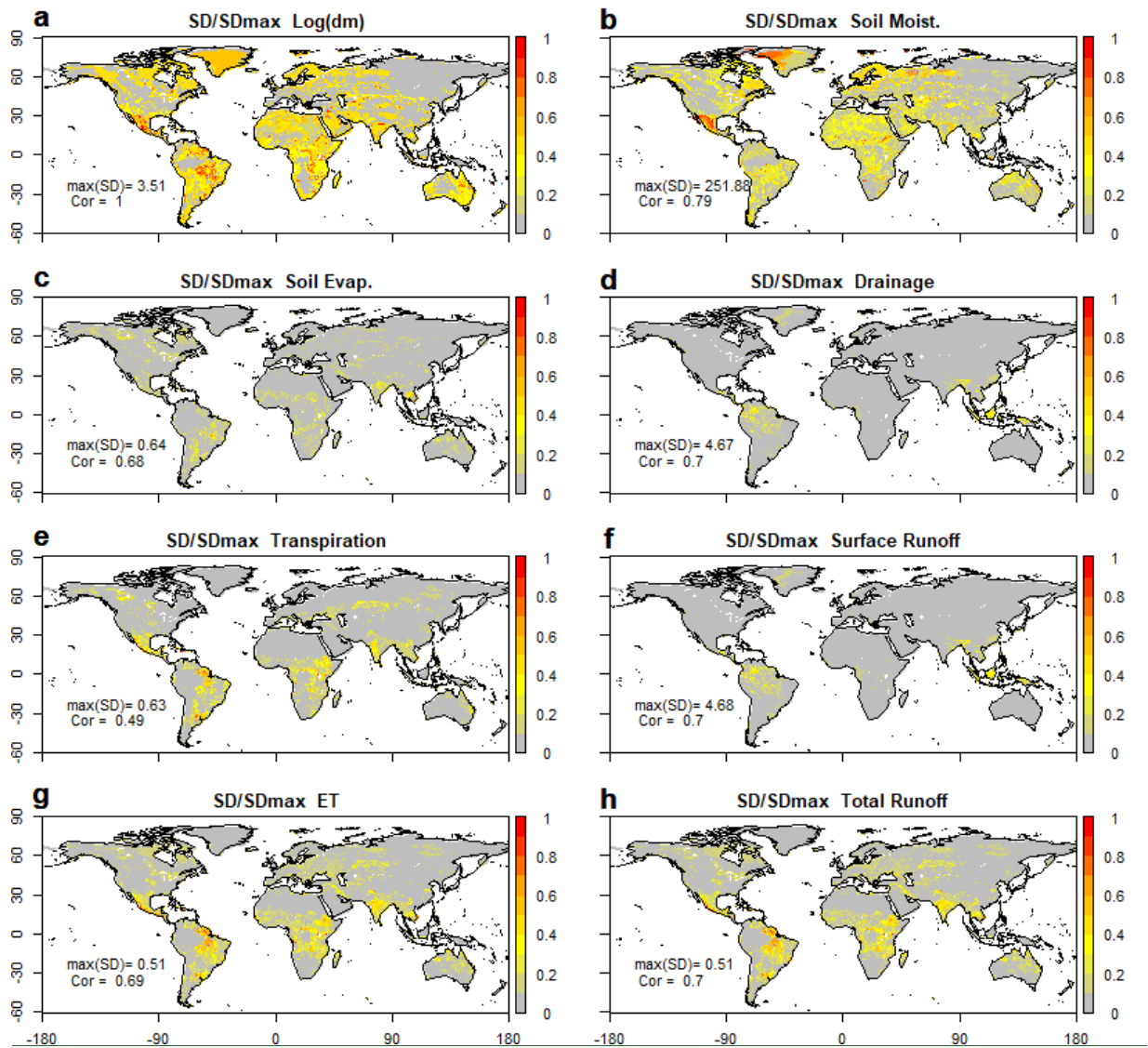
Figure 56. Spatial distribution of simulated annual mean evapotranspiration (averaged over 1980-2010): (left) differences between selected pairs of simulations (a: EXP6-EXP5, b: EXP3- EXP2, c: EXP2-EXP4, d: EXP1-EXP2); (right) biases with respect to GLEAM product (e: EXP4, f: EXP3, g: EXP2, h: EXP1). Grey color indicates that the difference is not statistically significant based on Student's t-test (with a p-value of 5% < 0.05). The printed means and standard deviation correspond to the full land area excluding Antarctica. Maps of GLEAM and simulated evapotranspiration of the 9 experiments are presented in Supplementary Figure S2.

750

755



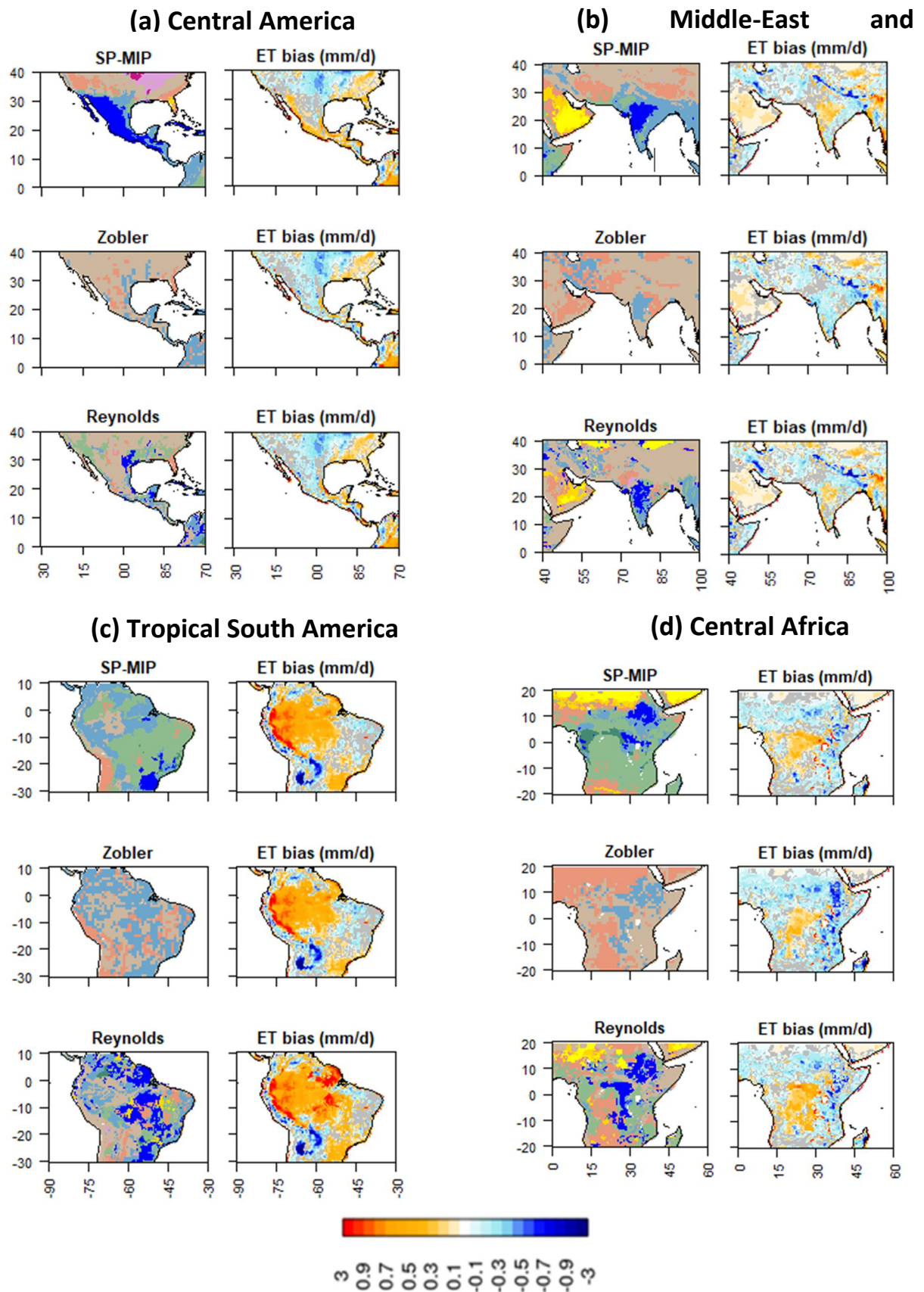
760 Figure 67. Difference in simulated variables (averaged over the period 1980-2010) when Reynolds map is replaced by a Zobler map (EXP3 – EXP2), averaged over the period 1980-2010. The corresponding difference for evapotranspiration is shown in Fig. 56b. Grey color indicates that the difference is not statistically significant based on Student's t-test (with a p-value $\leq 0.05\%$). Mean and standard deviation are averaged over the globe excluding Antarctica.



765

Figure 7. Maps of the standard deviation (SD) of (a) the logarithm of median particle diameter (dm) given by the three complex soil texture maps (Reynolds, Zobler, SP-MIP), and (b-h) the mean annual simulated variables (in mm/d except for soil moisture in mm) using the three different maps. For easier comparison, each SD map is normalized by the maximum standard deviation of the map (maxSD), indicated in each map, with the spatial correlation coefficient (Cor) between the standard deviation of $\log(dm)$ and the standard deviation of each variable.

770



775

Figure 8. Regional zooms on soil texture maps and the corresponding evapotranspiration bias maps (with respect to the GLEAM product) in four different areas. The colors scale on the right corresponds to the evapotranspiration bias maps, in which the grey color indicates that the bias is not statistically significant using Student's t-test with a p-value < 0.05 . The colors of the soil texture maps are defined in Figure 1d.

780

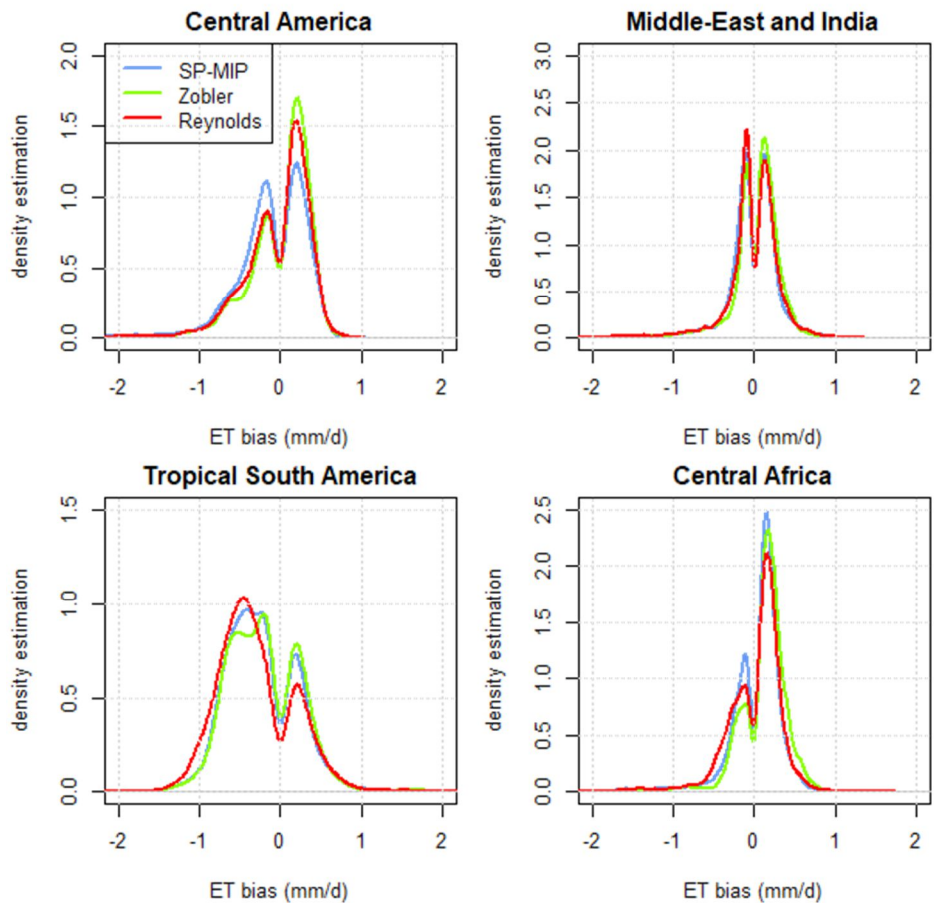


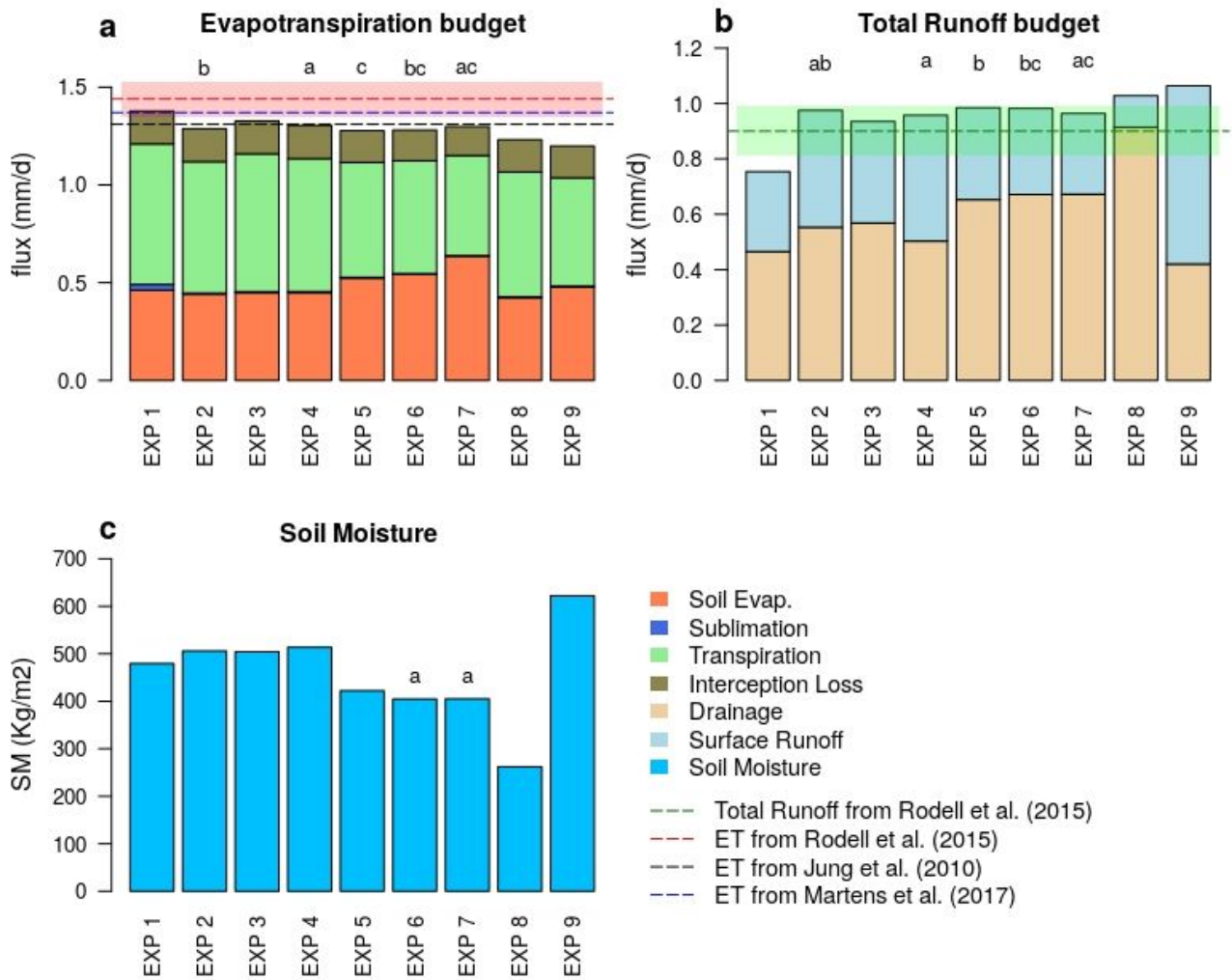
Figure 9. Probability distribution of evapotranspiration bias in the 4 regions of Figure 8, for simulations EXP2, EXP3, EXP4 in red, green and blue respectively.

(a)	SoilGrids	Reynolds	Zobler
SoilGrids	100		
Reynolds	41.2	100	
Zobler	46.0	52.0	100
Unif. Loam	48.5	43.9	64.3
Unif. Silt	3.3	0	0
Unif. Loamy Sand	2.1	6	0
Unif. Clay	2.7	5.8	0

(b)	SoilGrids	Reynolds	Zobler
SoilGrids	1		
Reynolds	0.27	1	
Zobler	0.34	0.43	1

785

Figure 8. Indicators of similarity between the different soil texture maps: (a) Percent overlap between the texture maps. (b) Correlation coefficients between maps of soil particles diameter (soil texture maps were converted to soil particles median diameter maps using Table 2).



790 Figure 105. Terrestrial water budget components for the nine simulations of Table 1, on average over 1980-2010 and over all land
areas but Antarctica: (a) Evapotranspiration budget; (b) Total runoff budget; (c) Soil moisture. Letters above bars describe
statistical significance: the mean difference between bars with the same letter is not statistically significant based on Student's t-test
(with a p-value < 0.05%). Red and green semi-transparent bands show the uncertainty range in the estimates of Rodell et al. (2015),
 795 for evapotranspiration and total runoff respectively. The estimated values of evapotranspiration and total runoff used for evaluation
are described in section 2.43.

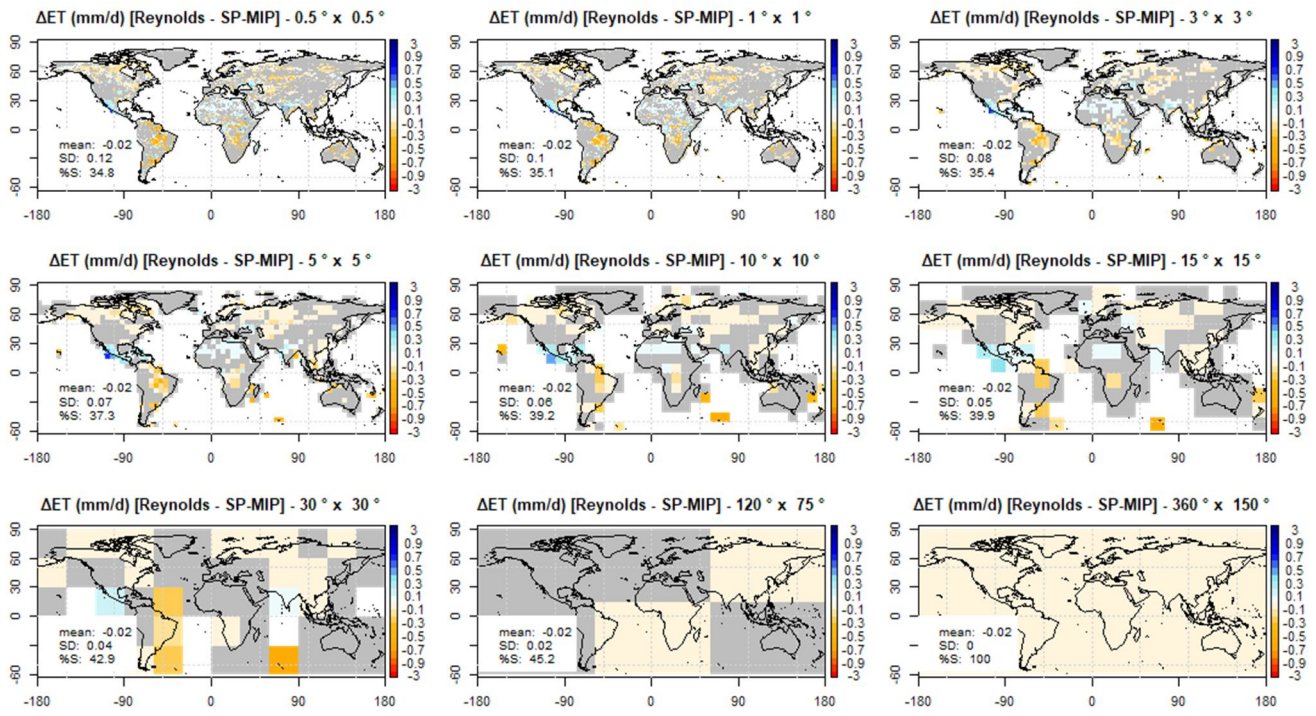


Figure 11. Spatial distribution of simulated annual mean evapotranspiration: difference between EXP2 and EXP4 (Reynolds – SP-MIP), upscaled to different resolutions. Grey color indicates that the difference is not statistically significant at the tested resolution based on Student’s t-test (with a p-value < 0.05). The printed means and standard deviations correspond to the full land area excluding Antarctica. %NS represents the percentage of land with non-significant differences.

800

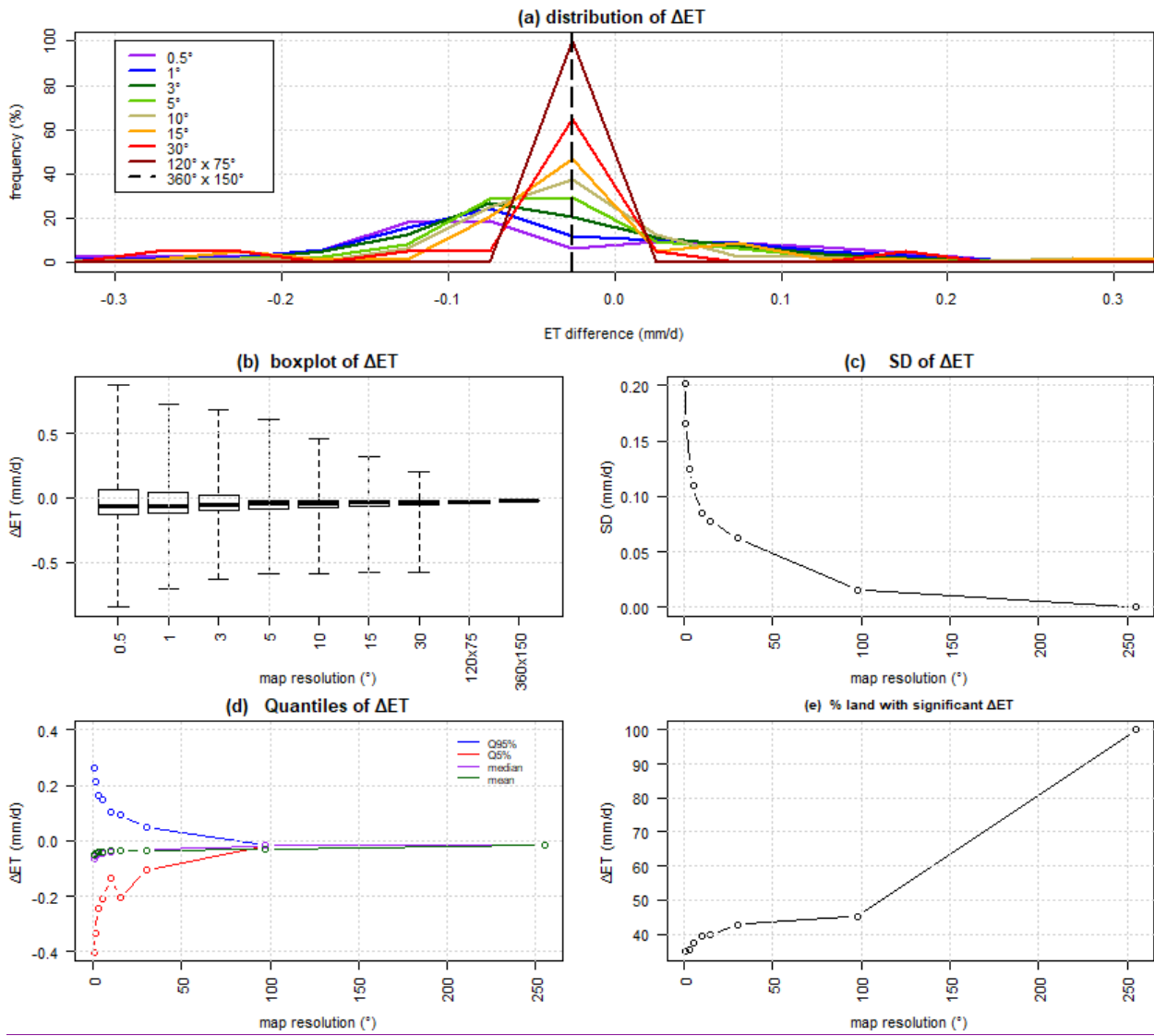


Figure 12. (a) Distribution of annual mean evapotranspiration difference (ΔET in mm/d) over land between EXP2 and EXP4, at different resolutions, (b-e) The corresponding statistical indicators (SD: standard deviation, and statistical significance assessed from a Student test with a p-value < 0.05).